UNIVERSITAT DE BARCELONA

Development and characterization of lung extracellular matrix-based models for respiratory research

Anna Ulldemolins Iglesias

UNIVERSITAT DE BARCELONA

DEVELOPMENT AND CHARACTERIZATION OF LUNG EXTRACELLULAR MATRIX - BASED MODELS FOR RESPIRATORY RESEARCH

Anna Ulldemolins Iglesias

Maig 2024

UNIVERSITAT DE BARCELONA

DEVELOPMENT AND CHARACTERIZATION OF LUNG EXTRACELLULAR MATRIX - BASED MODELS FOR RESPIRATORY RESEARCH

Memòria presentada per l'Anna Ulldemolins Iglesias per optar al títol de doctora per la Universitat de Barcelona

Programa de Biomedicina

Línea de Enginyeria Biomèdica

Director: Isaac Almendros López

Facultat de Medicina i Ciències de la Salut

Barcelona, Maig 2024

Anna Ulldemolins

Isaac Almendros

AGRAÏMENTS

Ara que poso en perspectiva tot el camí recorregut, soc capaç de contemplar la bellesa fins i tot en els moments que semblaven més durs. Molta gent durant aquests tres anys i mig ha tingut un paper fonamental en aquest trajecte. M'agradaria aquí dedicar unes paraules d'agraïment a totes aquestes persones.

Al meu director de tesi, el Dr. Isaac Almendros. Gràcies per la confiança dipositada i les llargues conversacions discutint ciència i la vida. També m'agradaria agrair al Dr. Ramon Farré per proveir-me d'ull crític en la pràctica científica.

Als professors de la Unitat de Biofísica i Bioenginyeria Dra. Roser Sala, Dra. Núria Gavara, Dr. Jordi Otero, Dr. Raimon Sunyer i Dr. Jordi Alcaraz.

No podria imaginar un camí millor, si no hagués estat per les hores de cafè invertides amb el Dr. Héctor. Segons el Dr. Ignasi, que retornà en el meu últim any de doctorat, ara seríem més rics si no fos per tants "anem a fer cafè?". Gràcies als dos per irradiar passió i dedicació envers la ciència.

D'una cosa puc estar segura, sola no m'he sentit en cap moment. Gràcies a l'Alicia per estar sempre allà i escoltar les meves frustracions. També a les meves portugueses preferides, Dra. Maria i Dra. Constança, gràcies per fer les nostres col·laboracions ben entretingudes. Si us plau Dra. Natalia, no em perdis com a referent de *"golden retriever energy"* i gràcies per oferir-me comprensió quan ho he necessitat. Gràcies a en Berni i l'Ale per estar disposats a escoltar-me sempre.

A la resta de companyes i companys de laboratori, per ordre d'aparició: Gràcies a l'Eli, Álvaro i Dra. Esther per acollir-me durant el meu primer any de doctorat. Gràcies al Dr. Brayan i al Dr. Ignacio per ajudar-me des de la distància. Gràcies al Dr. Rafa, Dra. Marta, Dra. Paula, Dra. Agnès Elba, Dra. Patricia, Mar, Dr. Marc, Dra. Carolina, Nanthilde, Àfrica, Marina i Sergio.

Finalment, totes aquelles persones que indirectament i amb la mateixa importància m'han donat suport i motivació. Gràcies a la meva família. Manel i Marga, res d'això hauria estat possible si no haguéssiu dedicat tots els mitjans per donar ales a la meva ment

curiosa des de ben petita. A les meves amigues, Clariss i Cristina per escoltar-me, interessar-vos en els meus experiments i les meves cèl·lules. I gràcies a l'Ivan per ser un suport imprescindible en l'últim tram d'aquest camí.

Aquesta tesi és tan vostre com meva.

Unitat de Biofísica i Bioenginyeria
Facultat de Medicina I Ciències de la Salut,
Universitat de Barcelona
Casanova 143, 08036 Barcelona

El Dr. **Isaac Almendros López**, professor de la Unitat de Biofísica i Bioenginyeria del Departament de Biomedicina de la Facultat de Medicina i Ciències de la Salut de la Universitat de Barcelona, i director de la tesi doctoral de la Sra. Anna Ulldemolins Iglesias,

INFORMA, sobre la participació personal de la Sra. Ulldemolins Iglesias en els articles científics inclosos a la seva Tesi Doctoral, que es presenta en el format de compilació d'articles. A continuació es fa referència als articles en el mateix ordre en que apareixen en la memòria de la Tesi doctoral:

Herranz-Díez C+, **Ulldemolins A**+, Farré R, Gavara N, Sunyer R, Almendros I, Otero J. Matrikines Released from Pepsin-Digested Lung Extracellular Matrix Hydrogels: Considerations for the in vitro Study of the Alveolar Epithelium. Manuscript in preparation.

+ Aquestes autores han contribuït equitativament en aquest treball

L'Anna Ulldemolins va ser responsable del cultiu celular, va realitzar les tècniques experimentals d'anàlisi (qRT-PCR i Wound Healing), i va processar les dades obtingudes. Així mateix, va tenir un paper protagonista en la redacció de l'article. A més, els resultats els ha presentat en congressos nacionals. *Aquest article no s'ha utilitzat ni formarà part, implícita o explícitament, de cap altra tesi doctoral.*

Ulldemolins A, Jurado A, Herranz-Diez C, Gavara N, Otero J, Farré R, Almendros I. Lung Extracellular Matrix Hydrogels-Derived Vesicles Contribute to Epithelial Lung Repair. Polymers (Basel). 2022;14(22):4907. Published 2022 Nov 14.

Índex d'impacte: 5.0, Q1.

En aquest estudi l'Anna Ulldemolins va desenvolupar el sistema experimental i va realitzar els experiments. També va a executar l'anàlisi dels resultats els quals va presentar en

congressos nacionals i internacionals. L'Anna Ulldemolins va escriure el primer esborrany de l'article i va participar en posteriors revisions.

Ulldemolins A, Jurado A, Otero J Farré R, Almendros I. Physiomimetic lung extracellular matrix hydrogel enhances pulmonary recovery in a rat model of acute respiratory distress syndrome. Preliminary results.

En aquest estudi l'Anna Ulldemolins va ser responsable de tot el desenvolupament experimental. Va posar a punt el sistema d'instil·lació de l'hidrogel de pulmó en rata i va contribuir en el disseny d'experiments. L'obtenció de mostres i anàlisi de les mateixes (immunohistoquímica i qRT-PCR) va ser realitzat per l'Anna Ulldemolins.

Ulldemolins A, Narciso M, Sanz-Fraile H, Otero J, Farré R, Gavara N, Almendros I. Effects of aging on the biomechanical properties of the lung extracellular matrix: Dependence on tissular stretch. Frontiers in Cell and Developmental Biology. 2024;12. Published 2024 April 5.

Índex d'impacte: 5.5, Q1

L'Anna Ulldemolins va ser responsable en la major part del disseny experimental. L'obtenció de pulmons i preparació de la mostra va ser realitzat per ella. Va posar a punt el sistema de cultiu en llesques de pulmó descelularitzades i va posteriorment va realitzar les tècniques experimentals d'anàlisi (viabilitat i immunohistoquímica), i va processar les dades obtingudes. Així mateix, va escriure el primer esborrany de l'article i va participar en posteriors revisions

A més, cal destacar que la Sra. Anna Ulldemolins ha col·laborat molt activament amb altres treballs de recerca del laboratori durant la realització de la seva Tesi Doctoral, com queda reflectit en la resta d'articles on la doctoranda és coautora al capítol XII d'aquesta mateixa tesi doctoral

Així ho faig constar pels efectes que siguin pertinents davant la corresponent Comissió de Doctorat de la Universitat de Barcelona

Isaac Almendros López

Science and everyday life cannot and should not be separated.

Rosalind Franklin

TABLE OF CONTENTS

ABREVIATIONS AND ACRONYMS

RBC	Red Blood Cell
ATI	Alveolar Type I Cell
ATII	Alveolar Type II Cell
TLR	Toll-like Receptor
AM	Alveolar Macrophage
ECM	Extracellular Matrix
PG	Proteoglycan
GAG	Glycosaminoglycan
MSC	Mesenchymal Stromal Cell
MMP	Matrix Metalloprotease
PGP	Pro-Gly-Pro matrikine
VGVAPG	Val-Gly-Val-Ala-Pro-Gly matrikine
ARDS	Acute Respiratory Distress Syndrome
IL-6	Interleukin 6
TNF-α	Tumor Necrosis Factor α
IL-1β	Interleukin 1β
IL-8	Interleukin 8
ROS	Reactive Oxygen Species
NET	Neutrophil Extracellular Trap
TRAIL	TNF-related apoptosis-inducing ligand
BASC	Bronchioalveolar stromal cell
ENaC	Epithelial Sodium Channel
MSC	Mesenchymal Stromal Cells
ALI	Acute Lung Injury
TV	Tidal Volume
IRV	Inspiratory Reserve
ERV	Expiratory Reserve

FV	Functional Volume
RV	Residual Volume
IC	Inspiratory Capacity
FRC	Functional Residual Capacity
VC	Vital Capacity
TLC	Total Lung Capacity
P_{Pl}	Intrapleural Pressure
P_{alv}	Intra-alveolar Pressure
P_{atm}	Atmospheric Pressure
3D	Three Dimension
2D	Two Dimension
VILI	Ventilator-Induced Lung Injury
SDS	Sodium Dodecyl Sulfate
SDC	Sodium Deoxycholate
L-HG	Lung extracellular matrix- derived Hydrogel
LC-MS/MS	Liquid Chromatography–Mass Spectrometry
EV	Extracellular Vesicle
LPS	Lipopolysaccharide
AFM	Atomic Force Microscopy

Chapter I.
INTRODUCTION

1. Respiratory Physiology and Acute Respiratory Distress Syndrome

Lung Architecture

The human respiratory system is responsible for the oxygen and carbon dioxide exchange between the body and the external environment. It is composed of organs and tissues being the lungs the pivotal organ of the system. They facilitate the exchange of gases during respiration which is vital for sustaining cellular metabolism and body's homeostasis (1).

Lungs are composed of a mesh of airways. The starting point is the trachea, which bifurcates into the two main bronchi that enter the right and left lungs. These bronchi are further divided into smaller bronchi and bronchioles, that finally leads to alveoli, tiny air sacs surrounded by blood vessels. The alveoli have an enormous surface area, allowing efficient diffusion of oxygen and carbon dioxide between air and the bloodstream (2). The oxygen is diffused to the capillaries and bound to haemoglobin inside the red blood cells (RBC) for their transportation across the whole body. Simultaneously, the waste product from the metabolism (carbon dioxide) is released from the capillaries to the alveoli to be released during exhalation.

The functional gas exchange executor: the alveolus

The structural features of the alveoli are unique to optimize the mentioned gas exchange (3). They are surrounded by a thin layer of type I alveolar cells (ATI), which are squamous epithelial cells. These cells are extremely thin allowing a rapid diffusion of gases. Neighbouring the ATI cells are the type II alveolar cells (ATII), also known as septal cells (4). ATII secrete surfactant, a substance that reduces surface tension within the alveoli (5) to prevent the collapse of the alveoli and facilitate the movement of gases (Figure 1).

The alveoli are surrounded by capillaries which have a thin endothelial monolayer, forming a thin respiratory barrier that promotes gas diffusion across it. Therefore, the oxygen can diffuse from the alveoli into the bloodstream and the carbon dioxide diffusing

in the opposite direction (6). Lung's vital role in respiration is fulfilled by collaborative effects between the alveolar structure, the circulatory system and ventilation.

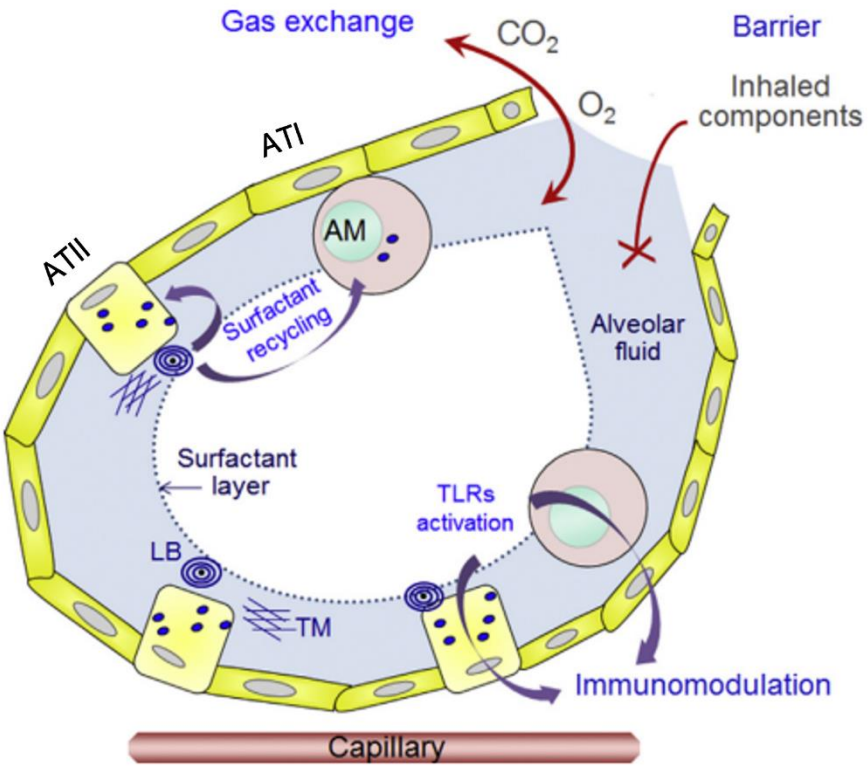

Figure 1. Alveolus structure and gas exchange. *Type I alveolar cells (ATI) and type II alveolar cells (ATII) play an important role within the alveoli, facilitating interaction between the external environment and the bloodstream. Alveolar cells are responsible for barrier maintenance, gas exchange, and immunomodulation necessary to maintain alveoli homeostasis. The immunomodulation requires the crosstalk between alveolar macrophages trough expression of specific molecules like toll-like receptors (TLRs). The surfactant layer is derived from lamellar bodies (LB) and tubular myelin (TM). ATII and alveolar macrophages (AM) play a role in recycling surfactant components. Adapted from (7).*

Lung Extracellular Matrix

The lung extracellular matrix (ECM) provides support for the cells and maintains the architecture of the lung tissue (8). It also preserves the mechanical properties of the tissue contributing to the elasticity and pulmonary compliance allowing it to expand and contract during respiration. Lung ECM is composed by a mesh of proteins, glycoproteins, proteoglycans, and other molecules that surround the cells and supports them within the lung tissue (9) (Figure 2).

In addition to provide a framework for the cells, the lung ECM also serves as a dynamic environment that regulates cell behaviour and signalling. Many proteins such as growth factors, cytokines and enzymes composing the lung ECM are involved in cell proliferation, differentiation, and tissue remodelling. The interaction between these molecules and the lung resident cells influences their responses to physiological and pathological stimuli (8). During lung development, the ECM guides the formation and composition of the lung tissue. Over the course of lung development, the composition and topography changes, and is very heterogeneous depending on the function of the different lung regions (10).

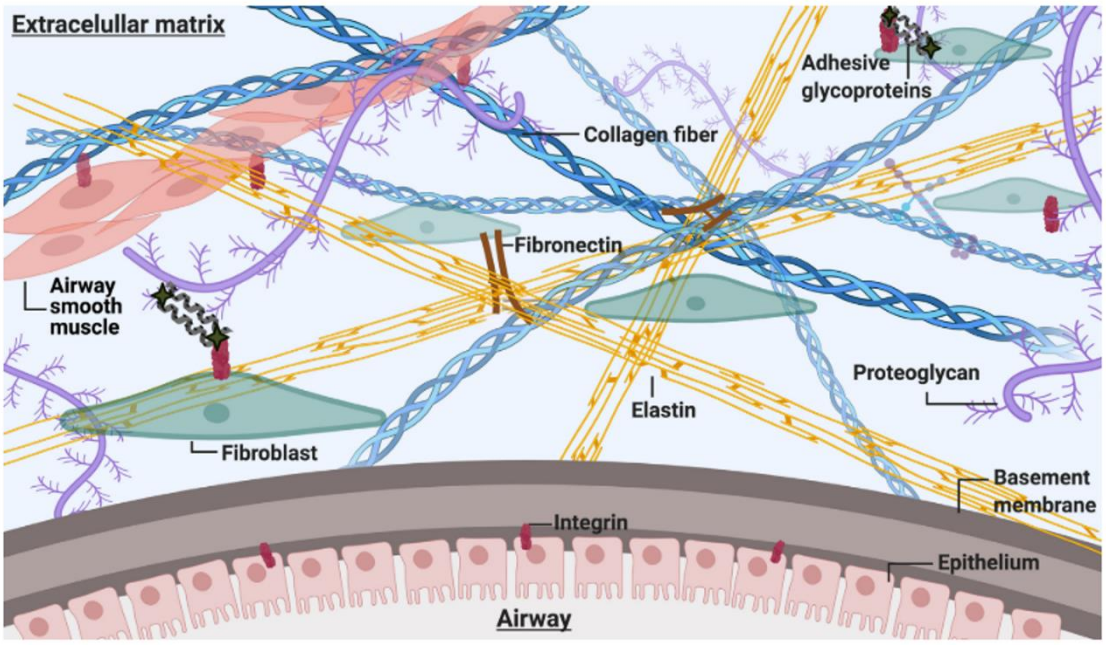

Figure 2. Schematic representation of the lung extracellular matrix. *The primary constituents of the extracellular matrix are collagens, proteoglycans, and adhesive glycoproteins. They are arranged in a mesh-like structure that interact with lung resident cells (epithelial and mesenchymal cells, fibroblasts and airway smooth muscle cells) through integrins. Adapted from* (11)

Here are listed the principal constituents of the lung ECM, essential for providing biomechanical support, cellular communication, and tissue homeostasis:

Collagen: This is the primary protein component of the ECM and it is characterised by triple-helix structure and intermolecular cross-links (12). There are nearly 30 member in the collagen family, including types I, II, III, V, and XI the most abundant types encountered in connective tissues (13). Collagens provide tensile strength to tissues and participate in cell adhesion, chemotaxis, and cell migration (14). Type I collagen constitutes approximately the 90% of the total collagen and assemble into collagen fibrils in the

extracellular space. The fibrils have a diameter between 10 to 300 nm, lengths reaching almost 100 μm and tend to aggregate into larger, cable-like bundle structures visible called collagen fibbers. These fibbers are generally stiff (between 3.75 and 11.5 GPa) (15) and inelastic, tending to fracture at low levels of deformation.

Elastin: Lung tissue requires both strength and elasticity. The lung ECM contains a network of elastic fibbers responsible for providing the necessary resilience, allowing tissues to recoil after being transiently stretched (16). Elastin is the primary component of these elastic fibbers, which are synthetized by the enzymatic cross-linking of tropoelastin monomers and microfibrillar proteins. Elastin structure is characterized by a high degree of conformational disorder, which enables it to stretch and recoil like a rubber band (17). Unlike collagen, elastin can sustain substantial deformation without breaking. Consequently, elastin fibbers have much lower stiffness than collagen (1-3 MPa), owing to their deformation properties (18).

Proteoglycans: The extracellular interstitial space in tissues is filled with proteoglycans (PGs) which are the primary non-fibrous protein in the ECM. PGs contribute to ECM hydration, provide force-resistance properties to tissues and mediate binding between fibrous proteins (19). They are formed of glycosaminoglycan (GAG) chains covalently attached. GAGs are composed by linear polysaccharide chains formed of repeating disaccharide units, and they can be divided into sulfated GAGs (e.g., chondroitin sulfate, heparan sulfate, and keratan sulfate) and non-sulfated components like hyaluronic acid. GAGs are highly negatively charged due to the abundance of sulfate and carboxyl groups, making them hydrophilic. Also they enable the ECM to endure high compressive forces (20).

Fibronectin: This is a glycoprotein which exists as dimers and forms an insoluble fibre meshwork. It is secreted by fibroblasts, supporting matrix construction. Cells bind to fibronectin through specific surface receptors known as integrins. The well-known integrin-binding motif in fibronectin is Arg-Gly-Asp (RGD). However, fibronectin can also bind to collagens GAGs, effectively connecting the ECM network (21).

Laminin: It is a major fibrillar glycoprotein found in the basal lamina, a specialized ECM layer underlying all epithelial cells. Laminin-1, the most common type within this family,

is a large, flexible protein consisting of three long polypeptide chains arranged in the shape of an asymmetric cross (22,23). The stabilization of the ECM structure is possible because laminin has multiple binding sites (i.e. collagen VI). Moreover, integrins are capable of recognize some peptide sequences from laminin. Their primary functional roles are in embryogenesis, tissue and organ formation, as well as cell attachment, proliferation, and differentiation (23).

Matrikines

The lung ECM continuously undergoes controlled remodelling. Cells are constantly rebuilding the lung ECM through synthesis, degradation, reassembly and chemical modification of its components. This process involves changes in the ECM, mediated by specific enzymes such as matrix metalloproteinases (MMP). This remodelling is necessary for tissue repair, but excessive or dysregulated ECM remodelling can contribute to the pathogenesis of lung diseases (8). Enzymatic hydrolysis upon degradation or remodelling can affect all ECM constituents, producing small peptides with biological activity known as matrikines (24). In Table 1, the most present matrikines and its effects in the lungs are summarized.

Table 1. Described lung extracellular matrix– matrikines and its effects. (PMN, Polymorphonuclear neutrophils).

ECM Protein	Matrikine	Action	Reference
Collagen	Pro-Gly-Pro (PGP) peptide	Vascular permeability	(25,26)
	N-ac-PGP	PMN influx	(27)
	Tumstatin	Anti-angiogenic, Anti-inflammatory	(28)
Elastin	Val-Gly-Val-Ala-Pro-Gly (VGVAPG) peptide	Monocyte influx	(29,30)
Proteoglycan	Low – molecular weight hyaluronan	Inflammation, wound repair	(31)
	Endorepillin	Modulates angiogenesis	(32)

Fibronectin	P1-P5 peptides	Increase MMP9,12, IL-1, IL-6, TNF-α	(33)
Laminin	γ2 ectodomain	Epithelial proliferation, wound repair, alveologenesis	(34,35)
	A13 peptide	Wound repair	(36)
	C16 peptide	Wound healing, angiogenic	(22)

These bioactive molecules have an impact on tissue repair, cell signalling, migration proliferation and tissue homeostasis (37). In the lung ECM, several matrikines have been identified that contribute to lung physiology and disease processes (25,38). An example is endostatin, a 20-kDa C-terminal fragment of collagen XVIII that inhibits angiogenesis. In the lungs, the combined action of MMPs and prolylendopeptidase releases the tripeptide matrikine Pro-Gly-Pro (PGP). PGP, present also in its acetylated form (N-ac-PGP), regulates repair processes but it also attracts neutrophils contributing to lung pathology (39). More examples are the Val-Gly-Val-Ala-Pro-Gly (VGVAPG) released fragment in the MMP-12 and neutrophil elastase degradation of elastin, low molecular weight hyaluronan produced in the hyaluronidase-mediated breakdown of high molecular weight hyaluronan and g2-ectodomain originating from MMP-3,-12,-14,-20, or neutrophil elastase fragmentation of laminin.

Lung in disease and extracellular matrix alterations

The course of many chronic lung diseases is associated with changes in the composition, content, and structural organization of the ECM components. Changes in the ECM, which are driven by multiple cell types in the lung, affect lung function and cell biology. Dysregulation of the ECM composition, remodelling and mechanical properties changes lead to functional impairments and disease progression. The disease-specific changes driven by the ECM that affect cell behaviour are unknown. Further research in this area is needed to provide significant improvements in the development of new approaches for the treatment of patients with lung diseases (40).

Acute Respiratory Distress Syndrome

Acute Respiratory Distress Syndrome (ARDS) is characterized by severe impairment in gas exchange leading to hypoxemic respiratory failure (41). Unfortunately, ARDS has a high mortality rate, and there is currently no effective treatment available (42). The prevalence and mortality of this respiratory syndrome have significantly increased in the recent months, particularly because patients with severe COVID-19 often develop end-stage ARDS (43).

ARDS is initiated by direct or indirect lung insults such as pneumonia, sepsis, aspiration of gastric acid, severe trauma, or inhalation of harmful substances. The pathophysiology of ARDS involves a rapid and severe inflammatory response that progress through three phases: inflammatory, proliferative, and fibrotic (44). The injury to the alveoli causes damage to the epithelial and endothelial barriers and leads to increased permeability of the alveolar membrane. Disruption of this barrier allows protein-rich fluid to enter the alveoli causing fluid accumulation in alveolar spaces creating pulmonary edema (45). Additionally, there is a recruitment of neutrophils in the interstitial spaces. In the initial phase of ARDS, several inflammatory mediators such as interleukin 6 (IL-6), tumor necrosis factor-α (TNF-α), interleukin 1β (IL-1β), and interleukin 8 (IL-8) are present (46). The persistent inflammation affects the production of surfactant by ATII cells.

The inflammatory phase is followed by a pro-fibrotic phase characterized by the necrosis of alveolar cells, disruption of the alveolar capillary barrier, and proliferation of stromal fibroblasts. These changes produce an enlargement of the interstitial space that contains secreted ECM components, cell debris, and edema. The loss of ATI cells impairs the exchange of CO_2 and O_2 and at the same time ATII proliferate attempting to repair the damaged epithelium (44). Subsequently, stromal populations migrate to the alveolar lumen, proliferate increasing the secretion of ECM proteins (47).

The lung epithelium, acting as an important regulator and effector tissue, plays a crucial role in the immune innate response to damage (48). The epithelial cells are highly sensitive to their surroundings and act as an early warning system to initiate immune responses (49). As a response to damage, epithelial cells can secrete a wide range of pro inflammatory cytokines and chemokines like IL-6 (50), IL-1β (51), TNF-α (52). They act as

chemotactic agents for other immune cells like monocytes, macrophages, T-cells and dendritic cells. IL-6 and TNF-α are pleiotropic cytokines that have been associated with poor prognosis in ARDS patients (53). IL-1β and TNF-α induce the production of other cytokines and can promote alveolar epithelial repair, spreading and migrating on the edge of wounds (51,54). They also activate the expression of adhesion molecules and stimulate growth. The combination of ECM alterations and inflammation contributes to the collapse and dysfunction of the alveoli (Figure 3).

Conventional treatment involves respiratory support trough mechanical ventilation and addressing the cause or trigger, such as treating infections or managing sepsis (56). Additionally, patients are administrated with anti-inflammatory medications to reduce lung edema. As the disease advances, the lungs become stiff and less compliant, leading to severe hypoxemia, even when patients are in treatment with supplemental oxygen. Abnormally low levels of oxygen in the blood can cause multiple organ failure and ultimately death. Even ARDS survivors experience lung damage and decreased lung function (57). Despite decades of research, current therapies have not shown a significant improvement in mortality rates (42,58). Therefore, a new therapeutic approach is needed.

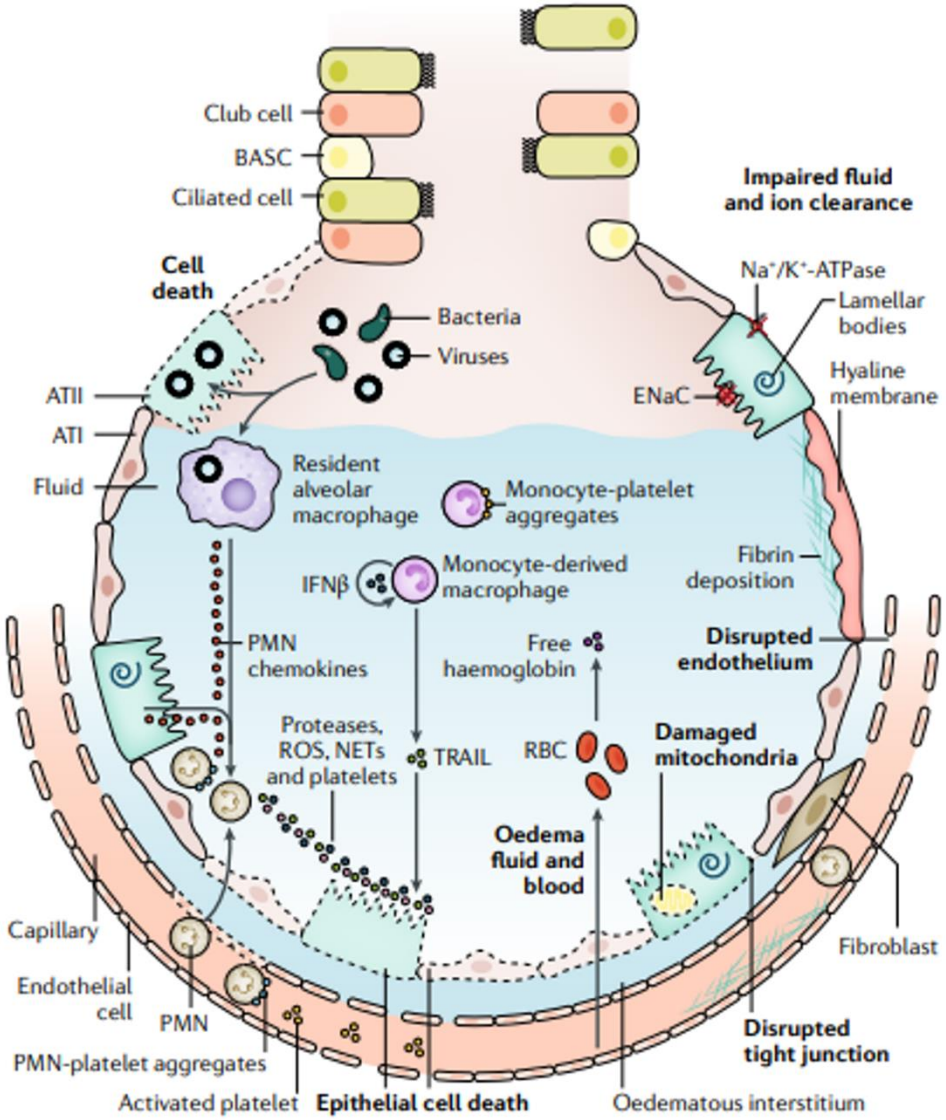

Figure 3. Schematic representation of the injured alveolus and its processes related. *The injured alveolus is subjected to various insults which directly harm the epithelial layer or induce inflammation, leading to subsequent epithelial damage. Toll-like receptors (TLRs) activate type II-alveolar (ATII) cells and resident alveolar macrophages (AM) to release chemokines, attracting immune cells into the airspaces. To eliminate pathogens, neutrophils across the epithelium release proteases, reactive oxygen species (ROS), and neutrophil extracellular traps (NETs), while monocytes can induce epithelial cell apoptosis by releasing tumor necrosis factor (TNF)-related apoptosis-inducing ligand (TRAIL). Red blood cells (RBC) release cell-free hemoglobin, aggravating injury through oxidant-driven mechanisms. Loss of cell–cell adhesion and plasma membrane wounds contribute to endothelial and epithelial permeability, allowing leukocyte migration and an influx of edematous fluid and RBCs into the airspaces. (BASC, bronchioalveolar stem cell; ENaC, epithelial sodium channel). Adapted from* (55)

2. Mechanobiology and its Effects in Mesenchymal Stromal Cell Therapy

Lung Mechanics

Biomechanical properties of the ECM including its stiffness and topography have an impact on the lung tissue behaviour. A quantitative measure used to assess these biomechanical forces is called stress, which represents the force applied to a specified area with the potential to alter its shape (measured in Newtons per square meter, or Pascal per area unit). Various types of stresses are induced by physical actions on the ECM: tensile stress (pulling), compressive stress (pressing), torsional stress (twisting), and shear stress (flowing parallel to a tissue) (59). When an applied stress is present it causes cell strain referring to the deformation experienced by the cell normalized to its initial length. Permanent changes caused by deformations are called plastic deformations, while temporary changes are known as elastic deformations indicating the resistance to changes of the material. To express tissue elasticity at low strain values, the Young's modulus is used. It is derived from stress-strain curves through mathematical modelling, helping to define the organ's passive stiffness (60).

However, it is essential to recognize that tissues are not entirely elastic and exhibit time-dependent mechanical changes and energy dissipation, similar to the viscous liquids. As a result, the components of the lung ECM display initial linear elasticity, which becomes nonlinear in response to increasing strain levels. The dual behaviour of the ECM, combining both elastic and viscous characteristics (viscoelasticity) (Figure 4), is a widely recognized feature present in all biological tissues (60) .

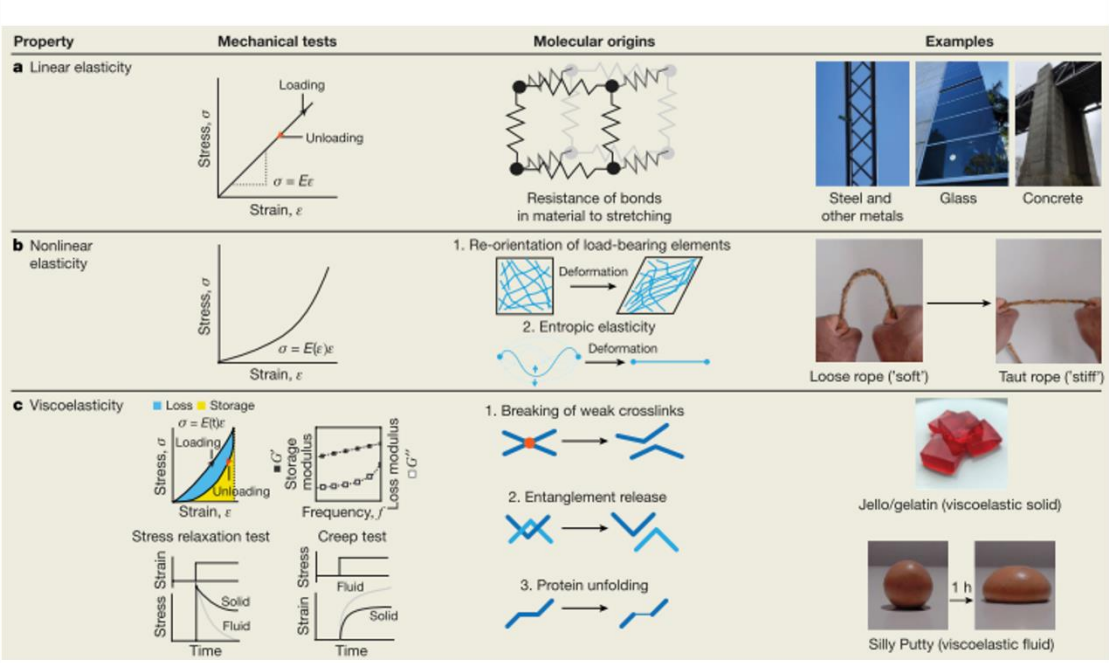

Figure 4. Mechanical behaviours relevant to biological tissues and extracellular matrices*. Materials can be classified based on their response to mechanical loading, observed in a stress-strain test. Biological tissues and extracellular matrices can display a blend of nonlinear elasticity and viscoelasticity. Adapted from* (60)

Tissular Stretch

In physiological conditions, air volume in the intrathoracic airways is determined by different factors: the properties of the lung parenchyma, surface tension, and the forces exerted by respiratory muscles. The lung is being continuously exposed to different levels of mechanical stresses due to its complex structure and cyclic deformation during spontaneous breathing.

During exhalation, the lungs contract inward while the chest wall expands outward. These opposed forces generate negative pressure between the parietal and visceral pleurae. The negative intrapleural pressure (P_{PI}) is essential for keep small airways open. Inhalation reduces P_{PI}, and allows air to enter alveoli, while also dilating small airways to enhance airflow. Exhalation reverses this process passively with an increase of P_{PI} and subsequently air exits the alveoli. The whole process is a rhythmic contraction of inspiratory muscles that causes cyclic changes in the thoracic cage dimension with a cyclic variation of P_{PI} (Figure 5).

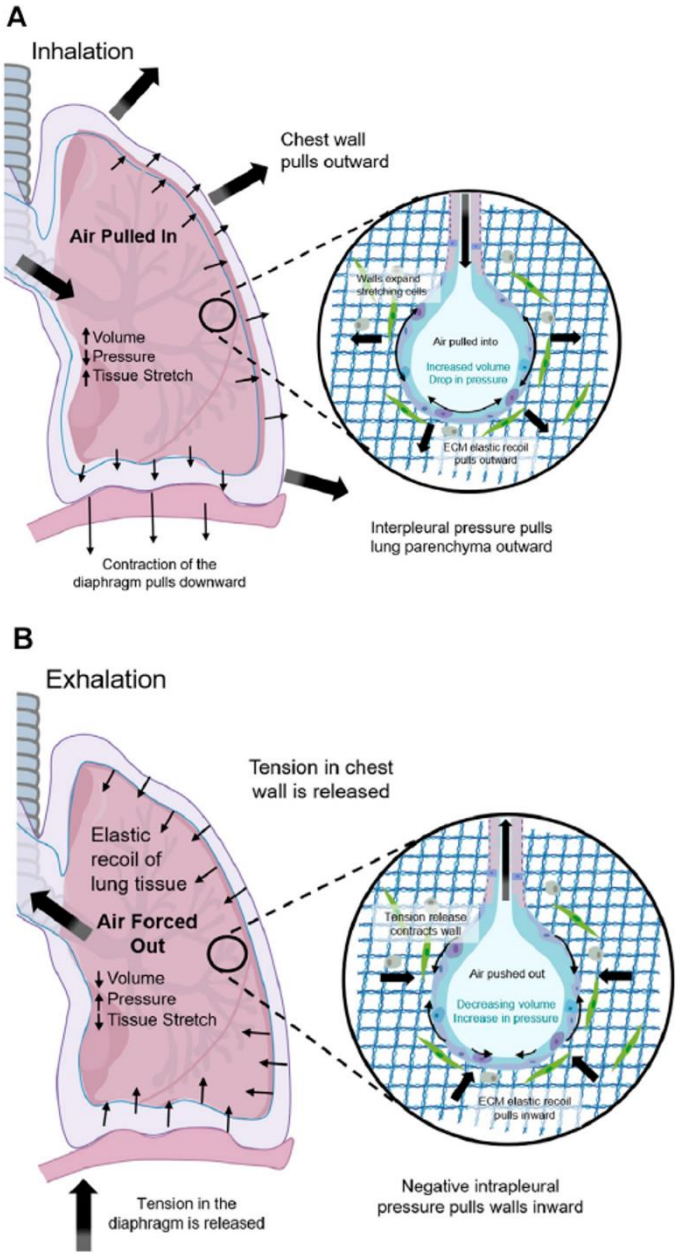

Figure 5. Mechanical forces within the lung. ***(A)*** *Contraction of the diaphragm and muscles in chest wall during inhalation lead to negative interpleural pressure that enlarges lung tissue, stretches the alveoli, and increases lung volume driving air inside.* ***(B)*** *Relaxation of the diaphragm and muscles in chest wall during exhalation permits elastic retreat that decreases lung volume and air compression that drives air outside. Adapted from* (61).

Four standard lung volumes, tidal (TV), inspiratory reserve (IRV), expiratory reserve (ERV), functional volume (FV) and residual volumes (RV) are described in the literature. Accordingly, the standard lung capacities are inspiratory (IC), functional residual (FRC),

vital (VC) and total lung capacities (TLC). Specifically, RV constitutes part of FRC as well as TLC and FV is equal to ½ of the TV and the FCR (Figure 6).

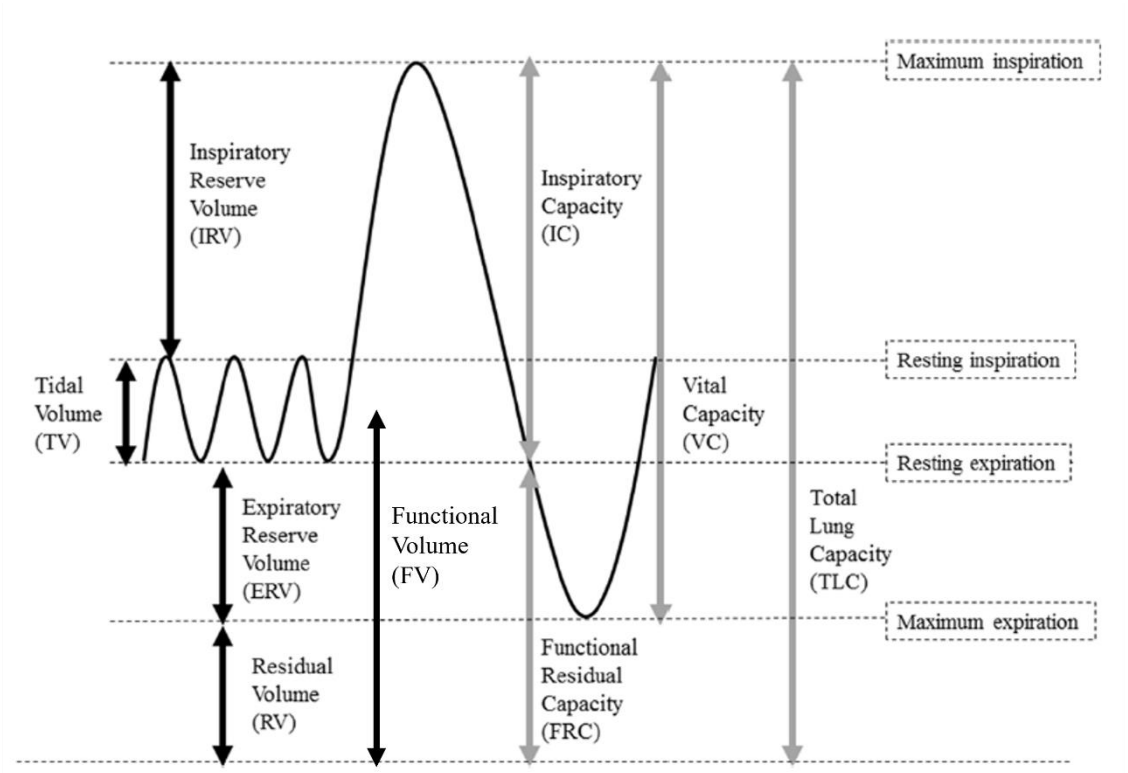

Figure 6. *Standard lung volumes (black arrows) and capacities (grey arrows). Adapted from* (62)

Tidal breathing maintains the airways open and deeper inhalations require the action of other inspiratory muscles for increased air delivery. On the other hand, exhalation below tidal levels activate the expiratory muscles. They compress the thoracic cage to its maximum and there is an increase in both P_{Pl} and intra-alveolar pressure (P_{alv}) above atmospheric pressure (P_{atm}). Even after a forced exhalation, there is air remaining in the lungs (RV). The lung–chest wall system is rested when P_{alv} is equal P_{atm} and the lungs are filled with FRC. At this point, the inward recoil tendency of the lungs is equal to the outward recoil tendency of the chest wall.

There are studies focusing on the lung biomechanics of ECM carried out at RV (63,64). On the other hand, there are others that examined the mechanical characteristics inherent in the ECM at FV (65,66). However, the consistency of the results of the lung mechanical properties using RV or FCR remains unknown.

Mesenchymal Stromal Cell Therapy in Acute Distress Respiratory Syndrome

In the last years, stem cell therapy has shown great promise in the development of new treatments. Mesenchymal Stromal Cells (MSCs) are a population of multipotent cells capable of differentiate into various cell types and release agents with immunomodulatory, anti-inflammatory, and antimicrobial effects (67). Also, these cells can migrate into the lungs and differentiate into ATII in cases of acute lung injury (ALI) and lung fibrosis (68). Due to their immunomodulatory properties, they interact with different immune cells, regulating both innate and adaptive immunity (69). Moreover, it is also widely recognized that MSCs possess antibacterial and tissue repair capabilities (70,71). Accordingly, a significant amount of research has been conducted in the application of MSCs for ARDS therapy with successful preclinical results in lung permeability, inflammatory cell infiltration and immunomodulation (69,72).

Despite the clear preclinical research outcomes, clinical trials have not shown strong evidence for MSC efficacy (67,73,74). There is a current need to address challenges in the use of cell therapies (75,76). The MSC conditioning, bioprocessing and therapeutic application methods are important factors to take into account to develop innovative strategies to ensure clinical translation and potentially to use MSC-based therapies as treatment for lung related conditions (69).

Extracellular Matrix- Mesenchymal Stromal Cell Crosstalk

Physical forces such as stress and strain influence cellular behaviour and function that ultimately affect tissue remodelling (76,77). This interaction between cells and the ECM, regulated by the lung's mechanical load, is crucial for maintaining healthy mechanical tissue homeostasis (78).

Additionally, MSCs interact with elements of their microenvironment, like ECM topography and mechanical forces (79). The MSCs-ECM crosstalk is mediated by biochemical and biomechanical cues that influence cell response. They play a significant role in a wide range of cellular functions, such as migration, wound healing, and differentiation, and are one of the hotspots for tissue engineering research (80). MSCs

also remodel their environment in response to environmental signals that results in a variation of ECM composition and concentration within and between tissues and organs (8,81,82). The abundance and distribution of ECM components significantly affect its physicochemical characteristics and its interaction with MSCs.

The process by which the cells respond to their microenvironment with the activation of signalling pathways that subsequently impact in cell migration and differentiation is known as mechanotransduction (83,84). Notably, the biophysical properties of the substrate where the cells are cultured have been used to influence MSCs fate *in vitro* (85).

Cells adhere to the ECM through surface receptors which enable them to sense mechanical cues from the ECM, such as stiffness and adhesive regions (86). Specifically, this interaction is possible because of the presence of focal adhesions, which connect the cytoskeleton of the cells to the ECM. These focal adhesions act as mechanosensors. They translate mechanical cues into biochemical signals that influence cell behaviour and function. Among its components, integrins are transmembrane proteins that directly bind to ECM components. Integrins play a vital role in this process because they transfer the mechanical forces to the cytoskeleton and trigger signalling pathways that affect cell adhesion, migration, proliferation, and differentiation (i.e. YAP/TAZ signalling) (86,87) (Figure 7).

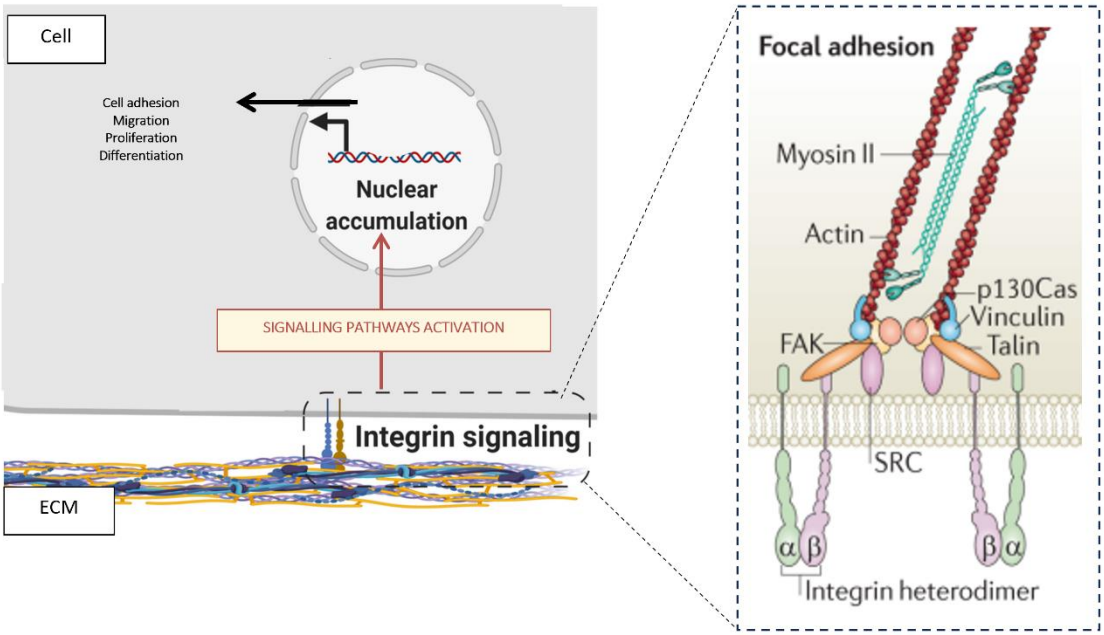

Figure 7. Key components in tissue mechanical homeostasis. *Cell-matrix adhesion complexes sense the physical characteristics of the extracellular matrix (ECM). These complexes incorporate protein sensors such as talin, p130Cas (or BCAR1), and integrins. They undergo alterations in conformation based on the applied force, and consequently they initiate downstream signalling responses. Focal adhesion kinase (FAK), Steroid receptor coactivator (SRC). Adapted from* (78) *and* (88)

Additionally, the cytoskeleton is composed of actin filaments, microtubules, and intermediate filaments that contribute to mechanosensing. Cells interact with the ECM pulling through the contraction of actomyosin-filaments and by pushing through actin polymerization and microtubules (Figure 8). These forces lead to a rearrangement in the cell cytoskeleton with the activation of signalling pathways (89).

In the context of lung diseases, the consideration of ECM mechanosensing becomes evident. Lung cells are exposed to microenvironments with different stiffness, and they experience mechanical stimuli due to ventilation (90). Therefore, it is evident to take into account ECM mechanosensing and consider the complexity of the native ECM in respiratory tissue engineering research. Thus, ECM-based therapies have been proposed as potential approaches for lung regeneration and for the treatment of severe lung diseases (91).

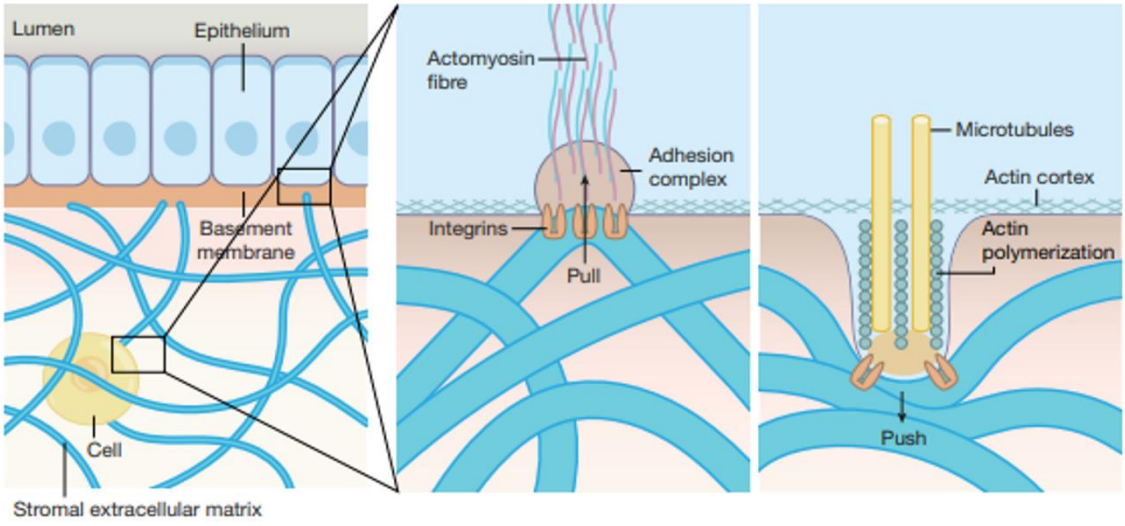

Figure 8. Mechanical interactions between cells and the extracellular matrix. *Cells interact with the extracellular matrix by pulling and pushing. Adapted from* (62).

Physiomimetic Preconditioning on Mesenchymal Stromal Cell Therapy

The use of physiomimetic and biophysically tuneable ECM scaffolds opens the opportunity to enhance the MSC therapy. However, to replicate the complex native ECM is a challenge since its sophisticated composition, structure, dynamics, biocompatibility, topography, and function.

Ideally, cells should experience a microenvironment similar to their native tissues. In addition to ECM components, static and dynamic biomechanical properties of the pulmonary microenvironment should be taken into consideration since they can activate repair pathways in MSCs. For example, substrate stiffness regulates the secretion of a wide range of cytokines, and shear stress and cell stretch can enhance angiogenic and anti-apoptotic capacities in MSCs (92-94).

Moreover, when MSCs are cultured in a 3D environment, it provides more physiological conditions and maintains stemness, increase cell survival, and preserves multipotency when MSCs are transplanted (95). Such 3D cultures have demonstrated enhanced angiogenic and anti-inflammatory potential in MSCs compared to conventional 2D microenvironments (95). Recent data from our research group showed that MSCs preconditioned in decellularized lung scaffolds and subjected to cyclic stretch significantly

increased their beneficial therapeutic effects after ventilator-induced lung injury (VILI) in rats (96). Given the specific features of ARDS, biophysical conditioning on MSCs before therapeutic use could significantly improve their therapeutic effects.

Therefore, the development of novel experimental scaffolds aiming to replicate the biological and biophysical microenvironment could enhance MSCs therapy.

Building a Physiomimetic Lung Environment

Decellularized lung scaffolds

To be able to generate a lung physiomimetic substrate, tissue decellularization has emerged as a technique that involves the removal of cellular components from biological tissues while preserving the ECM architecture (97). The posterior repopulation with cells to generate functional tissue constructs is possible. Also, it can be used for the cell-matrix interaction studies. Therefore, it has gained significant attention in regenerative medicine and tissue engineering (98).

In the last years, the tissue engineering field has considerably explored applications for decellularized ECM. Many studies have proven the removal of cellular components with preservation of structural and functional proteins from different organs including the lung, heart, kidney, liver, intestine, larynx, skin, and bladder by using detergents such as sodium dodecyl sulfate (SDS), sodium deoxycholate (SDC), and Triton X-100 (99).

Recently in our lab group, a *in situ* novel decellularization method for lung tissue slices has been developed (100). It offers the advantage of not removing the sample from the microscopic slide during the process, so it can be subsequently used for cell culture, biomechanical assays and immunohistochemical analysis.

Lung hydrogels

Following the tissue decellularization protocol, the obtention of hydrogels has been also possible. This highly hydrated polymeric materials that mimic the lung native ECM (biomechanics and topography) represent an exciting development in the field of tissue engineering and regenerative medicine. Since the first natural lung ECM derived hydrogel was recently synthesized (101), numerous applications have been described (i.e. design of lung on-a-chip models, disease models, ATII culture and ATII differentiation) (102-108).

In contrast with the synthetic (i.e. polyacrylamide, polyethylene glycol, polyurethane, poly(-ε-caprolactone) and natural hydrogels widely used (i.e. alginate, agarose, chitosan, hyaluronan, collagen, gelatin) (109), ECM – derived hydrogels present several advantages. ECM hydrogels replicate the stiffness (110) and composition of the lung and more importantly they are comprised of ECM bioactive components, such as growth factors and cytokines mimicking (111) the natural microenvironment (108).

To obtain a lung ECM-derived hydrogel (L-HG), once the lung is decellularized, it is lyophilised and subsequently cryomilled to obtain lung powder (Figure 9). This lung powder is first solubilized with pepsin in an acid environment to obtain the monomeric components of the ECM that are going to be further rearranged spontaneously into the homogeneous gel by controlling the pH and temperature (112). Several lung hydrogel protocols are found in the literature (96,101,112).

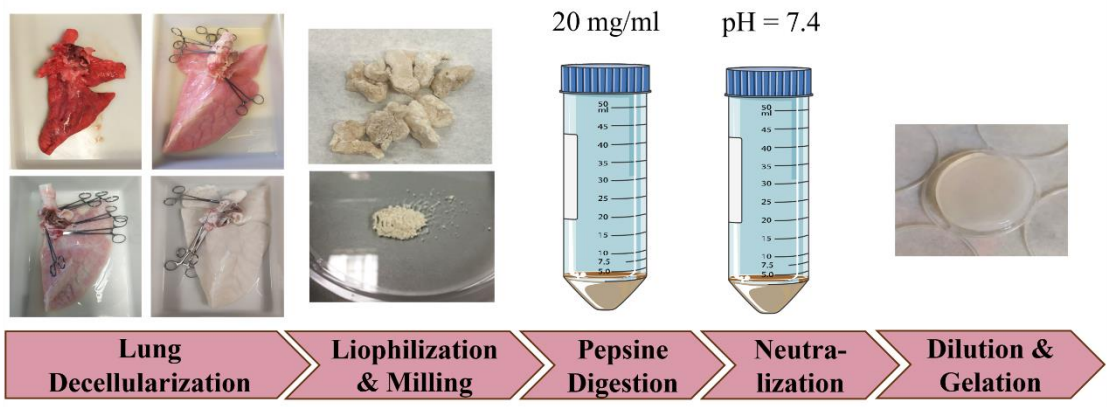

Figure 9. Lung extracellular matrix - derived hydrogel synthesis. *Successive images of the porcine right lung through all the decellularization protocol with consecutive risings of Triton X-100, sodium deoxycholate, sodium chloride and deoxyribonuclease. The final product is lyophilized and cryomilled to obtain a powder that is going to be digested with pepsin in an acid environment and neutralized for the final gelation.*

L-HGs have been recently used for MSCs culturing. For example, in contrast with the conventional culture conditions in plastic, L-HG maintains stemness and increases cell survival and multipotency of MSCs (110,113). Accordingly, it seems that ECM hydrogels could be further enhanced to be used as physiomimetic vehicle for applying MSCs or MSCs-derived release agents. In fact, the potential use of lung hydrogels not only relies in their capacity to mimic lung microenvironment. Although the mechanisms are not well elucidated, L-HGs can also release bioactive peptides (i.e. matrikines), nano-vesicles, chemokines, cytokines which the cells can interact with (114,115).

Lung Hydrogel-derived Matrikines

As expected, the range of matrikines discovered in ECM-derived hydrogels originates from the diverse proteins existing in the decellularized ECM framework (Table 1). Using proteomics-based techniques, the composition of decellularized lung ECM has been established. Li et al. conducted a label-free proteomic analysis of decellularized human lungs through liquid chromatography–mass spectrometry (LC-MS/MS) and identified 384 proteins (116). Calle et al. employed targeted quantitative proteomics to contrast the ECM composition between two lung decellularization techniques (117). This method enabled the effective quantification of 71 proteins. Proteomics are crucial for understanding the biological effects of ECM-derived hydrogel therapies, providing valuable insights into experiments conducted in animal models and even clinical trials.

Recent reports have shown that L-HGs reduce oxidative damage, protects from lung injury (91,118) and modulates fibrotic tissue remodelling (119), resulting in improved lung pulmonary health. One possible explanation for this phenomenon is because the enzymatic breakdown of ECM releases growth factors initially bound to the native scaffold (112,120). Another factor could be that the enzymatic digestion of the ECM produces matrikines with particular biological functions, which interact with membrane-bound mechanotransduction proteins that regulate gene expression (25,121). Additionally, the enzymatic breakdown of ECM protein structures might expose hidden protein sequences containing biological motifs (i.e. laminin-β1 chain fragments that hinder tissue fibrosis and remodelling by inhibiting MMP2 expression) (122). The proposed mechanisms of lung protection in ARDS exerted by the L-HG and the L-HG derived matrikines are summarized in Figure 10.

As reviewed by Saldin et al. (112), the proteomic profile of pepsin-digested ECM-derived hydrogels has been analysed for various tissues such as the liver (123), skeletal muscle (124), tendon (125), heart (126), kidney (127), pancreas (128) and umbilical cord (129) but not yet for the lung. The characterization of the protein fragment composition of lung ECM-derived hydrogels could be an opportunity for translational research. With the use of computational modelling, it may be possible to predict peptide interactions with biologically significant molecular targets and later test them *in vitro* or *in vivo.*

Hence, investigations should prioritize the identification and quantification of matrikines within lung ECM-derived hydrogels. While significant hydrogel constituents such as elastin, collagen, and glycosaminoglycans have been quantified (101,130,131), protein fragments resulting from ECM pepsin enzymatic digestion remain unexplored. Despite these possible explanations, there is no clear evidence of the molecular mechanisms responsible for ECM-derived hydrogel's lung protection against injury.

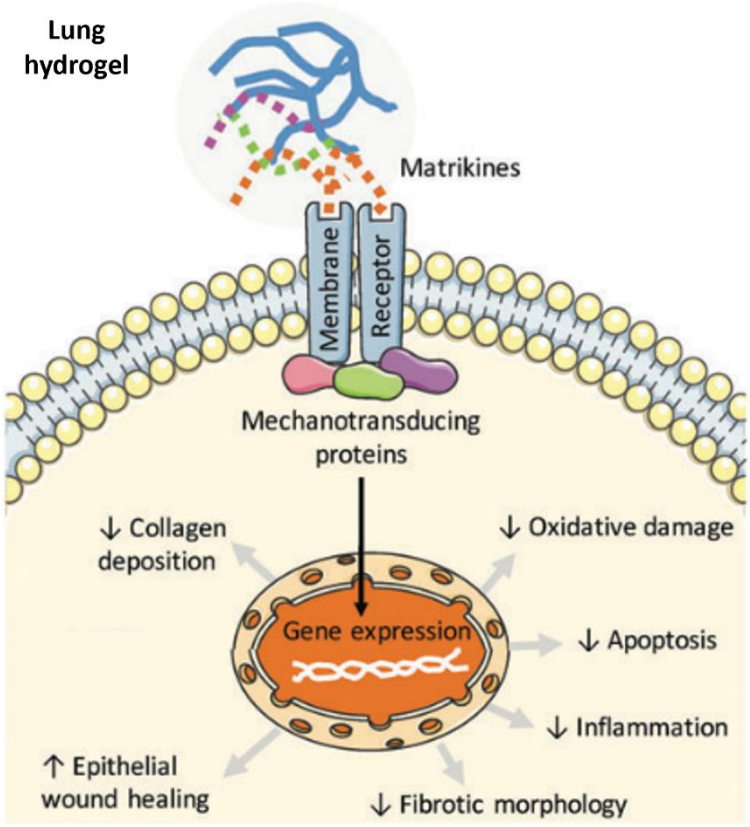

Figure 10. Proposed mechanism for extracellular matrix - derived hydrogels protection in acute respiratory distress syndrome. *Matrikines, created during the extracellular matrix digestion step to generate lung hydrogels, bind to receptors on the cell membrane. These receptors interact with mechanotransduction proteins that modulate gene expression and lead to different biological protecting effects. Adapted from* (132).

Instillation of the Lung Hydrogel for the Treatment of Acute Distress Respiratory Syndrome

In the last years, there has been a development in the use of decellularized ECM for tissue engineering applications. Although the use of the decellularized tissue as a physiomimetic substrate is evident, ECM-based therapies are promising novel strategies for regeneration/repair of the lung and for treating severe lung diseases. Following the tissue decellularization, the obtention of hydrogels is possible and the inherent fluidity of the pre-gel solutions allows for a variety of administration methods, such as instillation and nebulization (91). This is particularly advantageous for applying ECM-derived hydrogels to lung-related conditions. As early stated, it seems that ECM hydrogels could be used as a therapy since they can also release bioactive molecules by which the cells can interact.

Since the first ECM digested preparation to treat lung disorders was synthesised 14 years ago (119), there has been total of 3 more preclinical attempts to treat lung related conditions (91,118,133) , and only 2 in cases of lung injury (91,118). More specifically, the administration of the L-HG has been performed via instillation and nebulization (91). Notwithstanding, the first ECM-preparation used to treat a lung disorder was from urinary bladder at a pepsin digested concentration of 10mg/ml by intratracheal instillation. Its administration significantly reduced fibrosis in a bleomycin fibrosis mice model. It also protected against pulmonary injury (119). The following studies in ALI models showed that lung ECM-derived hydrogels protect against lung injury, potentially by reducing inflammation, and oxidative damage (91,118). The latest preclinical study that uses L-HG have also shown promising therapeutic advantages for alleviating lung fibrosis in a bleomycin rat model (133). The study indicates that the application of L-HG has the potential to impact processes related to tissue healing, the control of inflammation, restructuring of the cytoskeleton, and the cellular reaction to injury.

While several studies have presented preclinical indications of the therapeutic potential of ECM-derived hydrogel in animal models of lung diseases (Table 2), up until now, there is no clinic trial involving human participants employing L-HG.

Overall and given the current clinical demands of the COVID-19 pandemic, it appears clear that there is a need to enhance preclinical understanding and efficacy of L-HG therapy for treating ARDS.

Table 2. *Extracellular matrix - derived hydrogels used to treat lung diseases in preclinical in vivo experimentation (ALI, Acute Lung Injury; EMT, Epithelial – mesenchymal transition).*

Tissue	Disease model	Administration	Concentration	Outcome	Reference
Urinary Bladder	Bleomycin-induced Idiopathic pulmonary fibrosis	Intratracheal instillation	10 mg/mL 280 μg powder	Epithelial cell chemotaxis and reepithelization	(119)
Lung	Hyperoxia-induced ALI	Nebulization and Intratracheal instillation	3.2 mg/mL	Reduced hyperoxia-induced apoptosis and oxidative damage	(91)
	Radiation-induced ALI	Intratracheal instillation	10 mg/mL	Reduced inflammation, oxidative damage and EMT	(118)
	Bleomycin-induced Idiopathic pulmonary fibrosis	Intratracheal instillation	1 and 2 mg/mL	Reduced lung inflammation and oxidative damage	(133)

3. Therapeutic Effects of Mesenchymal Stromal Cells-Derived Extracellular Vesicles

The exact mechanism by which MSCs reduce lung inflammation and injury remains unknown. However, it involves several paracrine pathways influenced by the release of soluble factors, extracellular vesicles (EVs), and/or organelle transfer (134). Among the different EVs secreted by MSCs, exosomes are small vesicles typically measuring 30–100 nm in diameter. They are key mediators of cellular communication (135) through the transfer of proteins, lipids, and nucleic acids (136). Exosomes from MSCs have potent properties in immune modulation, signal transduction, tissue repair, and drug delivery. They have minimal immunogenicity and a proven therapeutic effect in numerous lung conditions (137-139).

Since MSCs can be derived from various sources, MSC-exosomes also originate from multiple sources such as bone marrow, adipose tissue, lungs and the human umbilical cord cells. While MSCs from different sources may possess slight variations in properties, they all contribute to tissue repair (140). Exosomes released from MSCs are capable of suppress pro-inflammatory factors, decrease cell apoptosis, promote cell proliferation, and mitigate oxidative stress (141) (Figure 11).

The use of MSCs supernatants, particularly their exosomes, instead of MSCs themselves offers significant advantages in the design of novel therapies. These advantages include:

- Elimination of the risk of neoplasia.
- Elimination of the risk of embolism.
- Ready to use in case of urgency.
- Ability to customize the dosage for each patient.
- Flexibility to stop the treatment at any time.
- No risk of immune rejection.
- Isolation of specific types of exosomes based on the lung disease being treated.

Due to these reasons, there is a growing interest in the use of exosomes and secretome products released from MSCs as a potential treatment for lung-related conditions and other diseases. Preclinical models of lung diseases have shown that the administration of

medium from MSCs have protective effects similar to those of the MSCs themselves (134). In the context of ARDS, studies have already demonstrated that the secretome derived from MSCs can improve ALI in mice (142).

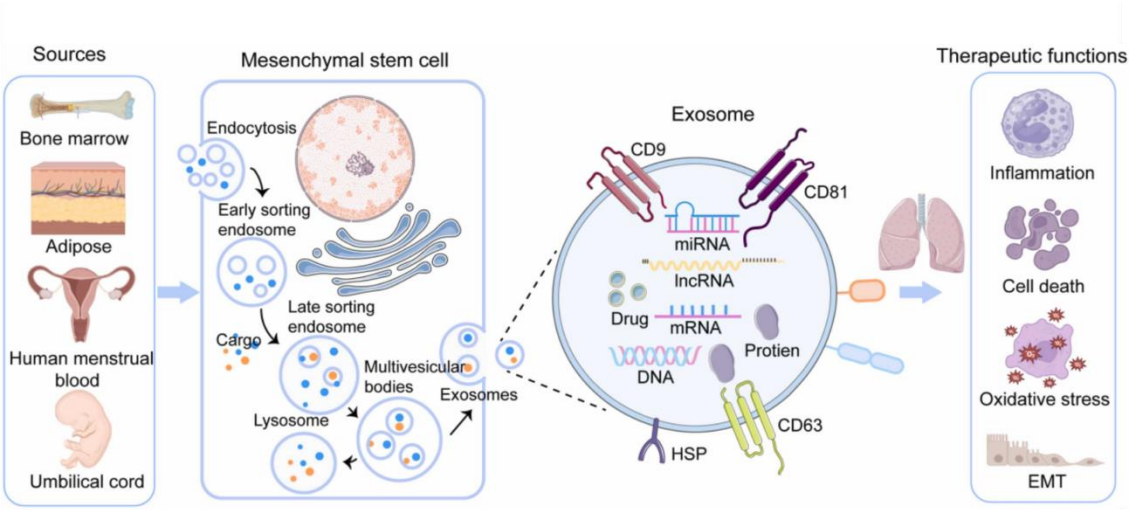

Figure 11. Mesenchymal stromal cell-derived exosomes for the treatment of lung diseases. *Exosomes are released by mesenchymal stromal cells (from the bone marrow, adipose tissue, human menstrual blood and umbilical cord) via the endosomal pathway, with membrane proteins CD9, CD81, and CD63 recognized as exosome markers. Exosomes contain abundant proteins and nucleic acids. Their therapeutic mechanism involves inflammation reduction, attenuation of cell death, mitigation of oxidative stress, and inhibition of epithelial-mesenchymal transition (EMT). Adapted from* (143).

Remarkably, MSC-derived exosomes appear to play an active role in ARDS recovery processes (144). Several studies have demonstrated the therapeutic potential of the administration of MSC-derived exosomes through inhalation or intravascular routes. For instance, in cases of ALI induced by *E. Coli* llipopolysaccharide (LPS) endotoxin, intratracheal instillation of MSC-derived exosomes improved pulmonary edema and preserved the integrity of the alveolar-capillary barrier with a reduced neutrophil infiltration and inflammation (111,144-148). Similarly, the human MSC-derived exosomes administration to mice with pneumonia mitigate the inflammatory response (149). In a mouse model of sepsis, the intravenous administration of MSC-derived exosomes significantly reduced the levels of inflammatory mediators (150). Also, these exosomes have shown positive effects on endothelial cells, improving permeability induced by LPS from *E.Coli*, reducing endothelial cell apoptosis, and modulating cytokine production (151). Furthermore, in a clinical cohort study with severe COVID-19 patients with moderate-to-severe ARDS, intravenous administration of EV's derived from bone marrow

MSCs reduced the elevated neutrophil count and improved patients' oxygenation status (152). Remarkably, MSCs can be preconditioned to enhance the synthesis of highly therapeutic soluble factors. For instance, treatment with the TLR-3 agonist has been shown to boost the therapeutic potential, immunomodulatory behavior, and antimicrobial activity of MSC-derived exosomes (153-155).

Nevertheless, the precise mechanisms by which preconditioning factors such as the use of physiomimetic substrate for cell culture can enhance the therapeutic potential of MSC-derived exosomes remain largely unknown.

4. Aging Effects on the Extracellular Matrix

Lung function is crucial for a healthy aging process and good life expectancy. A decline in pulmonary capacity increases the probability of illness and/or death from both respiratory and non-respiratory causes (156). As the lungs age, there is a decrease in the alveolar surface area together with an enlargement of alveoli and airspace dimensions (157).

The increase of aged population in developed countries prompt the need to comprehend the alterations that happen in the human lungs as humans age. It is crucial to investigate which are the factors associated with aging that could be targeted for therapeutic interventions to mitigate morbidity and mortality among the elderly (158). Respiratory conditions exhibit greater risks for older adults, with mortality rates 20-times higher for over 80 years old individuals compared to those in their 50s (159). Although advanced age constitutes the primary risk factor for chronic lung conditions, the primary mechanisms responsible for the aging process in the lung remain unidentified (160).

The cells and the ECM that form the lung airways and the lung epithelium from aged individuals show deficiencies in both composition and structure (Figure 12). The decline in the pulmonary function is a compilation of failures in both cell-intrinsic and external processes. In order to maintain an efficient gas exchange between the alveoli and the blood vessels, the ECM integrity needs to be preserved trough the aging process. Initial research conducted in both humans and rodent models in the lung ECM composition presented inconsistent findings. Some data indicated age-related increase in collagens and other ECM proteins, while others suggested declines (161,162).

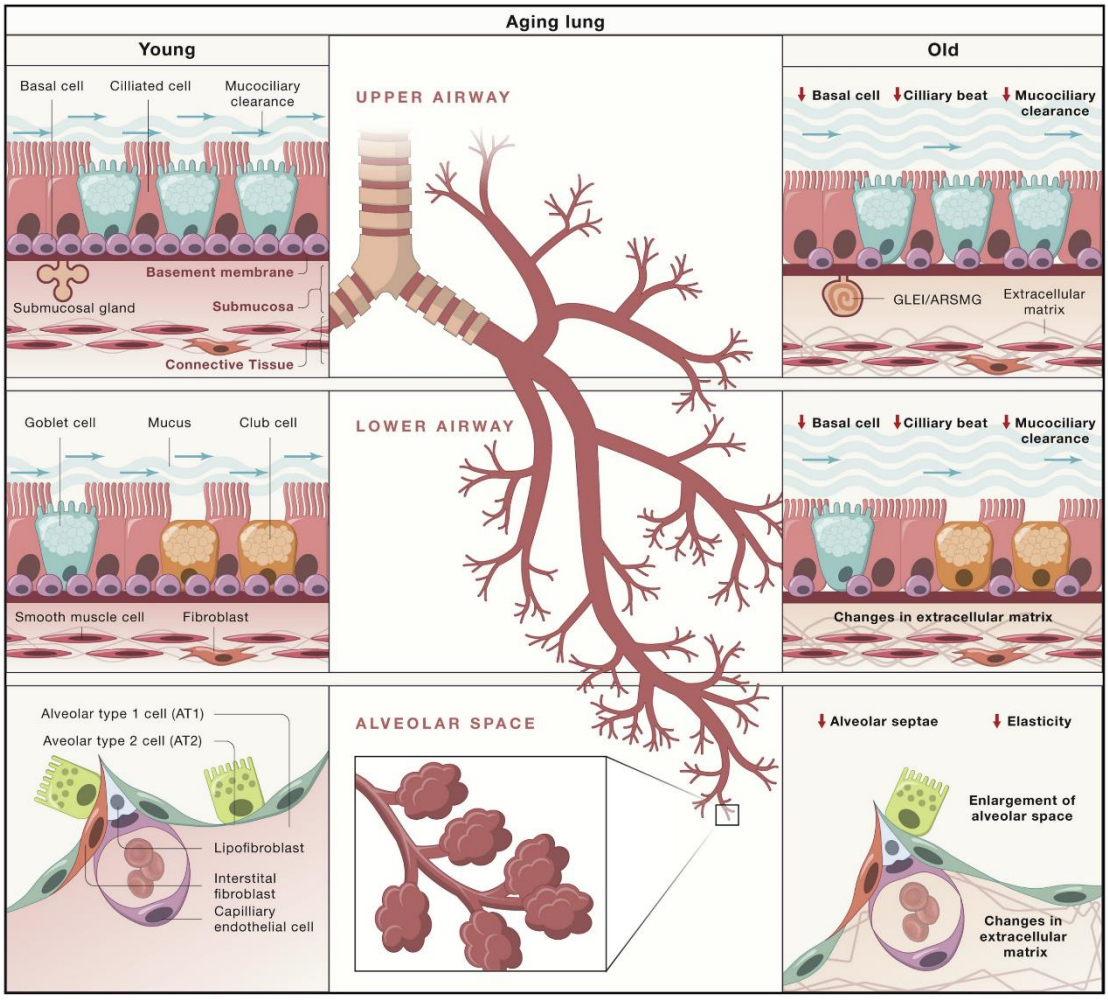

Figure 12. Cellular composition and functional changes in the aging lung. *Schematic representation of changes in young (left) and aged (right) lung show major changes in cellular composition and structure by anatomic region. Adapted from* (163).

Changes in the composition of ECM caused by aging can impact the mechanical properties of the airways and alveoli, leading to stiffening of the aging lung ECM (64,90) and contributing to an increased airway resistance and decreased lung compliance. In fact, the composition of the ECM determines its mechanical attributes (8). Accordingly, Godin et al. suggested that age-related alterations in ECM protein expression of laminin, elastin, and fibronectin, contribute to stiffening of the aged lungs (164). Consistently, Melo et al. studies utilizing atomic force microscopy (AFM) in FV inflated decellularized lungs from young and aged mice report a tendency of increase in local stiffness (66). However, there are conflicting findings, some studies report age-related increase in stiffness in lung parenchymal and vessel compartments (63) and others suggest a decrease (64). Consequently, the available data are inconclusive. Understanding the changes in the ECM

components with age is crucial since variations in the elastic properties of the human lung drastically influence lung function.

Recently, it was observed that stretch can induce strain-softening of acellular fibrotic lungs at the nanoscale (165), emphasizing the significance of conducting such measurements under physiomimetic conditions. Conversely, the majority of existing studies aimed to assess the biomechanical characteristics of the aging lung were conducted at RV (63,64) since the lung collapse upon removal. Whether mechanical measurements using residual (non-inflated), or functional volumes (inflated) provide consistent results in aging research remains also uncertain.

Chapter II.

HYPOTHESIS AND OBJECTIVES

According to the background previously explained, the hypotheses of this thesis are:

1. The ECM lung-derived hydrogels will release bioactive therapeutic molecules which could interact with epithelial alveolar cells.

2. Physiomimetic hydrogels derived from decellularized lungs will provide a most realistic substrate for culturing MSCs which will enhance the therapeutic effects of their secreted vesicles.

3. Therapeutic intratracheal administration of lung derived hydrogel will ameliorate the pulmonary outcomes and reduce the physiologic changes in an ALI rat model.

4. Aging has important implications in the ECM composition and stiffness, potentially modulating the behaviour of pulmonary cells and increasing the susceptibility to chronic lung diseases.

5. The difference in ECM composition during aging will affect the ECM stiffness at different level of tissular strain.

Therefore, in order to improve therapies in severe respiratory diseases, the general aim of the project is to characterize the ECM - based approaches to be used for better understanding and outcome in ARDS.

Specific aims

I. To characterize the proteins produced during the development of L-HG and released at different times and how they impact alveolar epithelial cells immunoresponse and migration capacity.

II. To characterize the secretome/EV's of MSCs cultured in conventional flasks and on lung hydrogels and to test the therapeutic effects of both EVs released

from MSCs and/or ECM-vesicles from lung-derived hydrogel in a wound-healing experimental model of lung repair.

III. To assess whether ARDS therapy can be improved by using L-HG for intratracheal instillation on an *in vivo* LPS – induced ALI model compared to the cellular approach using MSCs.

IV. To investigate how aging affects the composition and stiffness of the lung ECM and how it can modulate its crosstalk between MSCs.

Chapter III.

ARTICLES IN THIS THESIS

The scientific articles included in this thesis are here listed in relation to the aims of the thesis:

Aim I: To characterize the proteins produced during the development of L-HG and released at different times and how they impact alveolar epithelial cells immunoresponse and migration capacity.

- Herranz-Díez C, **Ulldemolins A**, Farré R, Gavara N, Sunyer R, Almendros I, Otero J. Matrikines Released from Pepsin-Digested Lung Extracellular Matrix Hydrogels: Considerations for the in vitro Study of the Alveolar Epithelium. Manuscript in preparation.

Aim II: To characterize the secretome/EV's of MSCs cultured in conventional flasks and on lung hydrogels and to test the therapeutic effects of both EVs released from MSCs and/or ECM-vesicles from lung-derived hydrogel in a wound-healing experimental model of lung repair.

- **Ulldemolins A,** Jurado A, Herranz-Diez C, Gavara N, Otero J, Farré R, Almendros I. Lung Extracellular Matrix Hydrogels-Derived Vesicles Contribute to Epithelial Lung Repair. *Polymers*. 2022; 14(22):4907. Published 2022 Nov 14. IF = 5.0 Q1.

Aim III: To assess whether ARDS therapy can be improved by using L-HG for intratracheal instillation on an in vivo LPS – induced ALI model compared to the cellular approach using MSCs.

- **Ulldemolins A**, Jurado A, Otero J Farré R, Almendros I. Physiomimetic lung extracellular matrix hydrogel enhances pulmonary recovery in a rat model of acute respiratory distress syndrome. Preliminary results.

Aim IV: To investigate how aging affects the composition and stiffness of the lung ECM and how it can modulate its crosstalk between MSCs.

- **Ulldemolins A,** Narciso M, Sanz-Fraile H, Otero J, Farré R, Gavara N, Almendros I. Effects of aging on the biomechanical properties of the lung extracellular matrix: Dependence on tissular stretch. Frontiers in Cell and Developmental Biology. 2024;12. Published 2024 April 5, IF = 5.5 Q1

Chapter IV.

MATRIKINES RELEASED FROM PEPSIN-DIGESTED LUNG EXTRACELLULAR MATRIX HYDROGELS: CONSIDERATIONS FOR THE IN VITRO STUDY OF THE ALVEOLAR EPITHELIUM

Matrikines Released from Pepsin-Digested Lung Extracellular Matrix Hydrogels: Considerations for the *in vitro* Study of the Alveolar Epithelium

Carolina Herranz-Díez[1+], Anna Ulldemolins[1+], Ramon Farré[1,2,3,5], Núria Gavara[1,4,5], Raimon Sunyer[1,5,6], Isaac Almendros[1,2,3] and Jorge Otero[1,2,4,5*]

[1]Unitat de Biofísica i Bioenginyeria, Universitat de Barcelona, Barcelona, Spain. [2]CIBER de Enfermedades Respiratorias (CIBERES), Madrid, Spain. [3]Institut d'Investigacions Biomèdiques August Pi i Sunyer (IDIBAPS), Barcelona, Spain. [4]The Institute for Bioengineering of Catalonia (IBEC), Barcelona, Spain. [5]Institute of Nanoscience and Nanotechnology (IN2UB), Universitat de Barcelona, Barcelona, Spain. [6]CIBER de Bioingeniería, Biomateriales y Nanomedicina (CIBER-BBN), Madrid, Spain.

[+]Carolina Herranz-Diez and Anna Ulldemolins contributed equally to this article.

[*]Correspondence.

ABSTRACT

Background: Scaffolds based on extracellular matrix hydrogels are nowadays the most promising physiomimetic environments for culturing cells. These hydrogels are produced by the digestion of decellularized tissues by using pepsin from the porcine gastric mucosa, a process known to produce matrix fragments that are further released from the structures. The impact of these matrikines in cell response is starting to be unravelled, so it is important to consider them when conducting experiments using pepsin-digested hydrogels. In the present work, we have characterized the matrikines released by lung extracellular matrix hydrogels and how they impact alveolar epithelial cells response.

Methods: Extracellular matrix hydrogels were produced by the digestion of decellularized porcine lungs and incubated at 37 °C. Hydrogel structural changes were measured by electron microscopy while protein release was quantified by bicinchoninic acid assay. Composition of the hydrogel and released products were studied by proteomic analysis using liquid chromatography-mass spectrometry. The effect of the released matrikines in

the inflammatory and migratory response of ATII-like rat lung epithelial cells was tested by RT-qPCR and wound healing assays respectively.

Results: Analysis of the initial composition of the hydrogel revealed the presence of a high number of non-matrix proteins which were being released mostly during the first week, confirmed by the observation of a reduction of the fibre size with time. Released matrikines at day 1 showed to have a clear inflammatory effect in the cells that was not observed with matrikines released at day 7. Noteworthy, an increased migratory capacity was also observed with matrikines from day 1 and the effect was preserved with the matrikines from day 7. Proteomic analysis revealed that there are several matrikines that are not anymore present at day 7 that are related with the inflammatory response, while basement membrane-associated matrikines are still being released at day 7 so they may be influencing cell adhesion and migration.

Conclusions: Many efforts have been focused on the characterization of the composition of scaffolds produced of extracellular matrix hydrogels to understand the response of the cells cultured on them. Our results showed that a deep understanding of what is being released from these hydrogels is also necessary to analyze the experiments conducted. Matrikines generated during the production of decellularized lung hydrogels have an inflammatory effect in alveolar epithelial cells, which can be mitigated by incubating the scaffolds for one week prior to seeding the cells. Nevertheless, there are several other matrikines that are still being released at that point that may be influencing different cellular processes, such adhesion and/or migration, as confirmed by the wound healing assays presented herein.

Keywords: extracellular matrix, decellularization, hydrogel, lung, inflammation, migration, matrikines, pepsin digestion.

BACKGROUND

The extracellular matrix (ECM) is a network composed by complex and active proteins and other biomolecules (1). It provides a framework for the cells and maintains the architecture and physico-chemical properties of the tissues (2). The ECM is known to be not only supportive but to interact with specific cell receptors to influence cell growth,

proliferation, differentiation, and function (3,4). The use of scaffolds based on tissue-specific ECM allows the study of cellular mechanisms in a more realistic scenario (5). ECM can be obtained from different sources by decellularization (6) of organs and/or tissues, and it can be used directly as scaffold or digested and reconstituted in the form of hydrogels (7). These latter are of special interest to develop scaffolds from heterogeneous and holey organs such as the lung (8).

Since the first natural lung ECM derived hydrogel was synthesized (9), numerous applications have been described (i.e. design of lung on-a-chip models, disease models, alveolar epithelial progenitor cells differentiation) (10-16). Lung ECM hydrogels (L-HG) are three-dimensional networks of hydrophilic polymers and represent nowadays the scaffolds which better mimic the lung native environment while preserving specific chemical and biochemical cues (9). On this way, there is a growing interest to understand how the physico-chemical properties of the developed L-HG impact the response of the cells (13,17-20). ECM hydrogel formation requires significant processing steps, including freeze-drying, milling in liquid N_2 to form a powder, and acid solubilization based on the digestion with pepsin from porcine gastric mucosa (21). Pepsin is a non-specific protease which cleaves peptide bonds in the protein backbone following aromatic residues (i.e., Tryptophan, Tyrosine, Phenylalanine) which is needed due to the acid-insoluble nature of certain ECM proteins. Pepsin's non-specific nature causes some other ECM proteins to be broken down as well, depending on the digestion time and particle size used to produce the L-HG (14). Proteins such as collagen, laminin, elastin, and hyaluronic acid may be fragmented by pepsin during digestion, thus producing small bioactive peptides, known as matrikines (22). It is then well reported that produced matrikines may impact several responses of the cells (Table 1).

Table 1 Described lung extracellular matrix matrikines and its effects. PMN, Polymorphonuclear neutrophils.

ECM Protein	Matrikine	Action	References
Collagen	Pro-Gly-Pro (PGP) peptide	Vascular permeability	(23, 24)
	N-ac-PGP	PMN influx	(25)

	Tumstatin	Anti-angiogenic, Anti-inflammatory	(26)
Elastin	Val-Gly-Val-Ala-Pro-Gly (VGVAPG) peptide	Monocyte influx	(27,28)
Proteoglycan	Low – molecular weight hyaluronan Endorepillin	Inflammation, wound repair Modulates angiogenesis	(29) (30)
Fibronectin	P1-P5 peptides	Increase MMP9,12, IL-1, IL-6, TNFa	(31)
Laminin	γ2 ectodomain A13 peptide C16 peptide	Epithelial proliferation, wound repair, alveologenesis Wound repair Wound healing, angiogenic	(32,33) (34) (35)

There is evidence that matrikines generated during the production of L-HG by pepsin digestion may be impacting the cells that are further cultured within the scaffolds. Nevertheless, the information about these matrikines and their impact in the cells is still scarce. There is a need for a better understanding of what matrikines are being released from the L-HG and which their effect on the cultured cells is. In the present work, we aim to characterize the matrikines produced during the development of L-HG and released at different times. We aim also to study how these matrikines impact alveolar epithelial cells immunoresponse and migration capacity.

MATERIALS AND METHODS

All the reagents were obtained from Sigma Aldrich, Missouri, USA unless otherwise specified.

Preparation of the Lung ECM-Derived Hydrogels

Porcine lungs were obtained from a local slaughterhouse and decellularized as previously described (19). Lungs were perfused through the trachea and the vasculature with 0.1% Triton X-100, sodium deoxycholate, DNase and 1 M sodium chloride, with intermediate perfusion with distilled water and PBS for rinsing purposes. To assess the effectiveness of decellularization, total genomic DNA was isolated using the PureLink Genomic DNA kit (ThermoScientific, Waltham, MA, USA) from native and decellularized scaffolds following

the manufacturer's instructions. The total amount of DNA was quantified using spectrophotometry and normalized to the sample tissue dry weight. The amount of remaining DNA was below the accepted threshold of 50 ng/mg for successful decellularization. Decellularized ECM was drained of excess water, freeze-dried in pieces, and lyophilized (Telstar Lyoquest55 Plus, Terrassa, Spain). Afterwards, the sample was pulverized into micron-sized particles at −180 °C by using a cryogenic mill (6755, SPEX, Metuchen, NJ, USA) for 5 min at maximum speed. The resulting powder was digested at 20 mg/mL concentration in a 0.01 M HCl solution with pepsin from porcine gastric mucosa (1:10 concentration) under magnetic stirring at room temperature for 16 h. The resulting (pregel) solution was then pH-adjusted to 7.4 (±0.4) by using 0.1 M NaOH and PBS 10X and frozen at −80 °C for subsequent use.

Determination of the passive release of species from the lung hydrogel

L-HGs were thaw and seeded on 24 well-plates. Once gellified, they were incubated in PBS 1X at 37 °C. Supernatant was collected at 1,2,3,4,7,14, and 21 days replaced with fresh PBS 1X at each time point. The protein release was quantitatively assessed by bicinchoninic acid assay assay according to manufacturer's protocol (Thermo Fisher Scientific, Waltham, MA, USA).

Scanning electron microscopy

The ultrastructure of L-HG was visualized with a JSM-6510 (JEOL, Tokyo, Japan) scanning electron microscopy (SEM). L-HG scaffolds were fixed in 4% paraformaldehyde (PFA) in PBS 1X for 48 h and then washed three times with 0.1M phosphate buffer (PB). Next, the samples were incubated in 4% osmium tetroxide for 90 min and then rinsed with deionized water. Subsequently, samples were dehydrated by washing them with ethanol 80% (x2), 90% (x3), 96% (x3), and 100% (x3) and preserved in absolute ethanol at 4 ℃ until critical point drying (Au-tosamdri-815 critical point dryer, Tousimis, Rockville, MD, US). Samples were then carbon coated and mounted using conductive adhesive tabs (TED PELLA, Redding, CA, US). Imaging was performed by using an SEM (JSM-6510, JEOL, Tokyo, Japan) at 15 kV.

The diameter of the fibres was assessed following the method developed in (36). Ten fibres of three different zones of each sample were randomly selected, and their diameter was computed with ImageJ Software (National Institute of Health, Bethesda, MD, US).

Inflammatory response

Alveolar type II-like Rat Lung Epithelial cells (RLE) (RLE-6TN, CRL-2300, ATCC) were used for experiments. Cells were cultured and expanded following manufacturer's instructions. For studying the expression of inflammatory cytokines after the exposure of the released L-HG proteins, RLE were cultured on TCP conditions at density of $2{\cdot}10^5$ cells/cm^2. When the confluency was reached, the L-HG supernatant collected from day 1 (L-HG D1) and after a week (L-HG D7) was added to the cells. An inflammatory hit consisting of Lipopolysaccharide (LPS) endotoxin from *Escherichia Coli* (O128:B12, Sigma) was also added at a concentration of 1 µg/mL and a control without L-HG was kept on parallel. RNA was subsequently extracted from samples by employing the RNeasy kit (Qiagen, Hilden, Germany). The cDNA was obtained by a reverse transcription-polymerase chain reaction (TaqMan Reverse Transcription Reagents, Invitrogen, Waltman, MA, USA) according to the manufacturer's instructions. The expression level of Interleukin 6 (IL-6) and tumor necrosis factor- α (TNFα) was studied using the Taqman Fast Advanced Master Mix and the TaqMan Gene Expression Assays in a StepOnePlus thermocycler (Applied Biosystems, Waltham, MA, USA). The expression level of genes was normalized to the constitutively expressed gene PPIA and calculated using the $2^{-\Delta\Delta Ct}$ method (37).

Wound Healing Assay

The wound closure on RLE after the exposure of L-HG supernatant was assessed by following the protocol presented in (38). Briefly, a density of $2{\cdot}10^5$ cells/cm^2 were seeded on top of TCP wells until reach confluency. Then, the epithelial cell monolayer was scratch-wounded using a sterile 200-µl pipette tip (Eppendorf, Hamburg, Germany), and cell debris was removed by washing with PBS 1X. Subsequently, PBS was discarded and replaced by L-HG supernatant collected from day 1 (L-HG D1) and after a week (L-HG D7). For any given condition, a parallel control group was included for further normalization of the wound healing rate, and a group with an LPS hit to study the migration under

inflammatory stress. For each experimental group, the wound healing measurements were carried out on 3 different days in triplicate (n = 3/experimental group).

The wound area was measured immediately after the performance of the scratch (0 h) and at the end of the experiment (24 h). Phase contrast images were recorded with an inverted microscope (Eclipse Ti, Nikon Instruments, Amsterdam, The Netherlands) equipped with a camera (C9100, Hamamatsu Photonics K.K., Hamamatsu, Japan) and a 10X objective. Wound closure was evaluated by utilizing ImageJ software to compare the initial and final areas of each epithelial wound. An impartial researcher used the freehand selection tool to mark the edges in all the images and calculate the respective areas. The percentage change between the initial and final measurements was then calculated to determine the extent of wound closure.

Proteomics

Proteins released from the L-HG were analyzed in a nanoAcquity liquid chromatographer (Waters) coupled to an LTQ-Orbitrap Velos (Thermo Scientific) mass spectrometer by the Proteomic Unit from Scientific and Technological Centers (CCiTUB), Universitat de Barcelona, using standardized proprietary methods. Briefly, the proteins present in the supernatants were precipitated and the pellets and the supernatants were analyzed. Both pellets and supernatants were resuspended in 1% formic acid solution and an aliquot per sample was injected for chromatographic separation. Peptides were trapped on a Symmetry C18TM trap column (Waters) and were separated using an ACQUITY UPLC BEH column (Waters). The raw data files obtained in the mass spectrometry analyses were used to search against a modified version of the public database SwissProt Plants, with a small database containing laboratory contaminants. Database search was performed with SequestHt search engine using Thermo Proteome Discover (v.2.5).

Statistical analysis

Fibre sized data was analyzed by Mann-Whitney test. Inflammation and wound healing data were analyzed by one way ANOVA with post-hoc Tukey. Statistical significance was considered for p-value < 0.05. In the figures, * indicates $p < 0.05$, ** indicates $p < 0.01$ and *** indicates $p<0.001$.

RESULTS

Passive release of species from the hydrogel and its effect in the L-HG mesh structure

The protein release presented a peak after 24 hours of L-HG preparation followed by a reduction until day 7 (Figure 1A). After one week, the matrikine release was negligible. The fibre diameter was quantified by ImageJ software, and it was observed a reduction of approximately 30% of the diameter of the fibres when the L-HG was 21 days incubated in PBS (Figure 1D). Although the fibres diameter size, the mesh structure typical of the ECM was maintained (Figure 1B, C).

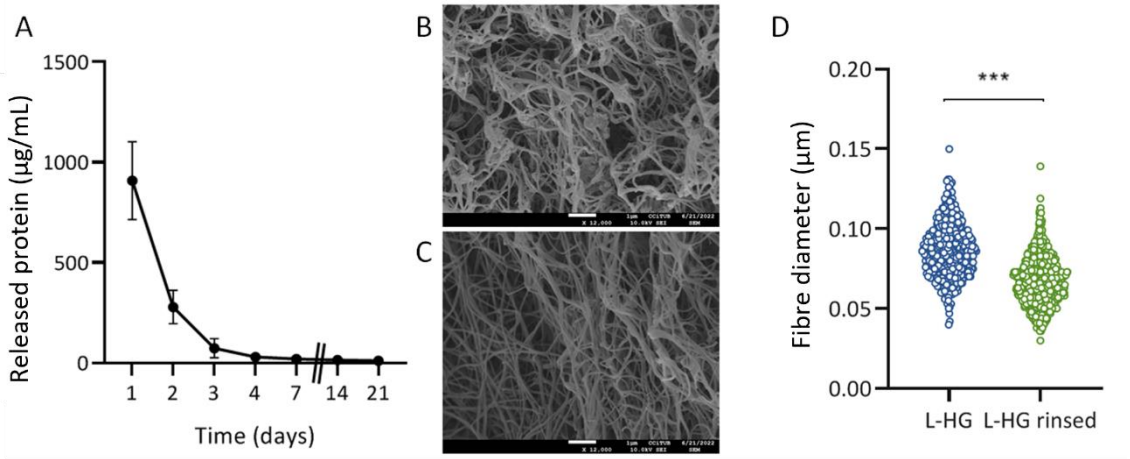

Figure 1. (A) Protein release from the L-HG for 21 days (n = 6). (**B)** L-HG structure assessed by SEM at day 1 of the formation and **(C)** after 21 days. **(D)** Quantification of the fibre diameter of the L-HG mesh structure at day 1 of the formation (blue) and at day 21 (green).

Matrikines released early from the L-HG promoted alveolar cells inflammation

The expression of IL-6 and TNF-α showed a 46-fold and 61-fold increase respectively when the epithelial cells were cultured with the supernatant of the L-HG collected at the first day of release (Figure 2). Noteworthy, this response was also higher than the one induced by the LPS hit. As it is shown in the Figure 2, this high inflammatory response was not observed when cells were subjected to matrikines from day 7.

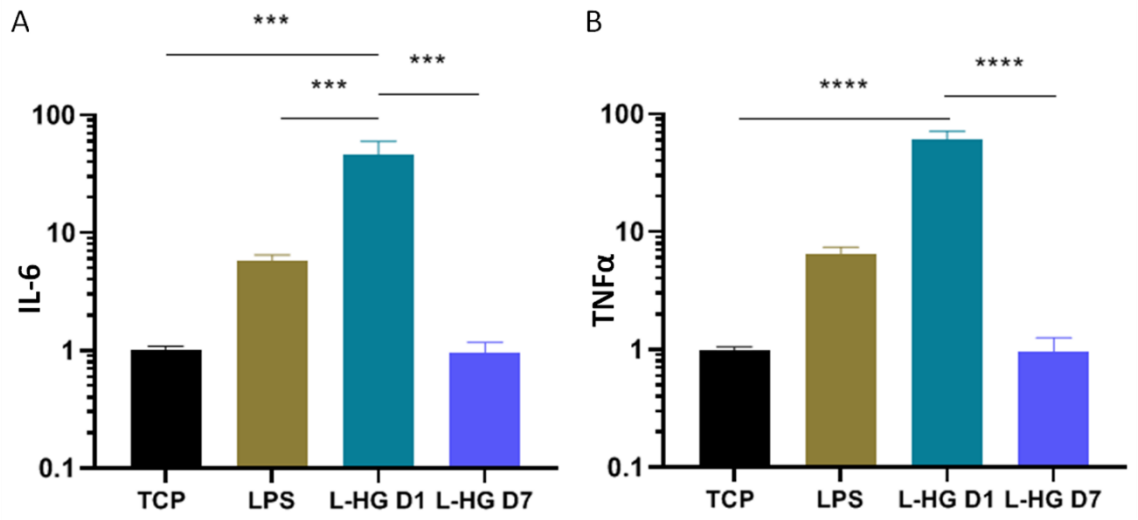

Figure 2. Rat lung epithelial cell inflammatory markers expression **(A)** IL-6 and **(B)** and TNF-α 24h after adding matrikines released at day 1 (L-HG D1), at day 7 (L-HG D7) from lung hydrogels or LPS to the cultures. Normalized by the expression under control conditions.

Matrikines released by the L-HG impacted cell migration

When cells were exposed at the matrikines released by the L-HG at both day 1 and 7 after the HG formation, the wound closure ratio of the lung epithelial model was significantly increased (1.89-fold and 1.76-fold increase respectively) (Figure 3). No differences were observed with the group where the LPS hit were applied.

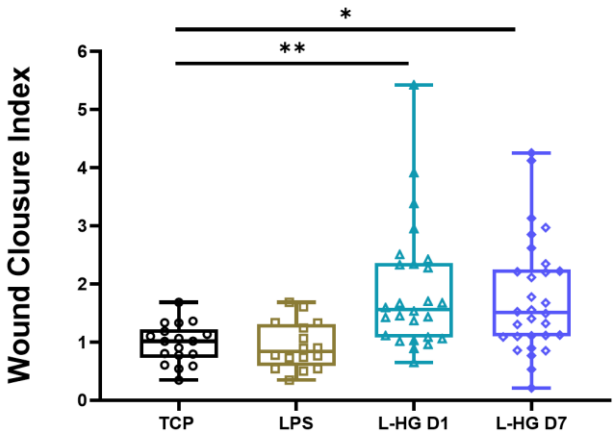

Figure. 3 Wound closure of rat lung epithelial cells at 0h and 24h when LPS and matrikines released at day 1 (L-HG D1) and day 7 (L-HG D7) from lung hydrogels were added

Proteomics analysis

The composition of the ECM L-HG was assessed by liquid mass spectrometry. A total of 181 proteins were detected and they were grouped according to matrisome classification (Figure 4A). Mainly there are collagens and glycoproteins, as well as a big percentage of non-ECM proteins, which should be residuals of the decellularization. Comparing the composition of the released species at days 1 and 7 (Figure 4B), we found that there were 25 proteins exclusively released at day 1, 8 proteins released at day 7, and 107 proteins that are being released at both times. If we compare the localization of exclusive proteins at both times (Figures 4C and 4D) we can confirm that ECM-related proteins are maintained while cell-related proteins are much more present at early stages.

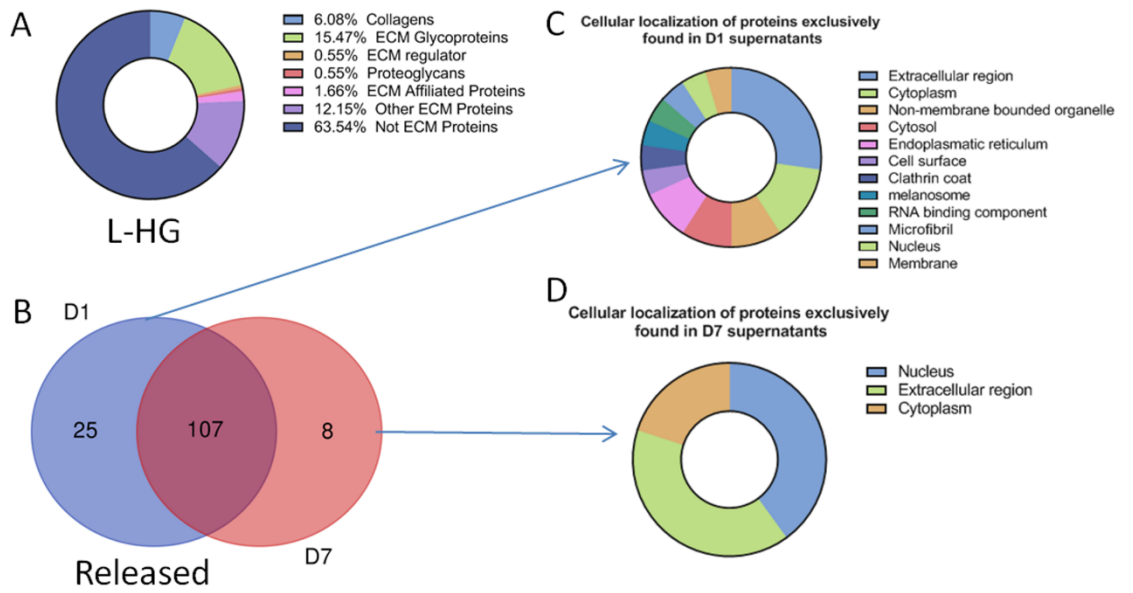

Figure 4. (A) Composition of the lung hydrogel (L-HG). **(B)** Venn diagram of the proteins detected with liquid mass spectrometry in the supernatant of L-HG at day 1 (D1) and day seven (D7), and identification of the localization of the exclusive proteins of **(C)** day 1 and of **(D)** day 7. Classification according to UniProt of the proteins detected in terms of cellular localization.

By looking at the abundances proteins that were released at both days 1 and 7 we can observe a huge heterogeneity (Figure 5A) in their release. If we focus on the proteins related with collagens, laminins and elastin that are known to be sources of matrikines in the lung (Figure 5B), there is a clear decrease in the release of most of them (note the collagen-α1 chain that is highly released early but almost not present at day 7) but for

certain collagens and laminin-α3. Looking at the proteins that present almost no variation in the release over time (Figure 5C), we can identify the proteins that will be acting on the cells even after 7 days of incubation.

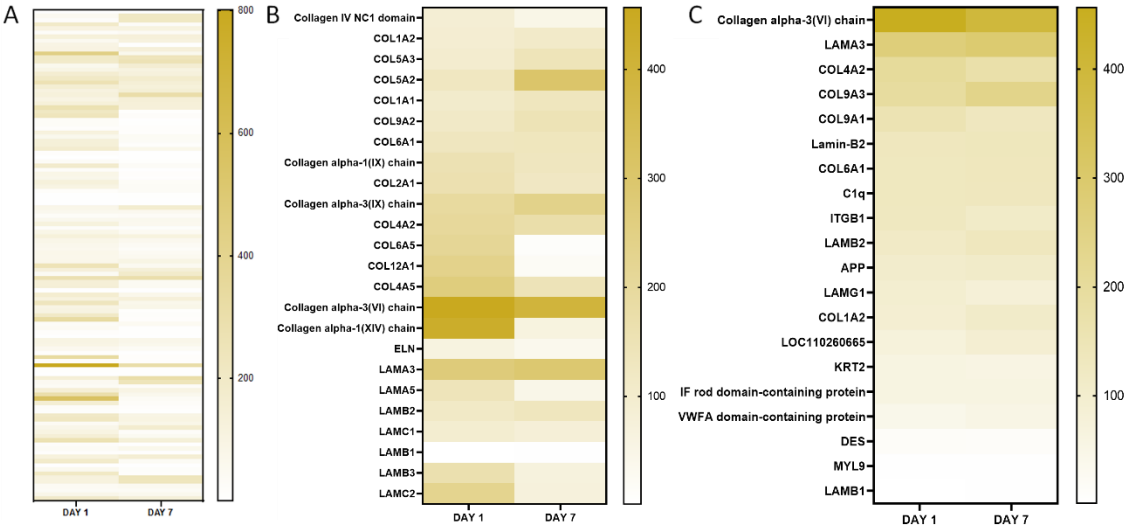

Figure 5. **(A)** Comparison of abundances of the 107 common proteins released from lung hydrogel both at days 1 and 7. (**B)** Abundances of proteins known as a source of matrikines in the lung found in the lung hydrogel release products at day 1 and day 7 **(C)** Abundances of common released proteins from the lung hydrogel with minor variations between days

DISCUSSION

The lung epithelium, acting as an important regulator and effector tissue, plays a crucial role in organizing the innate response to local damage (39). The epithelial cells are highly sensitive to their surroundings and act as an early warning system to initiate immune responses (40, 41). In this particular scenario, the matrikines released by the L-HG trigger a significant inflammatory reaction (Figure 2). Among the pro-inflammatory cytokines, IL-6 plays a crucial role in the transition to a reparative environment, which is essential for wound healing (42). Moreover, TNF-α induce the production of other cytokines and promotes alveolar epithelial repair (43,44). Both cytokines also activate the expression of adhesion molecules and stimulate growth. Our findings demonstrate the L-HG ability to promote cell migration (Figure 3) in concordance with recently published data (19). Interestingly, we observed that rinsing the L-HG for 7 days prior to its use effectively reduces the cell inflammatory response when cultured with L-HG released matrikines

(Figure 2). Indeed, the matrikine release peak is 24h after the formation of the L-HG (Figure 1A). Therefore, it indicates a clear relationship between matrikine presence and inflammation that regulates tissue repair pathways.

Among all the proteins secreted by the L-HG, the responsible actors may be the bioactive peptides. They are emerging from the digestion step of the L-HG formation, since pepsin cleaves peptic bonds next to aromatic amino acids such as phenylalanine, tryptophan, and tyrosine. Thus, because of the different enzyme specificity, the site of digestion will determine the type of peptides released, and consequently, their physiological properties (45).

When comparing all the proteomic data with all the already described matrikines found from lung ECM (Table 1), the predominant bioactive matrikine emerging from lung collagen at day 1 are Pro-Gly-Pro (PGP) fragments. While Pfister and colleagues were the first to show that PGP fragments possess potent neutrophil chemotaxis activity in an ocular injury model (46), it is now appreciated that PGP exhibits similar biological functions in the lung and various other tissues (47,48). More specifically, PGP may play an important role in facilitating wound repair and may restore demarcated airway epithelium as seen in Figure 3 and as already reported (23). Moreover, PGP-induced signalling is considered a feed-forward inflammatory signal (49). Other collagen fragment which is released at day 1 is collagen IV α5 chain, known as lamstatin. They have been implicated, together with the collagen IV α3 chain, known as tumstatin, in inhibiting pathological angiogenesis and suppressing proliferating endothelial cells and tumor growth (26,50,51). Together, collagen and elastin-derived matrikines further stimulate the recruitment of inflammatory cells to the lungs (52).

There are also proteins that present almost no variation in the release over time. Collagen VI-α3 chain, a pro-peptide called endotrophin, is equally released at day 1 and day 7. It is known to promote fibrosis and inflammation. Its effects include stimulating fibrosis, promoting endothelial cell migration, and enhancing macrophage infiltration into damaged tissue (53). Laminin-subunit α3 known to safeguard alveolar epithelial cells from the damaging effects of fibrosis, remains stable over time (54). By examining the sequence of peptides, various regions are identified as potential sites containing epidermal growth factor (EGF)-like domains linked to proliferation and migration (55,56). Moreover, it has

been described that Laminin α3 that contains angiogenic peptides (A13 an C16) that increase wound reepithelialization (34,35). Altogether, these peptides contribute to the prolonged epithelial migration effect from the L-HG release components.

These findings open a new window in the applications of lung derived hydrogels and the treatment of respiratory diseases. L-HG properties not only rely in their capacity to mimic the physiological environment in terms of topography and stiffness, but it also includes the biological cues and the ECM proteins released during physiological and pathophysiological processes. Further experiments are needed to identify other matrikines and clarify the specific role of lung-matrikines.

CONCLUSIONS

L-HG scaffolds are highly promising to study cell response under physiomimetic environments. Results presented in this work show that, as well as is of high importance to characterize the L-HG itself, it is necessary to take into account what is being released from these hydrogels. We observed that matrikines generated during the production of L-HG, and further released, have an inflammatory effect in alveolar epithelial cells. Interestingly, the inflammatory effect induced by the release of the L-HG disappeared after incubating the scaffolds for one week. Thus, this effect could be avoided if the L-HG is rinsed during one week prior to seeding the cells on top. Nevertheless, as observed by proteomic analysis, there are several other matrikines that are still being released at that point that may be influencing different cellular processes. In our experiments, we observed that migration capacity of the cells was sustained by the released matrikines after one week. From the data, we can conclude that the effect of the released matrikines should be either mitigated or at least taken into account when analyzing the results of experiments performed with L-HG scaffolds.

REFERENCES

1. Burgstaller, G., Oehrle, B., Gerckens, M., White, E. S., Schiller, H. B. and Eickelberg, O. (2017) 'The instructive extracellular matrix of the lung: basic composition and alterations in chronic lung disease', Eur Respir J, 50(1).
2. Suki, B. and Bates, J. H. (2008) 'Extracellular matrix mechanics in lung parenchymal diseases', Respir Physiol Neurobiol, 163(1-3), pp. 33-43.
3. Wagner, D. E., Bonenfant, N. R., Parsons, C. S., Sokocevic, D., Brooks, E. M., Borg, Z. D., Lathrop, M. J., Wallis, J. D., Daly, A. B., Lam, Y. W., Deng, B., DeSarno, M. J., Ashikaga, T.,

Loi, R. and Weiss, D. J. (2014) 'Comparative decellularization and recellularization of normal versus emphysematous human lungs', Biomaterials, 35(10), pp. 3281-97.

4. Busch, S. M., Lorenzana, Z. and Ryan, A. L. (2021) 'Implications for Extracellular Matrix Interactions With Human Lung Basal Stem Cells in Lung Development, Disease, and Airway Modeling', Front Pharmacol, 12, pp. 645858.
5. Kabirian, F. and Mozafari, M. (2019) 'Decellularized ECM-derived bioinks: Prospects for the future', Methods.
6. Guruswamy Damodaran, R. and Vermette, P. (2018) 'Tissue and organ decellularization in regenerative medicine', Biotechnol Prog, 34(6), pp. 1494-1505.
7. Wolf, M. T., Daly, K. A., Brennan-Pierce, E. P., Johnson, S. A., Carruthers, C. A., D'Amore, A., Nagarkar, S. P., Velankar, S. S. and Badylak, S. F. (2012) 'A hydrogel derived from decellularized dermal extracellular matrix', Biomaterials, 33(29), pp. 7028-38.
8. de Hilster, R. H. J., Sharma, P. K., Jonker, M. R., White, E. S., Gercama, E. A., Roobeek, M., Timens, W., Harmsen, M. C., Hylkema, M. N. and Burgess, J. K. (2020) 'Human lung extracellular matrix hydrogels resemble the stiffness and viscoelasticity of native lung tissue', Am J Physiol Lung Cell Mol Physiol, 318(4), pp. L698-L704.
9. Pouliot, R. A., Link, P. A., Mikhaiel, N. S., Schneck, M. B., Valentine, M. S., Kamga Gninzeko, F. J., Herbert, J. A., Sakagami, M. and Heise, R. L. (2016) 'Development and characterization of a naturally derived lung extracellular matrix hydrogel', J Biomed Mater Res A, 104(8), pp. 1922-35.
10. Marhuenda, E., Villarino, A., Narciso, M., Elowsson, L., Almendros, I., Westergren-Thorsson, G., Farré, R., Gavara, N. and Otero, J. (2022a) 'Development of a physiomimetic model of acute respiratory distress syndrome by using ECM hydrogels and organ-on-a-chip devices', Front Pharmacol, 13, pp. 945134.
11. Marhuenda, E., Villarino, A., Narciso, M. L., Camprubí-Rimblas, M., Farré, R., Gavara, N., Artigas, A., Almendros, I. and Otero, J. (2022b) 'Lung Extracellular Matrix Hydrogels Enhance Preservation of Type II Phenotype in Primary Alveolar Epithelial Cells', International Journal of Molecular Sciences, 23(9).
12. Martinez-Garcia, F. D., de Hilster, R. H. J., Sharma, P. K., Borghuis, T., Hylkema, M. N., Burgess, J. K. and Harmsen, M. C. (2021) 'Architecture and Composition Dictate Viscoelastic Properties of Organ-Derived Extracellular Matrix Hydrogels', Polymers (Basel), 13(18).
13. Nizamoglu, M., de Hilster, R. H. J., Zhao, F., Sharma, P. K., Borghuis, T., Harmsen, M. C. and Burgess, J. K. (2022) 'An in vitro model of fibrosis using crosslinked native extracellular matrix-derived hydrogels to modulate biomechanics without changing composition', Acta Biomater, 147, pp. 50-62.
14. Pouliot, R. A., Young, B. M., Link, P. A., Park, H. E., Kahn, A. R., Shankar, K., Schneck, M. B., Weiss, D. J. and Heise, R. L. (2020) 'Porcine Lung-Derived Extracellular Matrix Hydrogel Properties Are Dependent on Pepsin Digestion Time', Tissue Eng Part C Methods, 26(6), pp. 332-346.
15. Hoffman, E. T., Uriarte, J. J., Uhl, F. E., Eckstrom, K., Tanneberger, A. E., Becker, C., Moulin, C., Asarian, L., Ikonomou, L., Kotton, D. N. and Weiss, D. J. (2023) 'Human alveolar hydrogels promote morphological and transcriptional differentiation in iPSC-derived alveolar type 2 epithelial cells', Scientific Reports, 13(1), pp. 12057.
16. Park, S., Kim, T. H., Kim, S. H., You, S. and Jung, Y. (2021) 'Three-Dimensional Vascularized Lung Cancer-on-a-Chip with Lung Extracellular Matrix Hydrogels for In Vitro Screening', Cancers (Basel), 13(16).
17. Falcones, B., Sanz-Fraile, H., Marhuenda, E., Mendizábal, I., Cabrera-Aguilera, I., Malandain, N., Uriarte, J. J., Almendros, I., Navajas, D., Weiss, D. J., Farré, R. and Otero, J. (2021) 'Bioprintable Lung Extracellular Matrix Hydrogel Scaffolds for 3D Culture of Mesenchymal Stromal Cells', Polymers (Basel), 13(14).

18. Falcones, B., Söderlund, Z., Ibáñez-Fonseca, A., Almendros, I., Otero, J., Farré, R., Rolandsson Enes, S., Elowsson Rendin, L. and Westergren-Thorsson, G. (2022) 'hLMSC Secretome Affects Macrophage Activity Differentially Depending on Lung-Mimetic Environments', Cells, 11(12).
19. Ulldemolins, A., Jurado, A., Herranz-Diez, C., Gavara, N., Otero, J., Farré, R. and Almendros, I. (2022) 'Lung Extracellular Matrix Hydrogels-Derived Vesicles Contribute to Epithelial Lung Repair', Polymers (Basel), 14(22).
20. Link, P. A., Pouliot, R. A., Mikhaiel, N. S., Young, B. M. and Heise, R. L. (2017) 'Tunable Hydrogels from Pulmonary Extracellular Matrix for 3D Cell Culture', J Vis Exp, (119).
21. Freytes, D. O., O'Neill, J. D., Duan-Arnold, Y., Wrona, E. A. and Vunjak-Novakovic, G. (2014) 'Natural cardiac extracellular matrix hydrogels for cultivation of human stem cell-derived cardiomyocytes', Methods Mol Biol, 1181, pp. 69-81.
22. Sivaraman, K. and Shanthi, C. (2018) 'Matrikines for therapeutic and biomedical applications', Life Sci, 214, pp. 22-33.
23. Patel, D. F. and Snelgrove, R. J. (2018) 'The multifaceted roles of the matrikine Pro-Gly-Pro in pulmonary health and disease', Eur Respir Rev, 27(148).
24. Weathington, N. M., van Houwelingen, A. H., Noerager, B. D., Jackson, P. L., Kraneveld, A. D., Galin, F. S., Folkerts, G., Nijkamp, F. P. and Blalock, J. E. (2006) 'A novel peptide CXCR ligand derived from extracellular matrix degradation during airway inflammation', Nat Med, 12(3), pp. 317-23.
25. Akthar, S., Patel, D. F., Beale, R. C., Peiró, T., Xu, X., Gaggar, A., Jackson, P. L., Blalock, J. E., Lloyd, C. M. and Snelgrove, R. J. (2015) 'Matrikines are key regulators in modulating the amplitude of lung inflammation in acute pulmonary infection', Nat Commun, 6, pp. 8423.
26. Burgess, J. K., Boustany, S., Moir, L. M., Weckmann, M., Lau, J. Y., Grafton, K., Baraket, M., Hansbro, P. M., Hansbro, N. G., Foster, P. S., Black, J. L. and Oliver, B. G. (2010) 'Reduction of tumstatin in asthmatic airways contributes to angiogenesis, inflammation, and hyperresponsiveness', Am J Respir Crit Care Med, 181(2), pp. 106-15.
27. Senior, R. M., Griffin, G. L., Mecham, R. P., Wrenn, D. S., Prasad, K. U. and Urry, D. W. (1984) 'Val-Gly-Val-Ala-Pro-Gly, a repeating peptide in elastin, is chemotactic for fibroblasts and monocytes', J Cell Biol, 99(3), pp. 870-4.
28. Taddese, S., Weiss, A. S., Jahreis, G., Neubert, R. H. and Schmelzer, C. E. (2009) 'In vitro degradation of human tropoelastin by MMP-12 and the generation of matrikines from domain 24', Matrix Biol, 28(2), pp. 84-91.
29. Scheibner, K. A., Lutz, M. A., Boodoo, S., Fenton, M. J., Powell, J. D. and Horton, M. R. (2006) 'Hyaluronan fragments act as an endogenous danger signal by engaging TLR2', J Immunol, 177(2), pp. 1272-81.
30. Bix, G. and Iozzo, R. V. (2008) 'Novel interactions of perlecan: unraveling perlecan's role in angiogenesis', Microsc Res Tech, 71(5), pp. 339-48.
31. López-Moratalla, N., del Mar Calonge, M., López-Zabalza, M. J., Pérez-Mediavilla, L. A., subirá, M. L. and Santiago, E. (1995) 'Activation of human lymphomononuclear cells by peptides derived from extracellular matrix proteins', Biochim Biophys Acta, 1265(2-3), pp. 181-8.
32. Koshikawa, N., Schenk, S., Moeckel, G., Sharabi, A., Miyazaki, K., Gardner, H., Zent, R. and Quaranta, V. (2004) 'Proteolytic processing of laminin-5 by MT1-MMP in tissues and its effects on epithelial cell morphology', FASEB J, 18(2), pp. 364-6.
33. Sadowski, T., Dietrich, S., Koschinsky, F., Ludwig, A., Proksch, E., Titz, B. and Sedlacek, R. (2005) 'Matrix metalloproteinase 19 processes the laminin 5 gamma 2 chain and induces epithelial cell migration', Cell Mol Life Sci, 62(7-8), pp. 870-80.
34. Ponce, M. L. and Kleinman, H. K. (2003) 'Identification of redundant angiogenic sites in laminin alpha1 and gamma1 chains', Exp Cell Res, 285(2), pp. 189-95.

35. Malinda, K. M., Wysocki, A. B., Koblinski, J. E., Kleinman, H. K. and Ponce, M. L. (2008) 'Angiogenic laminin-derived peptides stimulate wound healing', Int J Biochem Cell Biol, 40(12), pp. 2771-80.
36. Baker, S. C., Atkin, N., Gunning, P. A., Granville, N., Wilson, K., Wilson, D. and Southgate, J. (2006) 'Characterisation of electrospun polystyrene scaffolds for three-dimensional in vitro biological studies', Biomaterials, 27(16), pp. 3136-46.
37. Livak, K. J. and Schmittgen, T. D. (2001) 'Analysis of Relative Gene Expression Data Using Real-Time Quantitative PCR and the 2−ΔΔCT Method', Methods, 25(4), pp. 402-408.
38. Campillo, N., Falcones, B., Montserrat, J. M., Gozal, D., Obeso, A., Gallego-Martin, T., Navajas, D., Almendros, I. and Farré, R. (2017) 'Frequency and magnitude of intermittent hypoxia modulate endothelial wound healing in a cell culture model of sleep apnea', J Appl Physiol (1985), 123(5), pp. 1047-1054.
39. Gomez, J. C., Yamada, M., Martin, J. R., Dang, H., Brickey, W. J., Bergmeier, W., Dinauer, M. C. and Doerschuk, C. M. (2015) 'Mechanisms of interferon-γ production by neutrophils and its function during Streptococcus pneumoniae pneumonia', Am J Respir Cell Mol Biol, 52(3), pp. 349-64.
40. Ratner, A. J., Hippe, K. R., Aguilar, J. L., Bender, M. H., Nelson, A. L. and Weiser, J. N. (2006) 'Epithelial cells are sensitive detectors of bacterial pore-forming toxins', J Biol Chem, 281(18), pp. 12994-8.
41. Waters, C. M., Roan, E. and Navajas, D. (2012) 'Mechanobiology in lung epithelial cells: measurements, perturbations, and responses', Compr Physiol, 2(1), pp. 1-29.
42. Johnson, B. Z., Stevenson, A. W., Prêle, C. M., Fear, M. W. and Wood, F. M. (2020) 'The Role of IL-6 in Skin Fibrosis and Cutaneous Wound Healing', Biomedicines, 8(5).
43. Li, Z., Mao, Z., Lin, Y., Liang, W., Jiang, F., Liu, J., Tang, Q. and Ma, D. (2008) 'Dynamic changes of tissue factor pathway inhibitor type 2 associated with IL-1beta and TNF-alpha in the development of murine acute lung injury', Thromb Res, 123(2), pp. 361-6.
44. Katsura, H., Kobayashi, Y., Tata, P. R. and Hogan, B. L. M. (2019) 'IL-1 and TNFα Contribute to the Inflammatory Niche to Enhance Alveolar Regeneration', Stem Cell Reports, 12(4), pp. 657-666.
45. Amigo, L. and Hernández-Ledesma, B. (2020) 'Current Evidence on the Bioavailability of Food Bioactive Peptides', Molecules, 25(19).
46. Haddox, J. L., Pfister, R. R., Muccio, D. D., Villain, M., Sommers, C. I., Chaddha, M., Anantharamaiah, G. M., Brouillette, W. J. and DeLucas, L. J. (1999) 'Bioactivity of peptide analogs of the neutrophil chemoattractant, N-acetyl-proline-glycine-proline', Invest Ophthalmol Vis Sci, 40(10), pp. 2427-9.
47. Snelgrove, R. J. (2011) 'Targeting of a common receptor shared by CXCL8 and N-Ac-PGP as a therapeutic strategy to alleviate chronic neutrophilic lung diseases', Eur J Pharmacol, 667(1-3), pp. 1-5.
48. Abdul Roda, M., Fernstrand, A. M., Redegeld, F. A., Blalock, J. E., Gaggar, A. and Folkerts, G. (2015) 'The matrikine PGP as a potential biomarker in COPD', Am J Physiol Lung Cell Mol Physiol, 308(11), pp. L1095-101.
49. Gaggar, A. and Weathington, N. (2016) 'Bioactive extracellular matrix fragments in lung health and disease', J Clin Invest, 126(9), pp. 3176-84.
50. Hamano, Y., and Kalluri, R. (2005). 'Tumstatin, the NC1 domain of alpha3 chain of type IV collagen, is an endogenous inhibitor of pathological angiogenesis and suppresses tumor growth'. Biochem Biophys Res Commun., 333(2), pp. 292–298.
51. Weckmann, M., Moir, L. M., Heckman, C. A., Black, J. L., Oliver, B. G., and Burgess, J. K. (2012). 'Lamstatin--a novel inhibitor of lymphangiogenesis derived from collagen IV'. J Cell Mol Med, 16(12), pp. 3062–3073
52. Schaefer L and Schaefer RM (2010). 'Proteoglycans : from structural compounds to signaling molecules', Cell Tissue Res. 339(1), pp. 237–46

53. Rønnow, S. R., Langholm, L. L., Karsdal, M. A., Manon-Jensen, T., Tal-Singer, R., Miller, B. E., Vestbo, J., Leeming, D. J., & Sand, J. M. B. (2020). 'Endotrophin, an extracellular hormone, in combination with neoepitope markers of von Willebrand factor improves prediction of mortality in the ECLIPSE COPD cohort.' Respir res, 21(1), pp. 202.
54. Morales-Nebreda, L. I., Rogel, M. R., Eisenberg, J. L., Hamill, K. J., Soberanes, S., Nigdelioglu, R., Chi, M., Cho, T., Radigan, K. A., Ridge, K. M., Misharin, A. V., Woychek, A., Hopkinson, S., Perlman, H., Mutlu, G. M., Pardo, A., Selman, M., Jones, J. C., & Budinger, G. R. (2015). 'Lung-specific loss of α3 laminin worsens bleomycin-induced pulmonary fibrosis'. Am J Respir Cell Mol Biol., 52(4), pp. 503–512.
55. Hamill KJ, Paller AS, Jones JCR (2010). 'Adhesion and migration, the diverse functions of the laminin alpha3 subunit.', Dermatol Clin.,28(1), pp.79–87.
56. Engel J(1989). 'EGF-like domains in extracellular matrix proteins: Localized signals for growth and differentiation?', FEBS Letters, 251.

Chapter V.

LUNG EXTRACELLULAR MATRIX HYDROGELS-DERIVED VESICLES CONTRIBUTE TO EPITHELIAL LUNG REPAIR

polymers

MDPI

Article

Lung Extracellular Matrix Hydrogels-Derived Vesicles Contribute to Epithelial Lung Repair

Anna Ulldemolins [1], Alicia Jurado [1], Carolina Herranz-Diez [1], Núria Gavara [1,2], Jorge Otero [1,2,3], Ramon Farré [1,3,4] and Isaac Almendros [1,3,4,*]

1 Unitat de Biofísica i Bioenginyeria, Facultat de Medicina i Ciències de la Salut, Universitat de Barcelona, 08036 Barcelona, Spain
2 The Institute for Bioengineering of Catalonia (IBEC), The Barcelona Institute of Science and Technology (BIST), 08028 Barcelona, Spain
3 CIBER de Enfermedades Respiratorias, 28029 Madrid, Spain
4 Institut d'Investigacions Biomèdiques August Pi i Sunyer, 08036 Barcelona, Spain
* Correspondence: isaac.almendros@ub.edu

Abstract: The use of physiomimetic decellularized extracellular matrix-derived hydrogels is attracting interest since they can modulate the therapeutic capacity of numerous cell types, including mesenchymal stromal cells (MSCs). Remarkably, extracellular vesicles (EVs) derived from MSCs display similar functions as their parental cells, mitigating tissue damage in lung diseases. However, recent data have shown that ECM-derived hydrogels could release other resident vesicles similar to EVs. Here, we aim to better understand the contribution of EVs and ECM-vesicles released from MSCs and/or lung-derived hydrogel (L-HG) in lung repair by using an in vitro lung injury model. L-HG derived-vesicles and MSCs EVs cultured either in L-HG or conventional plates were isolated and characterized. The therapeutic capacity of vesicles obtained from each experimental condition was tested by using an alveolar epithelial wound-healing assay. The number of ECM-vesicles released from acellular L-HG was 10-fold greater than EVs from conventional MSCs cell culture revealing that L-HG is an important source of bioactive vesicles. MSCs-derived EVs and L-HG vesicles have similar therapeutic capacity in lung repair. However, when wound closure rate was normalized by total proteins, the MSCs-derived EVs shows higher therapeutic potential to those released by L-HG. The EVs released from L-HG must be considered when HG is used as substrate for cell culture and EVs isolation.

Keywords: extracellular matrix; hydrogel; mesenchymal stem cells; extracellular vesicles; lung epithelial cells; lung repair

Citation: Ulldemolins, A.; Jurado, A.; Herranz-Diez, C.; Gavara, N.; Otero, J.; Farré, R.; Almendros, I. Lung Extracellular Matrix Hydrogels-Derived Vesicles Contribute to Epithelial Lung Repair. *Polymers* **2022**, *14*, 4907. https://doi.org/10.3390/polym14224907

Academic Editors: Francesco Lopresti and Manuela Ceraulo

Received: 20 October 2022
Accepted: 9 November 2022
Published: 14 November 2022

1. Introduction

The development and use of extracellular matrix (ECM)-derived hydrogels is attracting interest in cell therapy. The ECM is one of the most important cell niche components since it provides structural support for cells and is also critical in developmental organogenesis, homeostasis, and injury-repair responses. In particular, the physical signals exerted by the ECM composition, topography, and rigidity are translated to the cells via mechanotransduction which has been found to be crucial in regulating stem cell fate [1]. In contrast to traditional cultures, the biomechanical properties of hydrogels can be modulated to provide a physiomimetic 3D environment reproducing physiological and disease conditions in vitro [2–5]. The stemness and differentiation characteristics of mesenchymal stromal cells (MSCs) in decellularized ECM hydrogels are significant for stem cell therapy and for designing new treatments [3,4]. Among the different opportunities and challenges, ECM-derived hydrogels are biomechanically tunable and have been recently used as MSCs delivery systems [6] and bioinks for 3D bioprinting [5] opening new possibilities for tissue engineering.

Regarding lung diseases, the most severe manifestation of acute lung injury is acute respiratory distress syndrome (ARDS), a hypoxemic respiratory failure characterized by severe impairment in gas exchange and lung mechanics with a high case fatality rate since there is no effective treatment [7]. From pre-clinical studies, MSCs seem to be effective in ameliorating lung permeability, modulating inflammatory mediators and facilitating lung repair [8]. However, clinical trials to date have not provided strong evidence for MSC efficacy [9,10]. Potential limitations are the safety of these cells, their obtention procedure, and their viability after transplantation. Interestingly, MSCs cultured on decellularized lung scaffolds [11] and native lung-derived hydrogels [3] increased their therapeutic potential compared to conventional cell cultures. In a recent study, hydrogel-encapsulated MSCs could further alleviate acute lung injury, increasing the expression of several growth factors and interleukin-10 [12]. In addition, hydrogel-encapsulated MSCs showed better cell survival and could increase their engraftment in the injured tissue [13]. Thus, biomechanical preconditioning of cultured MSCs in physiomimetic hydrogels is a promising strategy to improve cell therapy in future clinical trials.

During the last few years, several studies have emerged showing that the therapeutic effects of MSCs are largely mediated by paracrine factors, which are transported within extracellular vesicles (EVs). Increasing evidence suggests that MSCs-derived EVs might represent a novel cell-free cell therapy with compelling advantages, compared with using parent MSCs, such as no risk of tumor formation and even lower immunogenicity. Re- garding ARDS, MSC-derived EVs seem to actively participate during the normal recovery process [14]. Moreover, several groups have revealed a therapeutic advantage when admin- istering MSC-derived EVs by intratracheal infusion or intravascular route. Intratracheal instillation of MSC-derived EVs in *Escherichia coli* lipopolysaccharide (LPS)-induced lung in- jury improved pulmonary edema, inflammation, and the integrity of the alveolar-capillary barrier [15,16]. However, how the physicochemical preconditioning of MSC cultured on physiomimetic hydrogels can modulate the therapeutic capacity of their secreted EVs is still largely unknown.

In contrast to conventional culturing, isolation and characterization of EVs secreted by MSCs cultured in decellularized ECM-derived hydrogels may pose a challenge since ECM bioscaffolds can also release bioactive vesicles with a structure (round vesicles) and size (50 to 400 nm) similar to EVs released by cells [17]. Thus, these ECM-vesicles represent another source of bioactive vesicles which can be mixed with the EVs released by the MSCs cultured on ECM derived-hydrogels. In addition, it has been reported that ECM-vesicles released from ECM fibrils by digestion contain miRNAs which have been associated with cellular development, proliferation, survival, migration, and cell cycle activity [17]. Regarding lung diseases, ECM infusion was able to improve cell survival and alveolar morphology and reduced hyperoxia-induced apoptosis and oxidative damage in a murine model of acute lung injury [18]. Moreover, recent studies have shown that some ECM components released from the hydrogel could provide some beneficial functions including antibacterial activity [19], and cell proliferation and chemotaxis [20]. However, the mechanisms involved are unknown. Herein, we hypothesize that ECM-bound vesicles could be an important component released from the hydrogels facilitating lung repair synergistically with those EVs released from MSCs. To this end, we tested the potential therapeutic effects of both EVs released from MSCs and/or ECM-vesicles from lung-derived hydrogel (L-HG) in a wound-healing experimental model of lung repair. The EVs and ECM-vesicles were characterized and quantified, and their contribution to repairing an alveolar epithelial cell monolayer was tested.

2. Materials and Methods

2.1 Preparation of the Lung ECM-Derived Hydrogels

Porcine lungs were obtained from a local slaughterhouse and decellularized as previ- ously described [5]. Lungs were perfused through the trachea and the vasculature with 0.1% Triton X-100, sodium deoxycholate, DNase and 1 M sodium chloride, with intermediate

perfusion with distilled water and PBS for rinsing purposes. To assess the effectiveness of decellularization, total genomic DNA was isolated using the PureLink Genomic DNA kit (ThermoScientific, Waltham, MA, USA) from native and decellularized scaffolds following the manufacturer's instructions. The total amount of DNA was quantified using spectrophotometry and normalized to the sample tissue dry weight. The amount of DNA was 16.26 ± 4.24 ng per mg of dry tissue which is below the accepted threshold of 50 ng/mg for successful decellularization (Supplementary Figure S1) [21].

Decellularized ECM were drained of excess water, freeze-dried in pieces, and lyophilized (Telstar Lyoquest55 Plus, Terrassa, Spain). Afterward, the sample was pulverized into micron-sized particles at −180 °C by using a cryogenic mill (6755, SPEX, Metuchen, NJ, USA) for 5 min at maximum speed. The resulting powder was digested at 20 mg/mL concen-tration in a 0.01 M HCl solution with pepsin from porcine gastric mucosa (1:10 concentration) under magnetic stirring at room temperature for 16 h. The resulting (pregel) solution was then pH-adjusted to 7.4 (±0.4) by using 0.1 M NaOH and PBS 10X and frozen at −80 °C for subsequent use. The biocompatibility of the L-HG has been confirmed as well as the attachment and growth of the cells within the lung ECM construct [4,5].

2.2 Rat Bone Marrow Mesenchymal Stromal Cells Isolation

Primary rat bone marrow-derived MSCs were isolated following an adapted protocol from [22] and approved by the Ethical Committee for Animal Research of the University of Barcelona. Bone marrow from the femurs and tibias of Sprague-Dawley rats (250 g) was flushed with a 19 G needle and syringe with prewarmed supplemented DMEM (Gibco) medium. The whole mesh was collected and disaggregated. Subsequently, cells were centrifuged at 350× *g* for 5 min and cultured on conventional plastic vessel T-75 (Techno Plastic Products AG, Trasadingen, Switzerland) with αMEM supplemented with 10% FBS and incubated with 5% CO_2 balanced-air incubator at 37 °C. After three days, the medium was replaced to discard all non-adhered cells and trypsinized for 5 min with TrypLE express trypsin (Gibco) before they reached confluence. MSCs were phenotypically characterized by flow cytometry. Fluorescein isothiocyanate (FITC)- or phycoerythrin (PE)-conjugated monoclonal antibodies specific for CD29, CD44H, CD45, CD11b/c, and CD90 (BioLegend, San Diego, CA, USA) were used.

2.3 Extracellular Vesicles Isolation

Vesicles were isolated and quantified from L-HG alone, and MSCs supernatants cultured on L-HG or on conventional plastic plates. Briefly, 10 mL of medium was collected and centrifuged at 2000× *g* for 30 min, and 5 mL of Total Exosomes Isolation Reagent (Life Technologies) was added. The mixtures were incubated overnight at 4 °C, followed by centrifugation at 10,000× *g* for 1 h. The pellets were suspended in 1 mL of PBS 1X and stored at −80 °C for further use. The concentration and size of EVs were analyzed by Nanoparticle Tracking Analysis (NTA).

2.4 F-Actin Staining

After EVs' isolation, cells were fixed with PFA 4% for 15 min, permeabilized with 0.1% Triton X-100, blocked with a 10% FBS solution and counter-stained for nuclei (NucBlue, ThermoScientific, Waltham, MA, USA) and F-actin (phalloidin, Thermoscientific, Waltham, MA, USA), and finally imaged with the Nikon D-Eclipse Ci confocal microscope ×20 Plan Apo immersion oil objective (Nikon, Minato ku, Japan).

2.5 Scanning Electron Microscopy

The hydrogel was freshly prepared and fixed in glutaraldehyde 2.5% in phosphate buffer (PB) 0.1 M, pH 7.4 for 24 h. After the fixation, it was washed ×4 with PB 0.1 M and treated with osmium tetraoxide 1% in PB at 4 °C for 90 min. Then, the sample was cleaned with ultrapure water until no yellow color was observed in the sample and water. The sample was cleaned with ethanol 50% followed by ethanol 70% and kept at 4 °C overnight.

Then, it was dried by using serial dilutions of ethanol from 80% to 100%. Finally, the sample was critical point dried (Autosamdri-815 critical point dryer, Tousimis, Rockville, MD, USA), gold coated, and mounted using conductive adhesive tabs (TED PELLA, Redding, CA, USA). Imaging was performed by using scanning electron microscopy (SEM) (JSM-6510, JEOL, Tokyo, Japan) at 15 kV.

2.6 Transmission Electron Microscopy

A 30 µL measure of the sample was placed in a clean parafilm piece and on top of the drop, a 400 copper mesh grid with formvar membrane and incubated for 25 min. The face of the grid that was in contact with the sample was then placed on top of a 30 µL staining agent (uranyl acetate 2%) drop and kept in contact for 30 s. Subsequently, samples were allowed to dry on a petri dish with filter paper for at least 1 h before being observed with transmission electron microscopy (TEM). The images were performed using a J1010 (Jeol) coupled with Orius CCD camera (Gatan) on the TEM-SEM Electron Microscopy Unit from Scientific and Technological Centers (CCiTUB) at the University of Barcelona.

2.7 Protein Quantification

First, to investigate the delivery of total protein and proteins from ECM-vesicles from acellular L-HG to the medium, the isolation protocol and quantification were measured in supernatants on different days. To this end, L-HG were washed with PBS 1× for 1 week. Every day, the PBS 1× was removed, and αMEM basal medium (without FBS) was added for 48 h to replicate cell culture conditions. After that, the EVs isolation protocol was applied. In parallel, L-HG were cultured for 1 week in PBS 1×, and the supernatant was collected daily. The protein content either from de L-HG supernatant or after the EVs isolation was assessed by BCA Protein kit (23225, Thermo Scientific™, Waltham, MA, USA).

These results showed that the delivery of vesicles from hydrogels reached a plateau after 3 days. Thus, experiments with MSCs embedded in L-HG were carried out after 3 days of L-HG washes in parallel to acellular L-HGs and MSCs in plastic cultures.

2.8 Wound Healing Assay

Rat lung epithelial cells (RLE) (CRL-2300, ATCC, Manassas, VA, USA) were used. The wound closure on RLE after the exposure of EVs and/or ECM-vesicles was assessed as pre- viously described [23]. Briefly, a density of $2 \cdot 10^5$ cells/cm^2 were seeded until cell reached confluency. Then, the epithelial cell monolayer was scratch-wounded using a sterile 200-µL pipette tip (Eppendorf, Hamburg, Germany), and cell debris was removed by washing with PBS 1×. Subsequently, PBS was discarded and replaced by a free-serum medium with a 1/10 dilution of the vesicles isolated from the different culture conditions. For any given condition, a parallel control group (PBS 1X instead of EVs) was included to further normal- ize the wound healing rate. For each experimental group, the wound healing measurements were carried out on 3 different days in duplicate (n = 5/experimental group).

The wound area was measured immediately after the scratch performance (0 h) and at the end of the experiment (24 h). Phase contrast images were recorded with an inverted microscope (Eclipse Ti, Nikon Instruments, Amsterdam, The Netherlands) equipped with a camera (C9100, Hamamatsu Photonics K.K., Hamamatsu, Japan) and a 10 × objective. Wound closure was assessed by comparing each epithelial wound's initial and final area with ImageJ 2.1.0/1.53c software, (NIH, Bethesda, MD, USA). Briefly, using the freehand selection tool by a researcher unaware of the experiment cell group, the edges were marked in all images, and the areas were calculated. The wound closure was computed as the percentage change between the two time points.

2.9 Statistical Analysis

Data are presented as mean ± standard error (SE). Comparisons between groups were made by one-way analysis of variance (ANOVA), except for the release of proteins at different time points where repeated two-way ANOVA was done. Student–Newman–Keuls

post hoc test was used for multiple comparisons. Differences were considered significant for $p < 0.05$. Statistical analyses were performed with SigmaPlot (v13.0 Systat Software, San Jose, CA, USA).

3. Results

3.1 Acellular Lung Hydrogel Is an Important Source of Extracellular Vesicles

SEM images of the L-HG hydrogels showed the fibrillary architecture of the scaffold (Supplementary Figure S2A). MSCs cultured on plastic and on L-HG showed a spread morphology indicative of their normal attachment (Supplementary Figure S2B). Actin filaments were distributed in a similar way in both conditions and with the characteristic spindle-like morphology.

As expected, L-HG releases a large amount of ECM-bonded proteins to the medium (1250 µg/mL) that decreases after consecutive daily washes (61.9 µg/mL after 7 days) (Figure 1). The proportion of proteins corresponding to those encapsulated in vesicles was approximately a 1/6 ratio with respect to the total protein release (227 µg/mL). Similarly, the proteins from ECM-bonded vesicles were reduced after daily washes, reaching a plateau on the third day (19 µg/mL) (Figure 1).

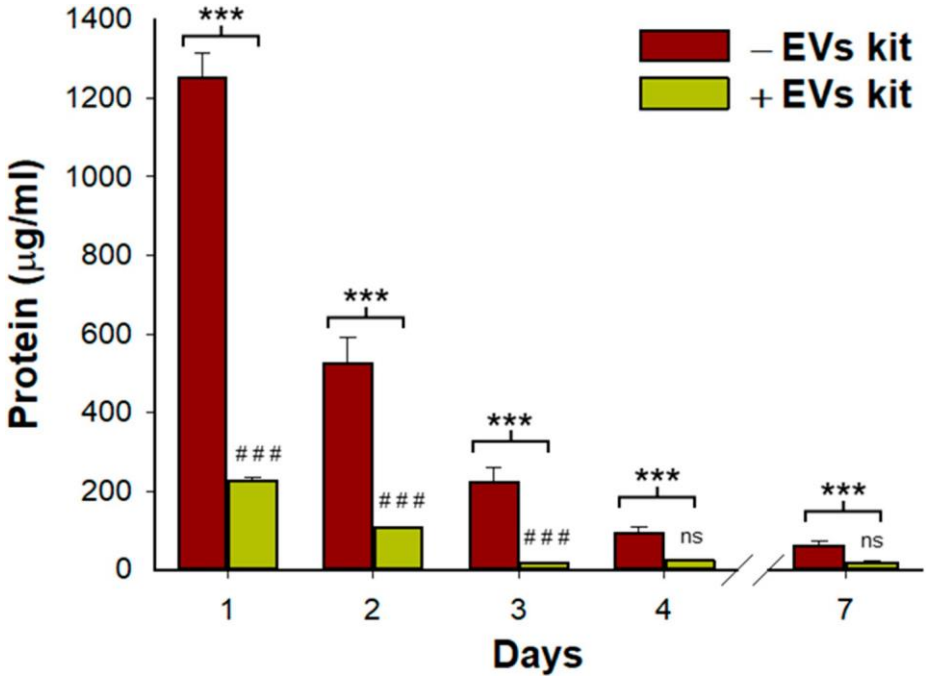

Figure 1. Total protein content and proteins released from bond-ECM vesicles measured in L-HG supernatants and after different daily washes. Whereas total protein was reduced every day, the portion of proteins from vesicles was reduced until day 3 reaching a plateau. (n = 3 per group).
* Comparisons between total protein and proteins from ECM-vesicles and # represents comparisons between consecutive days in proteins from ECM-vesicles. *** and ### $p < 0.001$.

Taking into consideration these data, we selected acellular L-HG after 3-day washing to use for MSCs culture in order to minimize the effects of L-HG-derived EVs on those secreted by the own cells. Interestingly, TEM images showed that after conventional EVs isolation protocol, there are isolated vesicles but also ECM-bound vesicles (Figure 2A). Although the amount of proteins released by the L-HG was reduced, NTA analysis revealed that there was still an important secretion of nanoparticles with similar physical characteristics to that released by MSCs (Figure 2). Vesicles isolated from MSCs cultured on conventional plastic and ECM-vesicles isolated from acellular L-HG presented a very similar NTA profile with a diameter of approximately 180 nm (Figure 2B). Therefore, the differential identification of

EVs and ECM-vesicles released from MSCs and L-HG, respectively, was not possible when MSCs are cultured on L-HG.

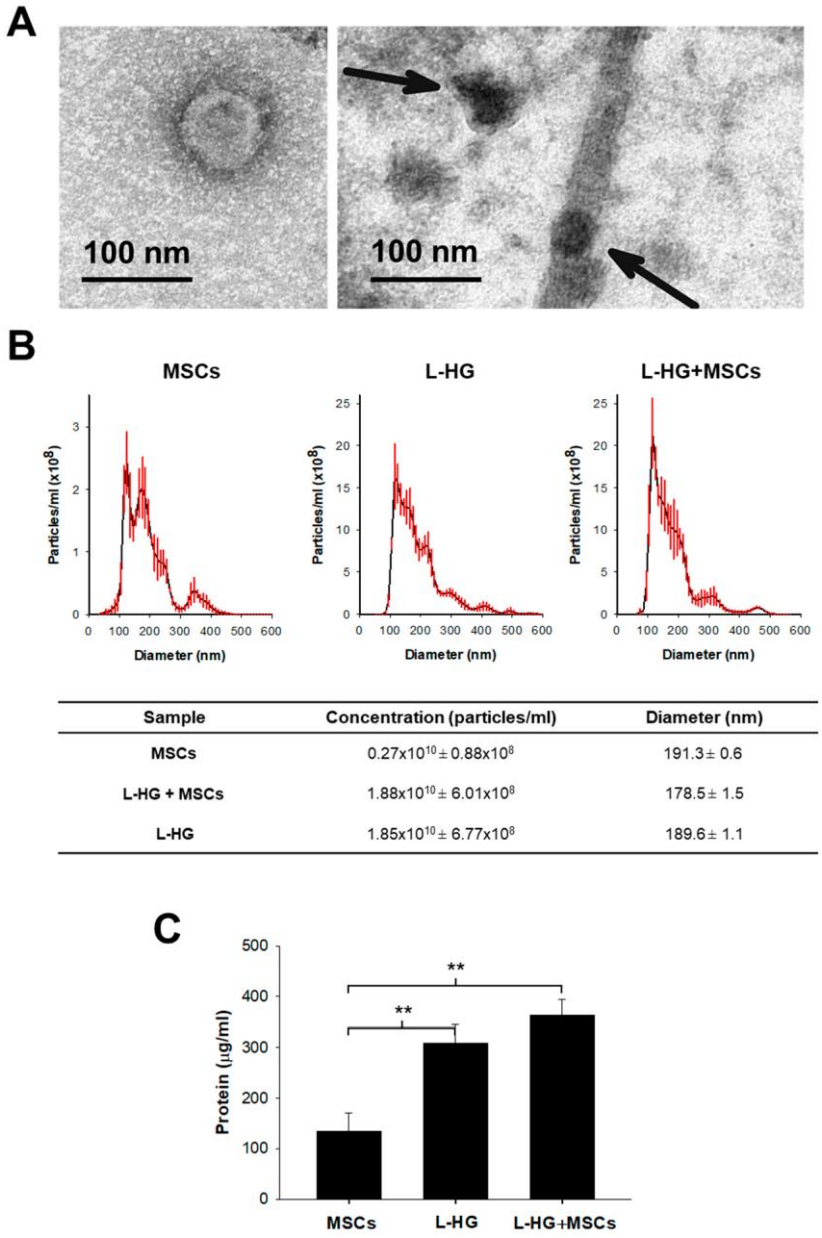

Sample	Concentration (particles/ml)	Diameter (nm)
MSCs	$0.27x10^{10} \pm 0.88x10^{8}$	191.3 ± 0.6
L-HG + MSCs	$1.88x10^{10} \pm 6.01x10^{8}$	178.5 ± 1.5
L-HG	$1.85x10^{10} \pm 6.77x10^{8}$	189.6 ± 1.1

Figure 2. Microvesicle quantification and characterization in all groups. (**A**) TEM images showing an isolated vesicle (**left**) and ECM-bound vesicles (**right**). (**B**) NTA analysis revealed that the number of ECM-vesicles released from 3-days washed L-HG were still higher than EVs secreted by MSCs cultured in plastic. The NTA profile also shows that vesicles released from both L-HG and MSCs have a very similar profile in size distribution. (**C**) The protein content of the particles isolated in each condition confirmed the NTA quantification showing a 3-fold increase in L-HG with respect to MSCs. ** $p < 0.01$ ($n = 5$).

The protein content from isolated EVs and ECM-vesicles was also measured to better estimate the total amount of EVs released in each condition. In accordance with NTA analysis, the protein amount obtained from isolated vesicles was 3-fold higher in those isolated from acellular L-HG (309 µg/mL, $p < 0.01$) and from L-HG with MSCs (363 µg/mL, $p < 0.01$) with respect to that obtained in MSCs cultured in plastic (134 µg/mL) (Figure 2C).

3.2 Woung Healing Is Enhanced by MSCs and L-HG-Derived EVs

The percentage of wound closure was increased when EVs and/or ECM-vesicles were applied (Figure 3). A group of ECM-vesicles isolated from L-HG without washes was also included in this assay. The greater closure was achieved when L-HG-derived vesicles were present and specifically for those obtained from non-washed L-HG (12.9% vs. 7.1% controls, $p < 0.05$) (Figure 3B). Considering that the number of vesicles released from MSCs was lower than that obtained from any other L-HGs condition when wound closure was normalized by the total amount of protein applied (Supplementary Table S1), the EVs derived from MSCs were the most efficient for wound healing (Figure 3C).

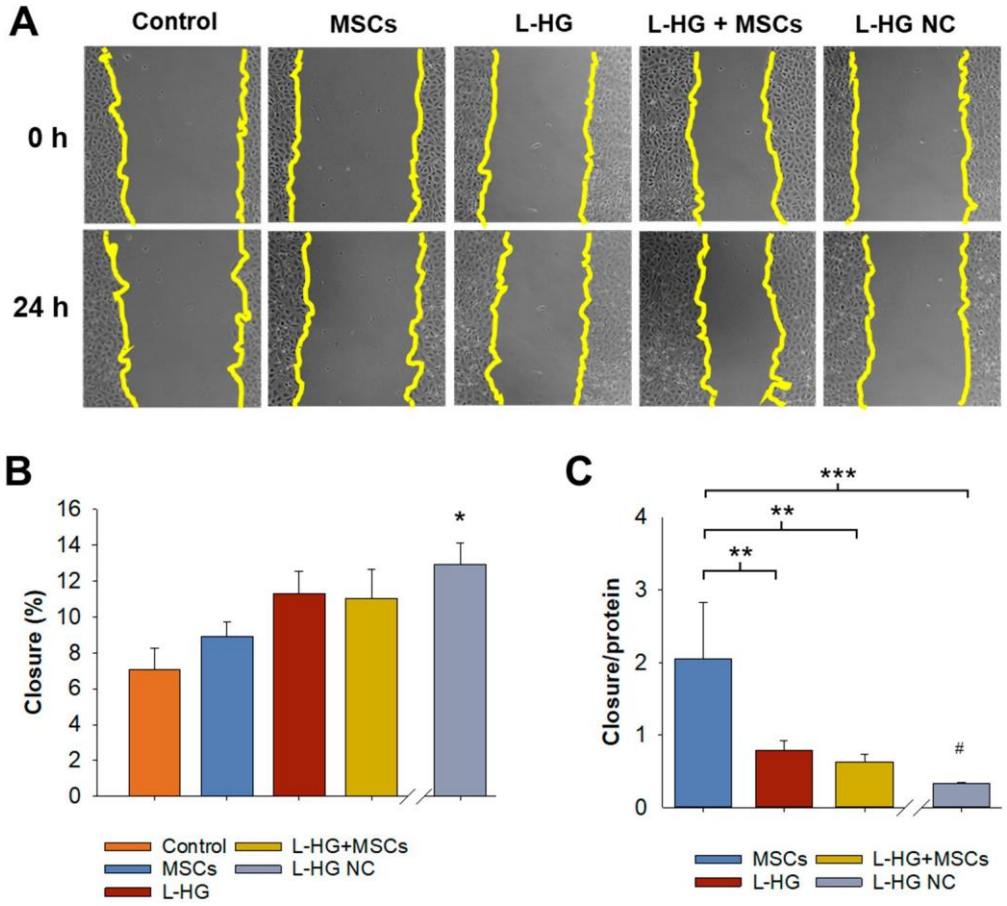

Figure 3. Functional characterization of EVs isolated from control, MSCs, pre-washed lung hydrogel (L-HG), L-HG with MSCs, and non-washed L-HG (L-HG NW). (**A**) Representative images of wound healing assay at 0 h and 24 h for each condition. (**B**) Wound closure was enhanced by applying MSCs, and L-HG-derived vesicles. (**C**) Wound closure normalized by total protein applied showed a higher effectivity of MSCs-derived EVs. * $p < 0.05$ and ** $p < 0.01$, *** $p < 0.001$ ($n = 5$). # Comparison between L-HG and L-HG NC, $p < 0.05$. Scale bar = 100 µm.

4. Discussion

Studies using physiomimetic ECM-derived hydrogels have recently emerged as a promising in vitro model that replicates many features of the cell environment in native healthy tissues or pathological conditions. Regarding cell therapy, hydrogels provide clear advantages to conventional culture. Their biophysical characteristics can be easily adjusted, other external physical stimuli (such as cyclic stretch) can be applied, are used as bioinks for bioprinting, and can be used as vehicle facilitating MSCs engraftment and viability after transplantation [12,13,24]. This work reveals that L-HG is also an important source of bioactive proteins and derived vesicles that can modulate multiple cellular mechanisms. Specifically, we demonstrate that they can interact with alveolar epithelial cells facilitating

lung repair. Interestingly, these results showed that the large amount of L-HG released vesicles have comparable therapeutic effects to those released by only MSCs when tested in a wound healing assay. Thus, the significance of these findings appears relevant since most studies carried out nowadays are not considering the presence of HG-derived vesicles (and their consequences) when hydrogels are used for cell culture.

Stem cell therapy has recently garnered much attention for treating respiratory diseases [25,26]. However, their therapeutic effects are minimal based on clinical trials [9,27,28]. The paracrine activity of MSCs, mediated partly by EVs, is being explored as a novel, promising approach to treating these diseases [29]. MSCs-derived EVs are generated and released into the extracellular environment to maintain tissue homeostasis. They are commonly characterized by a lipid membrane bilayer sharing some surface features [30]. However, their content, biogenesis, and release could depend on the surrounding environment [31]. As expected, here we found that MSCs derived from EVs can enhance wound healing in a model of lung repair. These findings support the notion that EVs could be used to treat severe ARDS patients that need an urgent and cell-free effective immunomodulatory treatment. In this work, MSCs were cultured in physiomimetic lung-derived hydrogels to understand how ECM components and MSCs could interact to improve the therapeutic capacity of their secretome. Surprisingly, the MSCs-derived EVs were a minor population among other ECM-vesicles released by the hydrogel, although results when normalized by the number of proteins showed that EVs have a greater effect in the cells than ECM-vesicles. In this way, MSCs-released particles showed to be much more specific for epithelial repair, confirming that ECM-vesicles present higher heterogeneity as expected.

It is known that hydrogels can contain subsets of EVs residing within the ECM [30,32,33]. Different types of vesicles have been very recently described from some decellularized tissues and scaffolds [17,32]. Although their role in repair and regeneration is still un- known, the scarce studies to date suggest that they could participate in modulating matrix remodeling [34] and tissue regeneration [33]. Interestingly, some of these ECM-vesicles seem to confer immunomodulatory effects on immune cells [35]. For instance, the applica- tion of matrix-bound vesicles on macrophages induces the expression of anti-inflammatory markers such as Fizz-1 and interleukin (IL)-4 indicating a polarization towards an M2 phenotype [30,35]. Accordingly, our results show that L-HG-derived vesicles also par- ticipate in tissue regeneration and repair based on a wound healing alveolar epithelial model. Our results could explain the protective role of intratracheal instillation of L-HG in a radiation-induced lung injury model [36], showing that L-HG could reduce epithelial– mesenchymal transition, inflammation, and oxidative damage induced by radiation [36]. In this context, further immunomodulatory studies are needed to assess the response generated by different cell types in the presence of the vesicles released by L-HG.

It should be also considered that hydrogels are degradable biomaterials. As previously reported [37], we observed a large amount of proteins released from the L-HG during the first 48 h after hydrogel gelation. These proteins are drastically reduced when a conventional EVs isolation protocol is applied (Figure 1). However, TEM images revealed the presence of small protein fragments from ECM degradation. Interestingly, we observed the presence of vesicles attached to these small ECM fragments confirming the existence of ECM-bound vesicles. These degradation products could confer some additional beneficial functions including antibacterial activity [19] and cell migration and proliferation [20]. However, the potential effect of these released products on alveolar epithelial wound healing needs to be studied in full detail in further studies.

5. Conclusions

The results obtained in this work provide novel insights into the therapeutic capacity of vesicles released from L-HG. These ECM-vesicles have the advantage of being present in the native lung, but their effects could differ from healthy or pathological conditions where ECM components are different (i.e., cystic fibrosis), opening new perspectives to better understand different diseases/conditions and their treatment. Moreover, the active

role of ECM-vesicles should be considered specifically when tissue-derived hydrogels are used for cell culture. As shown in this work, the large amount of ECM-vesicles released to supernatants can mask the effects of the MSCs-derived EVs for lung repair. In some mechanistic studies, the impact of ECM-vesicles could be reduced by previously washing the hydrogel. A better knowledge of ECM-vesicles could be crucial to interpreting the results obtained from the secretome obtained from cells cultured on hydrogels. Further analysis of the different types of ECM-vesicles released from hydrogels and the identification of the functional proteins released from the ECM are still needed to better understand their role in other cell populations and conditions.

Supplementary Materials: The following supporting information can be downloaded at: https://www.mdpi.com/article/10.3390/polym14224907/s1, Figure S1: Lung decellularization assessment; Figure S2: Scanning electron microscopy images and cell morphology of MSCs; Table S1: Total protein added in each experimental condition.

Author Contributions: Conceptualization, I.A.; methodology, A.U., A.J., C.H.-D., J.O., N.G., R.F. and I.A.; investigation, A.U., A.J., C.H.-D., J.O., N.G., R.F. and I.A.; software, I.A. and A.U.; resources, I.A., R.F., N.G. and J.O.; data curation, A.U. and I.A.; formal analysis, A.U., A.J., C.H.-D., J.O., N.G., R.F. and I.A.; validation, I.A. and A.U.; visualization, I.A. and A.U.; writing—original draft preparation, A.U. and I.A.; writing—review and editing, all; supervision, I.A.; project administration, I.A.; funding acquisition, I.A., R.F., N.G. and J.O. All authors have read and agreed to the published version of the manuscript.

Funding: Research was funded in part by the Spanish Ministry of Science, Innovation and Universities, grants numbers PID2019-108958RB-I00/AEI/10.13039/501100011033, PGC2018-097323-A-I00/AEI/10.13039/501100011033, PID2020-113910RB-I00-AEI/10.13039/501100011033, PID2020-11608RB-I00/AEI/10.13039/501100011033, and by SEPAR (900-2019).

Institutional Review Board Statement: The animal study protocol was approved by the Ethics Committee of the University of Barcelona (OB 168/19-2019).

Data Availability Statement: Data supporting the findings of this study are available from the corresponding authors upon reasonable request.

Acknowledgments: NTA analysis was performed by the ICTS "NANBIOSIS", more specifically by the Unit of the CIBER in Bioengineering, Biomaterials and Nanomedicne (CIBER-BBN) at the Universitat Autònoma de Barcelona. We thank the staff of the TEM-SEM Electron Microscopy Unit (Secientific and Technological Centers (CCiTUB), University of Barcelona) for their support and advice on TEM.

Conflicts of Interest: The authors declare no conflict of interest.

References

1. Jhala, D.; Vasita, R. A Review on Extracellular Matrix Mimicking Strategies for an Artificial Stem Cell Niche. *Polym. Rev.* **2015**, *55*, 561–595. [CrossRef]
2. Marhuenda, E.; Villarino, A.; Narciso, M.; Elowsson, L.; Almendros, I.; Westergren-Thorsson, G.; Farré, R.; Gavara, N.; Otero, J. Development of a physiomimetic model of acute respiratory distress syndrome by using ECM hydrogels and organ-on-a-chip devices. *Front. Pharmacol.* **2022**, *13*, 945134. [CrossRef] [PubMed]
3. Falcones, B.; Söderlund, Z.; Ibáñez-Fonseca, A.; Almendros, I.; Otero, J.; Farré, R.; Enes, S.R.; Rendin, L.E.; Westergren-Thorsson, G. hLMSC Secretome Affects Macrophage Activity Differentially Depending on Lung-Mimetic Environments. *Cells* **2022**, *11*, 1866. [CrossRef] [PubMed]
4. Marhuenda, E.; Villarino, A.; Narciso, M.L.; Camprubí-Rimblas, M.; Farré, R.; Gavara, N.; Artigas, A.; Almendros, I.; Otero, J. Lung Extracellular Matrix Hydrogels Enhance Preservation of Type II Phenotype in Primary Alveolar Epithelial Cells. *Int. J. Mol. Sci.* **2022**, *23*, 4888. [CrossRef] [PubMed]
5. Falcones, B.; Sanz-Fraile, H.; Marhuenda, E.; Mendizábal, I.; Cabrera-Aguilera, I.; Malandain, N.; Uriarte, J.; Almendros, I.; Navajas, D.; Weiss, D.; et al. Bioprintable Lung Extracellular Matrix Hydrogel Scaffolds for 3D Culture of Mesenchymal Stromal Cells. *Polymers* **2021**, *13*, 2350. [CrossRef]
6. Marusina, A.I.; Merleev, A.A.; Luna, J.I.; Olney, L.; Haigh, N.E.; Yoon, D.; Guo, C.; Ovadia, E.M.; Shimoda, M.; Luxardi, G.; et al. Tunable hydrogels for mesenchymal stem cell delivery: Integrin-induced transcriptome alterations and hydrogel optimization for human wound healing. *Stem Cells*

7. Han, S.; Mallampalli, R.K. The Acute Respiratory Distress Syndrome: From Mechanism to Translation. *J. Immunol.* **2015**, *194*, 855–860. [CrossRef]
8. Wang, F.; Fang, B.; Qiang, X.; Shao, J.; Zhou, L. The efficacy of mesenchymal stromal cell-derived therapies for acute respiratory distress syndrome—A meta-analysis of preclinical trials. *Respir. Res.* **2020**, *21*, 307. [CrossRef]
9. Matthay, M.A.; Calfee, C.S.; Zhuo, H.; Thompson, B.T.; Wilson, J.G.; E Levitt, J.; Rogers, A.J.; E Gotts, J.; Wiener-Kronish, J.P.; Bajwa, E.K.; et al. Treatment with allogeneic mesenchymal stromal cells for moderate to severe acute respiratory distress syndrome (START study): A randomised phase 2a safety trial. *Lancet Respir. Med.* **2019**, *7*, 154–162. [CrossRef]
10. Nagpal, A.; Choy, F.C.; Howell, S.; Hillier, S.; Chan, F.; Hamilton-Bruce, M.A.; Koblar, S.A. Safety and effectiveness of stem cell therapies in early-phase clinical trials in stroke: A systematic review and meta-analysis. *Stem Cell Res. Ther.* **2017**, *8*, 191. [CrossRef]
11. Nonaka, P.N.; Falcones, B.; Farre, R.; Artigas, A.; Almendros, I.; Navajas, D. Biophysically Preconditioning Mesenchymal Stem Cells Improves Treatment of Ventilator-Induced Lung Injury. *Arch. Bronconeumol.* **2020**, *56*, 179–181. [CrossRef] [PubMed]
12. Ding, J.; Dun, Y.; He, D.; Shao, Y.; Liu, F.; Zhang, L.; Shen, J. RGD-Hydrogel Improves the Therapeutic Effect of Bone Marrow- Derived Mesenchymal Stem Cells on Phosgene-Induced Acute Lung Injury in Rats. *Comput. Intell. Neurosci.* **2022**, *2022*, 2743878. [CrossRef] [PubMed]
13. Huang, Y.; Li, X.; Yang, L. Hydrogel Encapsulation: Taking the Therapy of Mesenchymal Stem Cells and Their Derived Secretome to the Next Level. *Front. Bioeng. Biotechnol.* **2022**, *10*, 859927. [CrossRef] [PubMed]
14. Shah, T.; Qin, S.; Vashi, M.; Predescu, D.N.; Jeganathan, N.; Bardita, C.; Ganesh, B.; DiBartolo, S.; Fogg, L.F.; Balk, R.A.; et al. Alk5/Runx1 signaling mediated by extracellular vesicles promotes vascular repair in acute respiratory distress syndrome. *Clin. Transl. Med.* **2018**, *7*, 19. [CrossRef] [PubMed]
15. Zhu, Y.-G.; Feng, X.-M.; Abbott, J.; Fang, X.-H.; Hao, Q.; Monsel, A.; Qu, J.-M.; Matthay, M.A.; Lee, J.W. Human Mesenchymal Stem Cell Microvesicles for Treatment of *Escherichia coli* Endotoxin-Induced Acute Lung Injury in Mice. *Stem Cells* **2014**, *32*, 116–125. [CrossRef]
16. Hu, S.; Park, J.; Liu, A.; Lee, J.; Zhang, X.; Hao, Q.; Lee, J.-W. Mesenchymal Stem Cell Microvesicles Restore Protein Permeability Across Primary Cultures of Injured Human Lung Microvascular Endothelial Cells. *Stem Cells Transl. Med.* **2018**, *7*, 615–624. [CrossRef]
17. Huleihel, L.; Hussey, G.S.; Naranjo, J.D.; Zhang, L.; Dziki, J.L.; Turner, N.J.; Stolz, D.B.; Badylak, S.F. Matrix-bound nanovesicles within ECM bioscaffolds. *Sci. Adv.* **2016**, *2*, e1600502. [CrossRef]
18. Wu, J.; Ravikumar, P.; Nguyen, K.T.; Hsia, C.C.W.; Hong, Y. Lung protection by inhalation of exogenous solubilized extracellular matrix. *PLoS ONE* **2017**, *12*, e0171165. [CrossRef]
19. Brennan, E.P.; Reing, J.; Chew, D.; Myers-Irvin, J.M.; Young, E.; Badylak, S.F. Antibacterial Activity within Degradation Products of Biological Scaffolds Composed of Extracellular Matrix. *Tissue Eng.* **2006**, *12*, 2949–2955. [CrossRef]
20. Reing, J.E.; Zhang, L.; Myers-Irvin, J.; Cordero, K.E.; Freytes, D.O.; Heber-Katz, E.; Bedelbaeva, K.; McIntosh, D.; Dewilde, A.; Braunhut, S.J.; et al. Degradation Products of Extracellular Matrix Affect Cell Migration and Proliferation. *Tissue Eng. Part A* **2009**, *15*, 605–614. [CrossRef]
21. Crapo, P.M.; Gilbert, T.W.; Badylak, S.F. An overview of tissue and whole organ decellularization processes. *Biomaterials* **2011**, *32*, 3233–3243. [CrossRef] [PubMed]
22. Carreras, A.; Almendros, I.; Farré, R. Potential Role of Bone Marrow Mesenchymal Stem Cells in Obstructive Sleep Apnea. *Int. J. Stem Cells* **2011**, *4*, 43–49. [CrossRef] [PubMed]
23. Campillo, N.; Falcones, B.; Montserrat, J.M.; Gozal, D.; Obeso, A.; Gallego-Martin, T.; Navajas, D.; Almendros, I.; Farré, R. Frequency and magnitude of intermittent hypoxia modulate endothelial wound healing in a cell culture model of sleep apnea. *J. Appl. Physiol.* **2017**, *123*, 1047–1054. [CrossRef] [PubMed]
24. Khayambashi, P.; Iyer, J.; Pillai, S.; Upadhyay, A.; Zhang, Y.; Tran, S.D. Hydrogel Encapsulation of Mesenchymal Stem Cells and Their Derived Exosomes for Tissue Engineering. *Int. J. Mol. Sci.* **2021**, *22*, 684. [CrossRef]
25. Azhdari, M.H.; Goodarzi, N.; Doroudian, M.; MacLoughlin, R. Molecular Insight into the Therapeutic Effects of Stem Cell-Derived Exosomes in Respiratory Diseases and the Potential for Pulmonary Delivery. *Int. J. Mol. Sci.* **2022**, *23*, 6273. [CrossRef]
26. Ji, H.-L.; Liu, C.; Zhao, R.-Z. Stem cell therapy for COVID-19 and other respiratory diseases: Global trends of clinical trials. *World J. Stem Cells* **2020**, *12*, 471–480. [CrossRef]
27. Horie, S.; Masterson, C.; Devaney, J.; Laffey, J. Stem cell therapy for acute respiratory distress

31. Han, S.; Mallampalli, R.K. The Acute Respiratory Distress Syndrome: From Mechanism to Translation. *J. Immunol.* **2015**, *194*, 855–860. [CrossRef]
32. Wang, F.; Fang, B.; Qiang, X.; Shao, J.; Zhou, L. The efficacy of mesenchymal stromal cell-derived therapies for acute respiratory distress syndrome—A meta-analysis of preclinical trials. *Respir. Res.* **2020**, *21*, 307. [CrossRef]
33. Matthay, M.A.; Calfee, C.S.; Zhuo, H.; Thompson, B.T.; Wilson, J.G.; E Levitt, J.; Rogers, A.J.; E Gotts, J.; Wiener-Kronish, J.P.; Bajwa, E.K.; et al. Treatment with allogeneic mesenchymal stromal cells for moderate to severe acute respiratory distress syndrome (START study): A randomised phase 2a safety trial. *Lancet Respir. Med.* **2019**, *7*, 154–162. [CrossRef]
34. Nagpal, A.; Choy, F.C.; Howell, S.; Hillier, S.; Chan, F.; Hamilton-Bruce, M.A.; Koblar, S.A. Safety and effectiveness of stem cell therapies in early-phase clinical trials in stroke: A systematic review and meta-analysis. *Stem Cell Res. Ther.* **2017**, *8*, 191. [CrossRef]
35. Nonaka, P.N.; Falcones, B.; Farre, R.; Artigas, A.; Almendros, I.; Navajas, D. Biophysically Preconditioning Mesenchymal Stem Cells Improves Treatment of Ventilator-Induced Lung Injury. *Arch. Bronconeumol.* **2020**, *56*, 179–181. [CrossRef] [PubMed]
36. Ding, J.; Dun, Y.; He, D.; Shao, Y.; Liu, F.; Zhang, L.; Shen, J. RGD-Hydrogel Improves the Therapeutic Effect of Bone Marrow- Derived Mesenchymal Stem Cells on Phosgene-Induced Acute Lung Injury in Rats. *Comput. Intell. Neurosci.* **2022**, *2022*, 2743878. [CrossRef] [PubMed]
37. Huang, Y.; Li, X.; Yang, L. Hydrogel Encapsulation: Taking the Therapy of Mesenchymal Stem Cells and Their Derived Secretome to the Next Level. *Front. Bioeng. Biotechnol.* **2022**, *10*, 859927. [CrossRef] [PubMed]
38. Shah, T.; Qin, S.; Vashi, M.; Predescu, D.N.; Jeganathan, N.; Bardita, C.; Ganesh, B.; DiBartolo, S.; Fogg, L.F.; Balk, R.A.; et al. Alk5/Runx1 signaling mediated by extracellular vesicles promotes vascular repair in acute respiratory distress syndrome. *Clin. Transl. Med.* **2018**, *7*, 19. [CrossRef] [PubMed]
39. Zhu, Y.-G.; Feng, X.-M.; Abbott, J.; Fang, X.-H.; Hao, Q.; Monsel, A.; Qu, J.-M.; Matthay, M.A.; Lee, J.W. Human Mesenchymal Stem Cell Microvesicles for Treatment of *Escherichia coli* Endotoxin-Induced Acute Lung Injury in Mice. *Stem Cells* **2014**, *32*, 116–125. [CrossRef]
40. Hu, S.; Park, J.; Liu, A.; Lee, J.; Zhang, X.; Hao, Q.; Lee, J.-W. Mesenchymal Stem Cell Microvesicles Restore Protein Permeability Across Primary Cultures of Injured Human Lung Microvascular Endothelial Cells. *Stem Cells Transl. Med.* **2018**, *7*, 615–624. [CrossRef]
41. Huleihel, L.; Hussey, G.S.; Naranjo, J.D.; Zhang, L.; Dziki, J.L.; Turner, N.J.; Stolz, D.B.; Badylak, S.F. Matrix-bound nanovesicles within ECM bioscaffolds. *Sci. Adv.* **2016**, *2*, e1600502. [CrossRef]
42. Wu, J.; Ravikumar, P.; Nguyen, K.T.; Hsia, C.C.W.; Hong, Y. Lung protection by inhalation of exogenous solubilized extracellular matrix. *PLoS ONE* **2017**, *12*, e0171165. [CrossRef]
43. Brennan, E.P.; Reing, J.; Chew, D.; Myers-Irvin, J.M.; Young, E.; Badylak, S.F. Antibacterial Activity within Degradation Products of Biological Scaffolds Composed of Extracellular Matrix. *Tissue Eng.* **2006**, *12*, 2949–2955. [CrossRef]
44. Reing, J.E.; Zhang, L.; Myers-Irvin, J.; Cordero, K.E.; Freytes, D.O.; Heber-Katz, E.; Bedelbaeva, K.; McIntosh, D.; Dewilde, A.; Braunhut, S.J.; et al. Degradation Products of Extracellular Matrix Affect Cell Migration and Proliferation. *Tissue Eng. Part A* **2009**, *15*, 605–614. [CrossRef]
45. Crapo, P.M.; Gilbert, T.W.; Badylak, S.F. An overview of tissue and whole organ decellularization processes. *Biomaterials* **2011**, *32*, 3233–3243. [CrossRef] [PubMed]
46. Carreras, A.; Almendros, I.; Farré, R. Potential Role of Bone Marrow Mesenchymal Stem Cells in Obstructive Sleep Apnea. *Int. J. Stem Cells* **2011**, *4*, 43–49. [CrossRef] [PubMed]
47. Campillo, N.; Falcones, B.; Montserrat, J.M.; Gozal, D.; Obeso, A.; Gallego-Martin, T.; Navajas, D.; Almendros, I.; Farré, R. Frequency and magnitude of intermittent hypoxia modulate endothelial wound healing in a cell culture model of sleep apnea. *J. Appl. Physiol.* **2017**, *123*, 1047–1054. [CrossRef] [PubMed]
48. Khayambashi, P.; Iyer, J.; Pillai, S.; Upadhyay, A.; Zhang, Y.; Tran, S.D. Hydrogel Encapsulation of Mesenchymal Stem Cells and Their Derived Exosomes for Tissue Engineering. *Int. J. Mol. Sci.* **2021**, *22*, 684. [CrossRef]
49. Azhdari, M.H.; Goodarzi, N.; Doroudian, M.; MacLoughlin, R. Molecular Insight into the Therapeutic Effects of Stem Cell-Derived Exosomes in Respiratory Diseases and the Potential for Pulmonary Delivery. *Int. J. Mol. Sci.* **2022**, *23*, 6273. [CrossRef]
50. Ji, H.-L.; Liu, C.; Zhao, R.-Z. Stem cell therapy for COVID-19 and other respiratory diseases: Global trends of clinical trials. *World J. Stem Cells* **2020**, *12*, 471–480. [CrossRef]
51. Horie, S.; Masterson, C.; Devaney, J.; Laffey, J. Stem cell therapy for acute respiratory distress

55. Kusuma, G.D.; Carthew, J.; Lim, R.; Frith, J.E. Effect of the Microenvironment on Mesenchymal Stem Cell Paracrine Signaling: Opportunities to Engineer the Therapeutic Effect. *Stem Cells Dev.* **2017**, *26*, 617–631. [CrossRef] [PubMed]
56. Hussey, G.S.; Molina, C.P.; Cramer, M.C.; Tyurina, Y.Y.; Tyurin, V.A.; Lee, Y.C.; El-Mossier, S.O.; Murdock, M.H.; Timashev, P.S.; Kagan, V.E.; et al. Lipidomics and RNA sequencing reveal a novel subpopulation of nanovesicle within extracellular matrix biomaterials. *Sci. Adv.* **2020**, *6*, eaay4361. [CrossRef] [PubMed]
57. Man, K.; Brunet, M.Y.; Federici, A.S.; Hoey, D.A.; Cox, S.C. An ECM-Mimetic Hydrogel to Promote the Therapeutic Efficacy of Osteoblast-Derived Extracellular Vesicles for Bone Regeneration. *Front. Bioeng. Biotechnol.* **2022**, *10*, 829969. [CrossRef] [PubMed]
58. Hao, D.; Swindell, H.S.; Ramasubramanian, L.; Liu, R.; Lam, K.S.; Farmer, D.; Wang, A. Extracellular Matrix Mimicking Nanofibrous Scaffolds Modified With Mesenchymal Stem Cell-Derived Extracellular Vesicles for Improved Vascularization. *Front. Bioeng. Biotechnol.* **2020**, *8*, 633. [CrossRef]
59. Huleihel, L.; Bartolacci, J.G.; Dziki, J.L.; Vorobyov, T.; Arnold, B.; Scarritt, M.E.; Pineda Molina, C.; Lopresti, S.T.; Brown, B.N.; Naranjo, J.D.; et al. Matrix-Bound Nanovesicles Recapitulate Extracellular Matrix Effects on Macrophage Phenotype. *Tissue Eng. Part A* **2017**, *23*, 1283–1294. [CrossRef]
60. Zhou, J.; Wu, P.; Sun, H.; Zhou, H.; Zhang, Y.; Xiao, Z. Lung tissue extracellular matrix-derived hydrogels protect against radiation-induced lung injury by suppressing epithelial–mesenchymal transition. *J. Cell. Physiol.* **2020**, *235*, 2377–2388. [CrossRef]
61. Pouliot, R.A.; Link, P.A.; Mikhaiel, N.S.; Schneck, M.B.; Valentine, M.S.; Gninzeko, F.J.K.; Herbert, J.A.; Sakagami, M.; Heise, R.L. Development and characterization of a naturally derived lung extracellular matrix hydrogel. *J. Biomed. Mater. Res. Part A* **2016**, *104*, 1922–1935. [CrossRef]

Chapter VI.

PHYSIOMIMETIC LUNG EXTRACELLULAR MATRIX HYDROGEL ENHANCES PULMONARY RECOVERY IN A RAT MODEL OF ACUTE RESPIRATORY DISTRESS SYNDROME

Physiomimetic lung extracellular matrix hydrogel enhances pulmonary recovery in a rat model of acute respiratory distress syndrome

Anna Ulldemolins[1], Alicia Jurado[1], Jorge Otero[1,2,4,5], Ramon Farré[1,2,3,5] and Isaac Almendros[1,2,3*]

[1]Unitat de Biofísica i Bioenginyeria, Universitat de Barcelona, Barcelona, Spain. [2]CIBER de Enfermedades Respiratorias (CIBERES), Madrid, Spain. [3]Institut d'Investigacions Biomèdiques August Pi i Sunyer (IDIBAPS), Barcelona, Spain. [4]The Institute for Bioengineering of Catalonia (IBEC), Barcelona, Spain. [5]Institute of Nanoscience and Nanotechnology (IN2UB), Universitat de Barcelona, Barcelona, Spain.

[*]Correspondence.

ABSTRACT

Rationale: Currently, the mortality of acute respiratory distress syndrome (ARDS) patients remains as high as 30-45% due to the scarcity of effective treatments. Mesenchymal stem cells (MSCs) have emerged as a promising cell therapy approach for ARDS treatment showing encouraging results from preclinical research studies but still with many challenges to solve into clinical practice. In addition, extracellular matrix (ECM)-based therapies have been recently emerged for tissue regeneration in lung injury.

Objective: To investigate the therapeutic capacity of lung ECM-derived hydrogel (L-HG) and its use as vehicle for MSCs instillation in a rat experimental model of ARDS.

Methodology: 24 Healthy and 24 ARDS LPS-induced Sprague-Dawley rats were randomly distributed into 4 experimental groups (n = 6) and intratracheally instilled as follows: (1) saline, (2) saline+MSCs, (3) L-HG, (4) L-HG + MSCs. 3 days after treatment, the lungs were excised and assessed for lung edema and histopathological analysis.

Results: Lung edema resulted 1.69 – fold greater (p = 0.04) in ARDS rats compared to controls. The use of conventional saline-MSCs, L-HG and L-HG+MSCS resulted in reduction of LPS- induced edema to 27.20%, 11% and 18%, respectively. Images of Hematoxylin &

Eosin staining showed a reduction of percentage of alveolar airspace in the ARDS rats (18.30 %) compared with the rats instilled with saline MSCs (33.19%, p = 0.072), L-HG (38.02%, p = 0.013) and L-HG+MSCs (40.51%, p =0.031).

Conclusion: The ECM-based therapy opens a new acellular approach in the treatment of ARDS with similar therapeutic results to those obtained in conventional MSCs instillation. Further immunomodulatory assays are still needed to assess how L-HG modulates local and systemic inflammation.

BACKGROUND

The Acute Respiratory Distress Syndrome (ARDS) is a condition characterized by impairment of gas exchange that leads to hypoxemic respiratory failure (1). It has a high case fatality rate and, unfortunately, there is no effective treatment available (2). ARDS prevalence and mortality have significantly increased in the recent years because patients with severe COVID-19 often develop end-stage ARDS (3). The actual treatment involves mechanical ventilation and the handeling of the underlying cause or trigger (i.e infection treatment, management of sepsis) (4). However, despite decades of research, current therapies have not shown a significant improvement in mortality rates (2,5).

Extensive research has focused on the use of Mesenchymal Stromal Cells (MSCs) as a potential therapy for ARDS, due to their antibacterial, immunomodulation, and tissue repair capabilities (6-8). Preclinical studies showed their efficacy in the improvement of lung permeability, inflammatory cell infiltration and immunomodulation in ARDS cases (9,10). However, despite promising results in preclinical studies, clinical trials have not yet provided strong evidence for MSC efficacy (7,11,12). Therefore, a new therapeutic approach is needed.

In the last years, the tissue engineering field has extensively explored applications for decellularized extracellular matrix (ECM). Many studies have proven the removal of cellular components with preservation of structural and functional proteins from organ scaffolds including the lung by using detergents such as sodium deoxycholate (SDC), and Triton X-100. Although the use of the decellularized tissue as a physiomimetic substrate is evident, ECM-based therapies are promising novel strategies for regeneration/repair of

the lung and for treating severe lung diseases. Following the tissue decellularization, the obtention of hydrogels is possible. This highly hydrated polymeric materials that mimic the lung native ECM represent an exciting development in the field of tissue engineering and regenerative medicine. The inherent fluidity of the pre-gel solutions allows for a variety of administration methods, such as instillation and nebulization (13). This is particularly advantageous for applying ECM-derived hydrogels to lung-related conditions. This study aimed to test the reparative and immunomodulatory effects of the lung ECM-derived hydrogel (L-HG) on a rat Lipopolysaccharide (LPS) – induced acute lung injury (ALI) model compared to the cellular approach using MSCs. We hypothesized that treatment with MSCs and L-HG would reduce the physiologic changes and early inflammatory in ALI.

MATHERIAL AND METHODS

Lung Hydrogel preparation

Porcine lungs were obtained from a local slaughterhouse and decellularized as previously described (14). Lungs were perfused through the trachea and the vasculature with 0.1% Triton X-100, sodium deoxycholate, DNase and 1M sodium chloride, with intermediate perfusion with distilled water and PBS for rinsing purposes. To assess the effectiveness of decellularization, total genomic DNA was isolated using the PureLink Genomic DNA kit (ThermoScientific, Waltham, MA, USA) from native and decellularized scaffolds following the manufacturer's instructions. The total amount of DNA was quantified using spectrophotometry and normalized to the sample tissue dry weight. Decellularized ECM was drained of excess water, freeze-dried in pieces, and lyophilized (Telstar Lyoquest55 Plus, Terrassa, Spain). Afterwards, the sample was pulverized into micron-sized particles at −180 °C by using a cryogenic mill (6755, SPEX, Metuchen, NJ, USA) for 5 min at maximum speed. The resulting powder was digested at 20 mg/mL concentration in a 0.01 M HCl solution with pepsin from porcine gastric mucosa (1:10 concentration) under magnetic stirring at room temperature for 16 h. The resulting (pregel) solution was then pH-adjusted to 7.4 (±0.4) by using 0.1 M NaOH and PBS 10X and frozen at −80 °C for subsequent use. For intratracheal instillation (IT), the pregel was diluted at 3 mg/ml with PBS 1X and let it self-assemble at 37ºC.

Acute Lung Injury Model

A total of 48 male Sprague-Dawley rats (Charles River, France), weighing 150 to 200 g at the beginning of the experiment were used. This study was approved by the animal experimentation ethics committee of the University of Barcelona (CECA – 159/19-10736). A Lipopolysaccharide (LPS) – induced Acute lung injury model was applied to the rats as previously described in (15). LPS from *Escherichia Coli (*O128:B12, Sigma) was used and rat bone marrow mesenchymal stromal cells (rBMMSCs) (SCR027, Sigma) were cultured on DMEM with 10% Fetal Bovine Serum. rBMMSCs from passages 3-6 were used for experiments.

The animals were randomly distributed into 6 experimental groups as follows:

- Control (C): saline intratracheal (IT) instillation at 0 hour and at 2 hours.
- C + MSCs: saline IT instillation as in control and IT instillation of MSCs (2×10^6 cells/animal) at 16 hours.
- C + L-HG: saline IT instillation as in control and IT instillation of L-HG 3mg/ml at 16 hours.
- ALI Control: HCl IT instillation at 0 hour and lipopolysaccharide (LPS) administration at 2 hours.
- ALI + MSCs: IT instillation as in ALI Control and instillation of MSCs (2×10^6 cells/animal) at 16 hours.
- ALI + L-HG: IT instillation as in ALI Control and instillation of L-HG 3mg/ml at 16 hours.

Cells were transplanted by IT instillation under 5% isoflurane sedation. Each animal received a dose of 2×10^6 cells suspended in 200 µl of sterile saline 16 hours after the instillation of HCl. The dose of the MSCs was taken from previous studies using cell therapies with MSCs and ATII cells in lung disease (16-18).

Lung histology and immunostaining studies

The lung right lobules were excised and immediately weighted. For histologic studies, the left lung was embedded in Optimum Cutting Temperature compound (OCT). Lungs were cut into 10-µm thick sections. The lung sections were stained with hematoxylin– eosin (H&E) and evaluated under NanoZoomer S60 Digital slide scanner (C13210-04,

Hamamatsu, Japan). The lung area and the quantification of both empty airspace and neutrophils were determined using Image J software (https://imagej.nih.gov/ij/).

Lung tissue inflammation

For studying the expression of local inflammatory cytokines, the lung was homogenized using a tissue homogenizer (Sigma, Z404586) in lysis buffer. RNA was subsequently extracted from homogenates by employing the RNeasy kit (Qiagen, Hilden, Germany). The cDNA was obtained by a reverse transcription-polymerase chain reaction (TaqMan Reverse Transcription Reagents, Invitrogen, Waltman, MA, USA) according to the manufacturer's instructions. The expression level of Interleukin 1β (IL-1β) and Interleukin 6 (IL-6) was studied using the Taqman Fast Advanced Master Mix and the TaqMan Gene Expression Assays in a StepOnePlus thermocycler (Applied Biosystems, Waltham, MA, USA). The expression level of genes was normalized to the constitutively expressed gene PPIA and calculated using the $2^{-\Delta\Delta Ct}$ method (19).

Statistical analysis

Results were expressed as mean ± standard deviation unless otherwise stated. GraphPad Prism 8.0 (GraphPad Software, Inc, San Diego, CA) was used for graphics and statistical analysis. One-way ANOVA was used for multiple group comparisons. Dunnett's post hoc test was used for comparisons with a control group, and Tukey's HSD posthoc test was used for multiple comparisons within each group. The results were statistically significant when $p < 0.05$.

RESULTS

Decellularized lung and ECM-derived hydrogel characterization

The decellularization and lung hydrogel synthesis process (Figure 1A) were analyzed for quality control. The amount of DNA in the decellularized samples (Figure 1B) was below the accepted threshold of 50 ng/mg for successful decellularization (20). The Live/Dead assay showed the biocompatibility of the lung hydrogel since rBMMSCs were alive after 72h (Figure 1C).

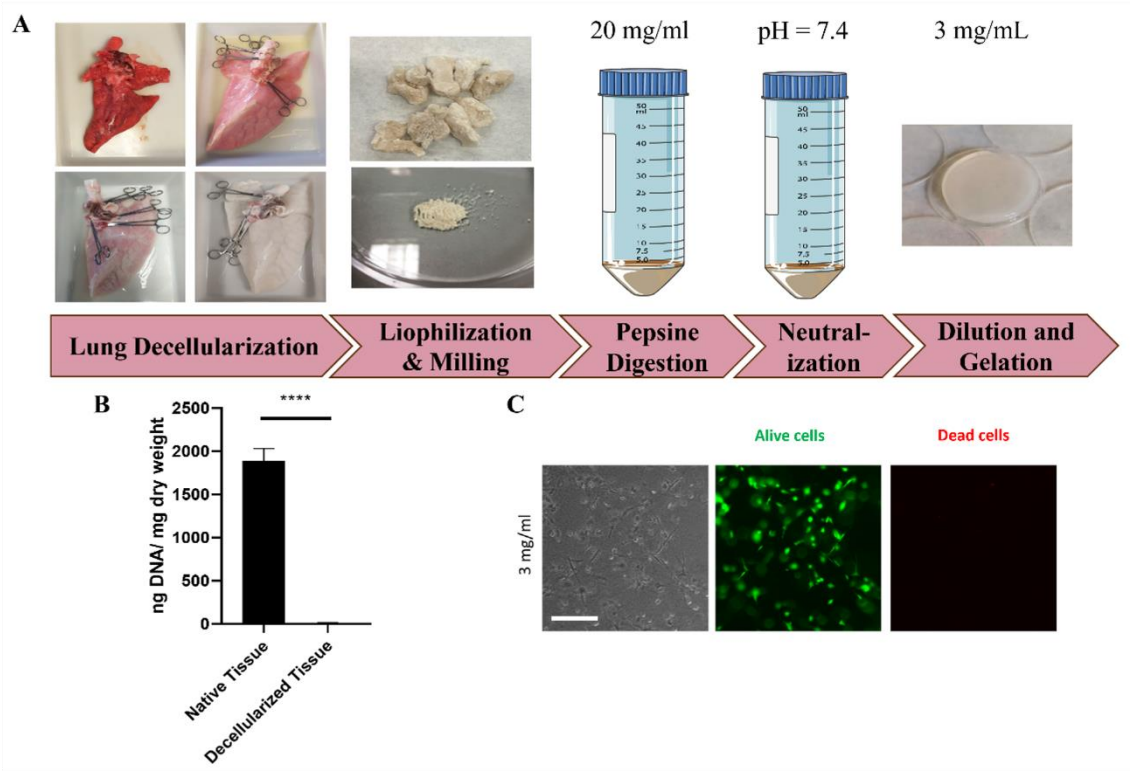

Figure 1. Lung ECM derived hydrogel synthesis and characterization. (A) Successive images of the porcine right lung through all the decellularization protocol, pepsine digestion and final gelation. (B) DNA quantification on the lung tissue. Data is representative from 3 independent experiments (**** $p < 0.0001$) **(C)** Live/Dead of rBMMSCs cultured on 3 mg/ml lung ECM derived hydrogel. Scale bar: 100 µm.

Analysis of Lipopolysaccharide – induced acute lung injury in rats treated with lung hydrogel

Following the experimental timeline (Figure 2A), HCl and LPS was administered to rats on day 0 by IT. After 16 hours of LPS + HCl instillation, rats underwent the same IT procedure, but this time, they received equal volumes of L-HG at concentrations of 3 mg/mL. A group in parallel was treated with 2×10^6 MSCs/animal by IT. Therefore, the administration of the L-HG treatment was intended to be an early intervention to prevent and protect against the advancement of lung injury. The lung hydrogel instillation resulted in a faster recovery of weight (Figure 2C) and increased survival. The ALI group treated with 0 mg/mL of lung hydrogel exhibited the lowest total weight gain between day 1 and day 4 (11 ± 14 %), while the other conditions showed approximately similar weight gains: ALI with 3 mg/mL of L-HG (16.61 ± 7.71%), saline with 0 mg/mL of L-HG (16.00 ± 6.05 %), saline with 3 mg/mL of L-HG (16.25 ± 5.83 %) and saline with 0 mg/mL of L-HG and MSCs (14.98 ±

4.23 %). Not surprisingly, the better weight gain recovery was obtained by ALI + MSCs group (21.42 ± 6.98 %). By contrast, IT instillation of L-HG in rats with ALI has the lowest survival (75%) (Figure 2B).

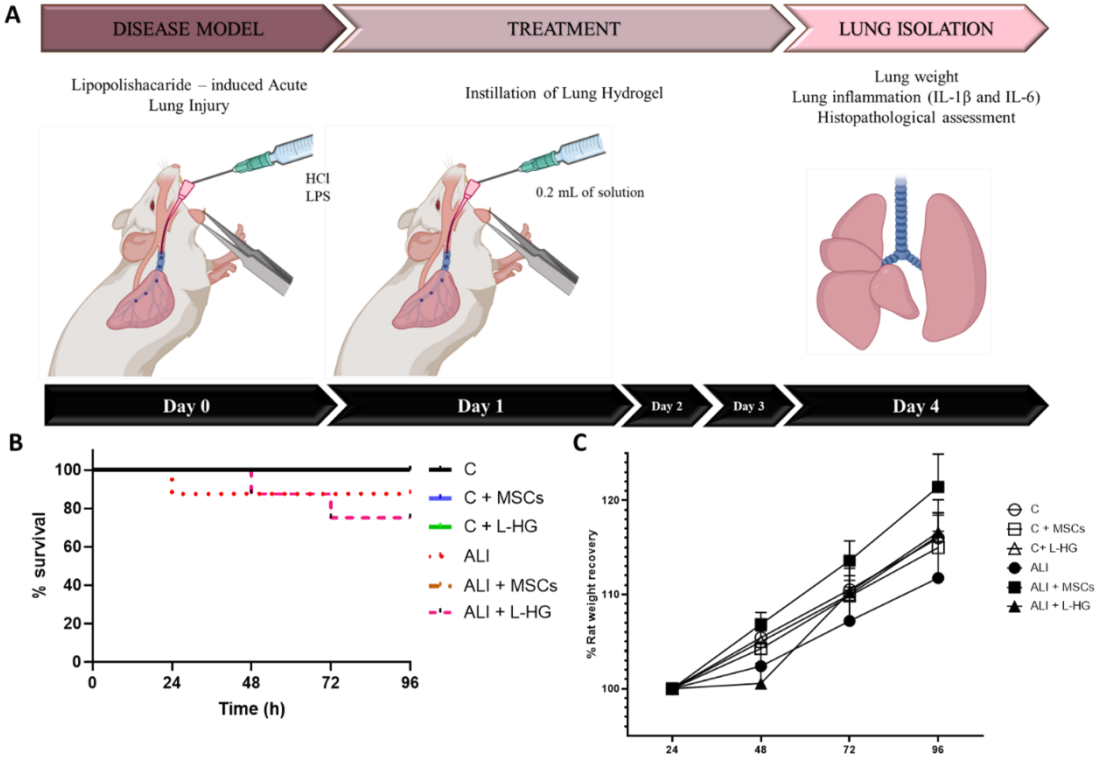

Figure 2. Physiologic parameters. (A) Rat surgeries scheduled in a timeline. **(B)** Survival shown by Kaplan-Meier curves in each of the experimental groups. **(C)** Body weight recovery over time starting at day 1 in each of the experimental groups.

Macroscopic and microscopic improvement in lipopolysaccharide- induced rat acute lung injury after lung hydrogel treatment

After euthanasia, there were different macroscopic appearances in whole rat lungs. Lungs treated with 0 mg/mL of L-HG and 0 cells appeared bigger, with damaged regions (data not shown). Lung weight at 72 hours after treatment was significantly greater in ALI rats than in the other conditions, suggesting an increase in lung edema (Figure 3B). Treatment with MSCs and L-HG reduced this effect, however not significantly.

To further examine the effect of L-HG and MSCs in this experimental ALI model, consecutive lung sections were stained with H&E and scanned (Figure 3A). Lung tissue sections from control rats showed no evidence of inflammation or epithelial damage. As expected, lung tissue sections from rats with ALI showed marked interstitial infiltration with inflammatory cells, hemorrhage, interstitial edema (Figure 3B, D). Although lungs

from rats treated with MSCs and L-HG had multifocal lesions, they had less edema, fewer inflammatory cells and considerably less hemorrhage than lungs from untreated ALI rats. Moreover, lungs from treated rats had large areas of undamaged tissue with normal alveolar architecture (Figure 3A). Accordingly, lung rats from ALI conditions and without treatment revealed thicker alveolar walls and reduced alveolar spaces in the H&E staining (Figure 3C).

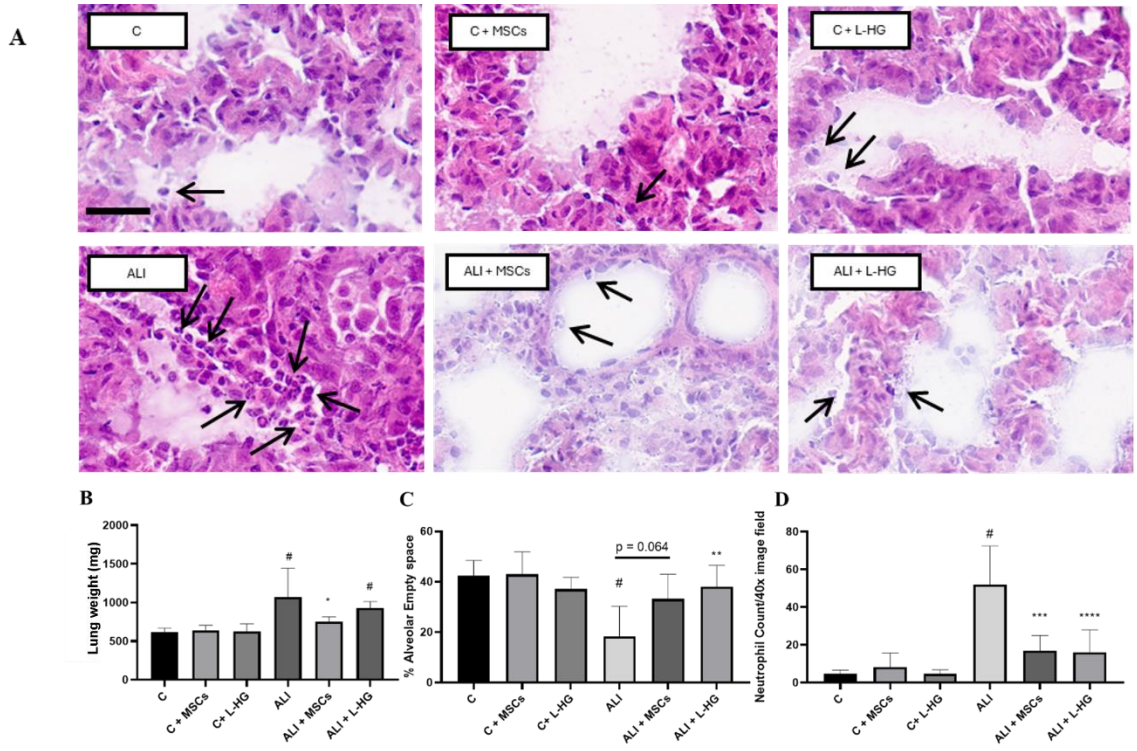

Figure 3. Histopathological analysis of the lung. (A) Representative images after H&E staining at 400× amplification. Arrows pointing the neutrophils present in the interstitial space. Scale bar: 50 µm **(B)** Rat right lung weight 72h after treatment (# $p < 0.001$ vs. control, *$p < 0.05$ vs. ALI from 6 independent experiments). **(C)** Alveolar empty space quantification from 100X H&E images (# $p < 0.001$ vs control, ** $p < 0.01$ vs ALI, from 5 images/animal group of 6 independent experiments). **(D)** Neutrophil Count from H&E images of 40x magnification (# $p < 0.0001$ vs control, *** $p < 0.001$ vs ALI from 3 images/animal group of 6 independent experiments).

Furthermore, lung damage resulted in an increased number of neutrophils in the interstitial space that were attenuated after treatment L-HG and MSCs diminishing the infiltration of inflammatory cells (Figure 3D). Finally, the MSCs were labelled before transplantation and followed in lung tissue by immunofluorescence analysis. We found MSCs cells engrafted in the lung tissue 72 hours after instillation (data not shown).

Rat lung inflammatory outcomes

Selected inflammatory markers were evaluated in lung homogenates. Pro-inflammatory cytokines (IL-1β, and IL-6) increased after instillation of HCl and LPS (Figure 4). After instillation of both L-HG and MSCs respectively, these markers decreased to control levels, demonstrating a reduction in the inflammatory response (Figure 4). However, no changes were observed in anti-inflammatory marker IL-1β after the instillation of L-HG.

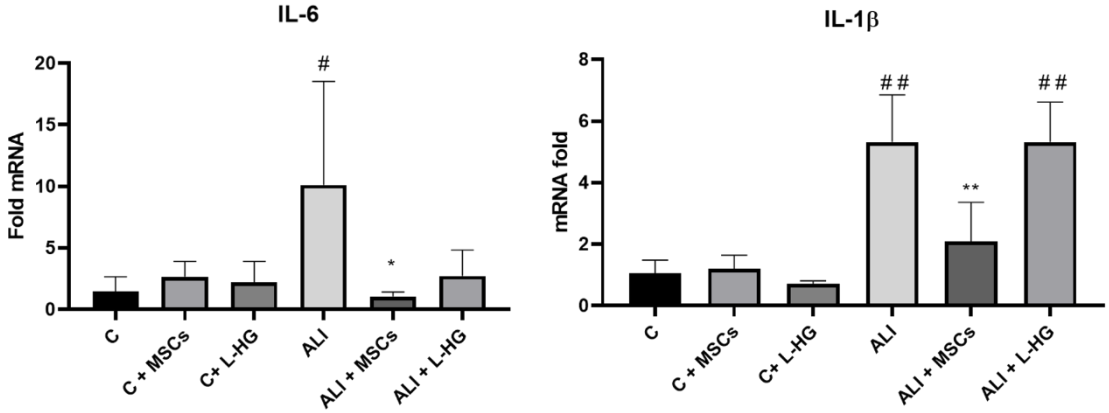

Figure 4. Lung inflammation. Relative expression of IL-1β (left) and IL-6 (right) cytokines on the rat lung after treatment with lung hydrogel (# $p < 0.05$, ## $p < 0.001$, vs. control; * $p < 0.05$, ** $p < 0.01$ vs ALI from 6 independent experiments).

DISCUSSION

ECM-derived hydrogels from decellularized tissues are promising biomaterials to enhance regeneration. This study produced and characterized a porcine lung ECM-derived hydrogel to be instilled intratracheally. The inherent fluidity of the L-HG makes it suitable for administration via instillation as shown here. This is particularly advantageous for applying ECM-derived hydrogels to lung-related conditions. Since the first hydrogel used to treat lung disorders was synthesised (21), there has been 3 more preclinical attempts to treat lung related conditions (13,22,23), and only 2 in cases of lung injury where the administration of the L-HG has been performed via instillation and nebulization (13,22). The lung hydrogel concentration of 3mg/ml used in this study is suitable for instillation since the particle diameter of the solution, which is less than 3 microns as reported by (13), does not overcome the rat lung small capillaries diameter of 6µm (14). Additionally, because of the many similarities between the pulmonary vasculatures in rat and human

(24), it is likely appropriate to assume that these experimental studies throw light on the L-HG treatment in humans.

As a response to damage, lung epithelial cells can secrete a wide range of pro inflammatory cytokines and chemokines like IL-6 (25) and IL-1β (26). They act as chemotactic agents for other immune cells like monocytes, macrophages, T-cells and dendritic cells. The use of L-HG in this study revealed that early intervention with ECM-derived hydrogel could prevent ARDS in a rat lung injury model, reduce morphology changes related to damage and modulate infiltration of pro-inflammatory cells (Figure 3 and 4). Likewise, there is a documented a study in which hydrogel derived from lung ECM exhibited a reduction in oxidative harm, inflammation in rats afflicted with lung injury caused by radiation exposure (22).

The local inflammation analysis in ALI lungs subjected to L-HG or MSCs showed a notable reduction in the expression of proinflammatory cytokines IL-6 and IL-1β. IL-6, recognized as a multifunctional pleiotropic cytokine involved in diverse physiological functions (27), along with IL-1β, known for playing a pivotal role in the initiation of lung injury (28), have been correlated with unfavourable prognoses in patients with ARDS (29,30). Our study demonstrated a downregulation in the levels of IL-6 following treatment with ECM-derived hydrogel, suggesting the potential of ECM-derived hydrogel to attenuate inflammation in rats. These results are in correlation with the latest preclinical study that uses L-HG as treatment for lung fibrosis in a rat model (23). The study indicates that the application of L-HG has the potential to impact processes related to tissue healing, the control of inflammation, restructuring of the cytoskeleton, and the cellular reaction to injury.

Although the use of lung hydrogel has been preclinically successful, the clear mechanisms associated with it remain unclear. Among others, mechanostransduction is the process by which cells sense and respond to mechanical cues from the surrounding ECM (31). It has been demonstrated that biophysical properties of the lung hydrogel have a high impact on cell mechanosensing pathways (32). It also has been proposed that in contact with a physiologic environment, cells activate lung cell proliferation, migration and response to treatment.

In fact, the potential use of lung hydrogels not only relies in their capacity to mimic lung microenvironment. Although the mechanisms are not well elucidated, L-HGs can also release bioactive peptides, nano-vesicles, chemokines, cytokines which the cells can interact with (33,34). These vesicles from the hydrogel have been described and demonstrated an increase in wound healing from epithelial cells (35). There is growing data that attributes the L-HG therapeutic properties to matrikines. These biologically active protein fragments formed during ECM enzymatic digestion to produce ECM-derived hydrogels influence gene expression, resulting in several biological effects that protect the lung from lung- related conditions (36). Recently in our research group, some of these matrikines release have been described and identified to be realesed from the L-HG (37).

Despite the noteworthy findings, it is important to acknowledge the limitations inherent in this study, which include a small number of animals, the absence of lung function tests, and limited information regarding immunomodulation effects of the L-HG treatment. Furthermore, for future therapeutic applications, it would be recommended to use human L-HG instead of porcine L-HG, especially considering the successful synthesis of human L-HG from alveolar regions (38). However, there are challenges regarding the obtention of a healthy human lung for hydrogel synthesis and it is crucial to recognize the potential immunogenicity of xenogeneic hydrogels in human applications (39). Addressing this concern, tissue engineers may explore solutions such as antigen removal during xenogeneic scaffold generation (40,41).

Finally, while several studies have presented preclinical indications of the therapeutic potential of ECM-derived hydrogel, up until now there is no clinic trial involving human participants employing them for the treatment of lung diseases. More information regarding the hydrogel and its effect in disease is needed to be reported.

CONCLUSION

In light of what have been discussed, our study demonstrates the potential of lung hydrogels from porcine decellularized ECM as an early intervention to combat lung injury in an LPS-induced ALI rat model. The ECM hydrogel treatment effectively reduced lung inflammation, lung edema and histologic evidence of lung injury. As a result, this study

opens the window for further research and development of lung hydrogels as a potential therapeutic strategy for treating ARDS.

REFERENCES

1. Tzotzos SJ, Fischer B, Fischer H, Zeitlinger M. Incidence of ARDS and outcomes in hospitalized patients with COVID-19: a global literature survey. 2020;1–4.
2. Han S, Mallampalli RK. The acute respiratory distress syndrome: from mechanism to translation. J Immunol. 2015 Feb;194(3):855–60.
3. Ji H-L, Liu C, Zhao R-Z. Stem cell therapy for COVID-19 and other respiratory diseases: Global trends of clinical trials. World J Stem Cells. 2020 Jun;12(6):471–80.
4. Griffiths MJD, Mcauley DF, Perkins GD, Barrett N, Blackwood B, Boyle A, et al. Guidelines on the management of acute respiratory distress syndrome. 2019.
5. Gotzev R, Kenarov P. Acute Respiratory Distress Syndrome (ARDS). Anaesthesiol Intensive Care. 2013;42(1):43–9.
6. Matthay MA. Therapeutic Potential of Mesenchymal Stromal Cells for Acute Respiratory Distress Syndrome. 2015;12(March).
7. Laffey JG, Matthay MA. Fifty Years of Research in ARDS. Cell-based Therapy for Acute Respiratory Distress Syndrome. Biology and Potential Therapeutic Value. Am J Respir Crit Care Med. 2017 Aug;196(3):266–73.
8. Wang F, Li Y, Wang B, Li J, Peng Z. The safety and efficacy of mesenchymal stromal cells in ARDS: a meta - analysis of randomized controlled trials. Crit Care [Internet]. 2023;1–11. Available from: https://doi.org/10.1186/s13054-022-04287-4
9. Zhang X, Wei X, Deng Y, Yuan X, Shi J, Huang W, et al. Mesenchymal stromal cells alleviate acute respiratory distress syndrome through the cholinergic anti-in fl ammatory pathway. 2022;(August 2021).
10. Wang F, Fang B, Qiang X, Shao J, Zhou L. The efficacy of mesenchymal stromal cell-derived therapies for acute respiratory distress syndrome—a meta-analysis of preclinical trials. Respir Res [Internet]. 2020;21(1):307. Available from: https://doi.org/10.1186/s12931-020-01574-y
11. Wilson JG, Liu KD, Zhuo H, Caballero L, McMillan M, Fang X, et al. Phase 1 Clinical Trial Designs Phase 1 Designs. Lancet Respir Med. 2015;3(1):24–32.
12. Qin H. Mesenchymal stem cell therapy for acute respiratory distress syndrome: from basic to clinics. Protein Cell [Internet]. 2020;11(10):707–22. Available from: https://doi.org/10.1007/s13238-020-00738-2
13. Wu J, Ravikumar P, Nguyen KT, Hsia CCW, Hong Y. Lung protection by inhalation of exogenous solubilized extracellular matrix. PLoS One. 2017;12(2):1–15.
14. Falcones B, Sanz-Fraile H, Marhuenda E, Mendizábal I, Cabrera-Aguilera I, Malandain N, et al. Bioprintable Lung Extracellular Matrix Hydrogel Scaffolds for 3D Culture of Mesenchymal Stromal Cells. Vol. 13, Polymers. 2021.
15. Puig F, Herrero R, Guillamat-Prats R, Gómez MN, Tijero J, Chimenti L, et al. A new experimental model of acid- and endotoxin-induced acute lung injury in rats. Am J Physiol Lung Cell Mol Physiol [Internet]. 2016/06/17. 2016 Aug 1;311(2):L229–37. Available from: https://pubmed.ncbi.nlm.nih.gov/27317688
16. Matthay MA, Goolaerts A, Howard JP, Lee JW. Mesenchymal stem cells for acute lung injury: preclinical evidence. Crit Care Med. 2010 Oct;38(10 Suppl):S569-73.
17. Guillamat-prats R, Puig F, Camprubí-rimblas M, Herrero R, Serrano-mollar A, Gómez N, et al. Intratracheal instillation of alveolar type II cells enhances recovery from acute lung injury in rats. J Hear Lung Transplant [Internet]. 2017;1–10. Available from: http://dx.doi.org/10.1016/j.healun.2017.10.025

18. Serrano-Mollar A, Nacher M, Gay-Jordi G, Closa D, Xaubet A, Bulbena O. Intratracheal transplantation of alveolar type II cells reverses bleomycin-induced lung fibrosis. Am J Respir Crit Care Med. 2007 Dec;176(12):1261–8.
19. Livak KJ, Schmittgen TD. Analysis of relative gene expression data using real-time quantitative PCR and the 2(-Delta Delta C(T)) Method. Methods. 2001 Dec;25(4):402–8.
20. Crapo PM, Gilbert TW, Badylak SF. An overview of tissue and whole organ decellularization processes. Biomaterials. 2011 Apr;32(12):3233–43.
21. Manni ML, Czajka CA, Oury TD, Gilbert TW. Extracellular matrix powder protects against bleomycin-induced pulmonary fibrosis. Tissue Eng- Part A. 2011;17(21–22):2795–804.
22. Zhou J, Wu P, Sun H, Zhou H, Zhang Y, Xiao Z. Lung tissue extracellular matrix-derived hydrogels protect against radiation-induced lung injury by suppressing epithelial–mesenchymal transition. J Cell Physiol. 2020;235(3):2377–88.
23. Evangelista-Leite D, Carreira ACO, Nishiyama MY, Gilpin SE, Miglino MA. The molecular mechanisms of extracellular matrix-derived hydrogel therapy in idiopathic pulmonary fibrosis models. Biomaterials. 2023;302(August).
24. Hislop A, Reid L. Normal structure and dimensions of the pulmonary arteries in the rat. J Anat [Internet]. 1978;125(Pt 1):71–83. Available from: http://www.ncbi.nlm.nih.gov/pubmed/632217%0Ahttp://www.pubmedcentral.nih.gov/articlerender.fcgi?artid=PMC1235567
25. Crestani B, Comillet P, Dehoux M, Rolland C, Guenounou M, Aubier M, et al. Alveolar Type II Epithelial Cells Produce Interleukin-6 In Vitro and In Vivo. Production. 1994;94(August):731–40.
26. Katsura H, Kobayashi Y, Tata PR, Hogan BLM. IL-1 and TNFα Contribute to the Inflammatory Niche to Enhance Alveolar Regeneration. Stem Cell Reports [Internet]. 2019;12(4):657–66. Available from: https://doi.org/10.1016/j.stemcr.2019.02.013
27. Babon JJ, Varghese LN, Nicola NA. Inhibition of IL-6 family cytokines by SOCS3. Semin Immunol. 2014 Feb;26(1):13–9.
28. Li Z, Mao Z, Lin Y, Liang W, Jiang F, Liu J, et al. Dynamic changes of tissue factor pathway inhibitor type 2 associated with IL-1beta; and TNF-alpha; in the development of murine acute lung injury. Thromb Res [Internet]. 2008 Dec 1;123(2):361–6. Available from: https://doi.org/10.1016/j.thromres.2008.03.019
29. Stukas S, Hoiland RL, Cooper J, Thiara S, Griesdale DE, Thomas AD, et al. The Association of Inflammatory Cytokines in the Pulmonary Pathophysiology of Respiratory Failure in Critically Ill Patients With Coronavirus Disease 2019. Crit Care Explor. 2020;2(9):e0203.
30. Meduri GU, Headley S, Kohler G, Stentz F, Tolley E, Umberger R, et al. Persistent elevation of inflammatory cytokines predicts a poor outcome in ARDS. Plasma IL-1 beta and IL-6 levels are consistent and efficient predictors of outcome over time. Chest. 1995 Apr;107(4):1062–73.
31. Urbanczyk M, Layland SL, Schenke-Layland K. The role of extracellular matrix in biomechanics and its impact on bioengineering of cells and 3D tissues. Matrix Biol [Internet]. 2020;85–86:1–14. Available from: https://doi.org/10.1016/j.matbio.2019.11.005
32. Marhuenda E, Villarino A, Narciso ML, Camprubí-Rimblas M, Farré R, Gavara N, et al. Lung Extracellular Matrix Hydrogels Enhance Preservation of Type II Phenotype in Primary Alveolar Epithelial Cells. Int J Mol Sci. 2022 Apr;23(9).
33. Huleihel L, Bartolacci JG, Dziki JL, Vorobyov T, Arnold B, Scarritt ME, et al. Matrix-Bound Nanovesicles Recapitulate Extracellular Matrix Effects on Macrophage Phenotype. Tissue Eng Part A. 2017 Nov;23(21–22):1283–94.
34. van der Merwe Y, Faust AE, Sakalli ET, Westrick CC, Hussey G, Conner IP, et al. Matrix-bound nanovesicles prevent ischemia-induced retinal ganglion cell axon degeneration and death and preserve visual function. Sci Rep [Internet]. 2019;9(1):1–15. Available from: http://dx.doi.org/10.1038/s41598-019-39861-4

35. Ulldemolins A, Jurado A, Herranz-Diez C, Gavara N, Otero J, Farré R, et al. Lung Extracellular Matrix Hydrogels-Derived Vesicles Contribute to Epithelial Lung Repair. Polymers (Basel) [Internet]. 2022;14(22). Available from: https://www.mdpi.com/2073-4360/14/22/4907
36. Evangelista-Leite D, Carreira ACO, Gilpin SE, Miglino MA. Protective Effects of Extracellular Matrix-Derived Hydrogels in Idiopathic Pulmonary Fibrosis. Tissue Eng - Part B Rev. 2022;28(3):517–30.
37. Herranz-Díez C, Ulldemolins A, Farre R, Gavara N, Sunyer R, Almendros I, Otero J. Matrikines Released from Pepsin-Digested Lung Extracellular Matrix Hydrogels: Considerations for the in vitro Study of the Alveolar Epithelium. In Manuscript
38. Hoffman ET, Uriarte JJ, Uhl FE, Eckstrom K, Tanneberger AE, Becker C, et al. Human alveolar hydrogels promote morphological and transcriptional differentiation in iPSC - derived alveolar type 2 epithelial cells. Sci Rep [Internet]. 2023;1–16. Available from: https://doi.org/10.1038/s41598-023-37685-x
39. Bayrak A, Tyralla M, Ladhoff J, Schleicher M, Stock UA, Volk HD, et al. Human immune responses to porcine xenogeneic matrices and their extracellular matrix constituents in vitro. Biomaterials [Internet]. 2010;31(14):3793–803. Available from: http://dx.doi.org/10.1016/j.biomaterials.2010.01.120
40. Kasravi M, Ahmadi A, Babajani A, Mazloomnejad R, Hatamnejad MR, Shariatzadeh S, et al. Immunogenicity of decellularized extracellular matrix scaffolds: a bottleneck in tissue engineering and regenerative medicine. Biomater Res [Internet]. 2023;27(1):1–24. Available from: https://doi.org/10.1186/s40824-023-00348-z
41. Wong ML, Griffiths LG. Immunogenicity in xenogeneic scaffold generation: antigen removal vs. decellularization. Acta Biomater. 2014 May;10(5):1806–16.

Chapter VII.

EFFECTS OF AGING ON THE BIOMECHANICAL PROPERTIES OF THE LUNG EXTRACELLULAR MATRIX: DEPENDENCE ON TISSULAR STRETCH

frontiers | Frontiers in Cell and Developmental Biology

TYPE Original Research
PUBLISHED 05 April 2024
DOI 10.3389/fcell.2024.1381470

OPEN ACCESS

EDITED BY
Karin Pfisterer,
Medical University of Vienna, Austria

REVIEWED BY
Mahesh Agarwal,
University of California, Los Angeles, United States
Béla Suki,
Boston University, United States

*CORRESPONDENCE
Isaac Almendros,
isaac.almendros@ub.edu
Núria Gavara,
ngavara@ub.edu

RECEIVED 03 February 2024
ACCEPTED 25 March 2024
PUBLISHED 05 April 2024

CITATION
Ulldemolins A, Narciso M, Sanz-Fraile H, Otero J, Farré R, Gavara N and Almendros I (2024), Effects of aging on the biomechanical properties of the lung extracellular matrix: dependence on tissular stretch. *Front. Cell Dev. Biol.* 12:1381470. doi: 10.3389/fcell.2024.1381470

Effects of aging on the biomechanical properties of the lung extracellular matrix: dependence on tissular stretch

Anna Ulldemolins[1], Maria Narciso[1,2], Héctor Sanz-Fraile[1], Jorge Otero[1,3], Ramon Farré[1,3,4], Núria Gavara[1,2]* and Isaac Almendros[1,3,4]*

[1]Unitat de Biofísica i Bioenginyeria, Facultat de Medicina i Ciències de la Salut, Universitat de Barcelona, Barcelona, Spain, [2]The Institute for Bioengineering of Catalonia (IBEC), The Barcelona Institute of Science and Technology, Barcelona, Spain, [3]CIBER de Enfermedades Respiratorias, Madrid, Spain, [4]Institut d'Investigacions Biomèdiques August Pi i Sunyer, Barcelona, Spain

Introduction: Aging induces functional and structural changes in the lung, characterized by a decline in elasticity and diminished pulmonary remodeling and regenerative capacity. Emerging evidence suggests that most biomechanical alterations in the lung result from changes in the composition of the lung extracellular matrix (ECM), potentially modulating the behavior of pulmonary cells and increasing the susceptibility to chronic lung diseases. Therefore, it is crucial to investigate the mechanical properties of the aged lung. This study aims to assess the mechanical alterations in the lung ECM due to aging at both residual (RV) and functional (FV) lung volumes and to evaluate their effects on the survival and proliferation of mesenchymal stromal cells (MSCs).

Methods: The lungs from young (4-6-month-old) and aged (20-24-month-old) mice were inflated with optimal cutting temperature compound to reach FV or non-inflated (RV). ECM proteins laminin, collagen I and fibronectin were quantified by immunofluorescence and the mechanical properties of the decellularized lung sections were assessed using atomic force microscopy. To investigate whether changes in ECM composition by aging and/or mechanical properties at RV and FV volumes affects MSCs, their viability and proliferation were evaluated after 72 h.

Results: Laminin presence was significantly reduced in aged mice compared to young mice, while fibronectin and collagen I were significantly increased in aged mice. In RV conditions, the acellular lungs from aged mice were significantly softer than from young mice. By contrast, in FV conditions, the aged lung ECM becomes stiffer than that of in young mice, revealing that strain hardening significantly depends on aging. Results after MSCs recellularization showed similar viability and proliferation rate in all conditions.

Discussion: This data strongly suggests that biomechanical measurements, especially in aging models, should be carried out in physiomimetic conditions rather than following the conventional non-inflated lung (RV) approach. The use of decellularized lung scaffolds from aged and/or other lung disease

murine/human models at physiomimetic conditions will help to better understand the potential role of mechanotransduction on the susceptibility and progression of chronic lung diseases, lung regeneration and cancer.

KEYWORDS

lung extracellular matrix, aging, lung volume, biomechanical properties, mesenchymal stromal cells

1 Introduction

During aging, lungs undergo structural and functional changes, including loss of elasticity and reduced pulmonary remodeling and regenerative capacity. These changes culminate in a decline in lung function and an increased susceptibility to chronic lung diseases (Cho and Stout-Delgado, 2020). There is growing evidence that most biomechanical changes are mediated by alterations in lung extracellular matrix (ECM) composition, as observed in chronic obstructive pulmonary disease (COPD), idiopathic pulmonary fibrosis (IPF), and aging (Burgstaller et al., 2017; Suki et al., 2022a; Burgess and Harmsen, 2022; Hoffman et al., 2023; Júnior et al., 2023; Mebratu et al., 2023). In fact, these alterations can lead to changes in ECM stiffness, and through mechanotransduction, they could modulate the behavior of pulmonary cells, facilitating disease progression. However, there is a scarcity of studies directly examining how age-related lung ECM alterations could modify ECM stiffness and, consequently, cellular responses (Faner et al., 2012).

The pulmonary connective tissue of the lung is composed of cells and the ECM, which is composed of a variety of biological macromolecules that are differently organized according to tissue or organ. Indeed, the mechanical properties of the ECM are determined by its composition, with collagen, elastin, and proteoglycans playing critical roles in the lung (Suki and Bates, 2008). Golding et al. postulated that the lungs gradually become more rigid with age due to altered expression of ECM proteins, including laminin, elastin, and fibronectin (Godin et al., 2016). Lung decellularization is a well-established technique for understanding the role of the composition and structural changes experienced by the ECM in different lung diseases and aging (Uriarte et al., 2018). Moreover, decellularized lungs can also be used as scaffolds for cell culture to better investigate specific ECM-cell interactions more effectively. The ECM protein content alterations induced by aging could lead to mechanical changes in the lung. In this regard, Melo et al. reported a tendency of increase in local stiffness measured by atomic force microscopy (AFM) in functional volume (FV) inflated decellularized lungs from young and aged mice (Melo et al., 2014). However, by using non-inflated lungs, other studies have observed significant age-related increases in stiffness in parenchymal and vessel compartments (Sicard et al., 2018) and even, a decrease (Miura, 2022). Therefore, the scarce available data are inconclusive.

The volume of gas in the intrathoracic airways is determined by the properties of the lung parenchyma, surface tension, and the forces exerted by respiratory muscles. In physiological conditions, because of the complex structure of the lung and its cyclic deformation during spontaneous breathing, pulmonary cells are continuously exposed to different levels of mechanical stresses. Interestingly, stretch can induce strain-softening of acellular fibrotic lungs at the nanoscale, as recently reported (Júnior et al., 2021), revealing the importance of conducting these measurements in physiomimetic conditions. Conversely, most available studies aiming to understand the biomechanical properties of the aged lung were done at residual volume (RV) (Sicard et al., 2018; Miura, 2022), since the lungs collapse after their removal. In fact, if mechanical measurements using residual (non-inflated) or functional volumes (Hopkins and Sharma, 2022) lead to consistent results in aging studies, is still unknown.

Here, we aimed to determine the biomechanical changes induced by aging in acellular lungs at RV and at physiologically-inflated conditions or functional volume (FV). The mechanical measurements were carried out at the nanoscale using AFM. To this end, an *in situ* decellularization method allowed us to decellularize the ECM for subsequent analysis of its mechanics and composition. Finally, the acellular lung scaffolds were repopulated with mesenchymal stromal cells (MSCs) to investigate whether their viability and proliferation are affected by aging and/or tissular stretch.

2 Materials and methods

2.1 Sample collection

This work was approved by the Ethical Committee of the University of Barcelona and Generalitat de Catalunya (OB 168/19 and 10972). Lungs were harvested *en bloc* with the heart from eight young (4-6-month-old) and eight aged (20–24-month-old) male C57BL/6J mice (Charles River Laboratories, Saint Germain sur L'arbresle, France). The lungs were subsequently inflated with 1:3 dilution of optimal cutting temperature (OCT, Tissue-Tek, Sakura, Torrance, CA, United States) compound with 0.3 mL to reach FV (Mitzner et al., 2001; Uriarte et al., 2016). Another group without inflation, at RV was sampled in parallel (Figure 1). Mice lungs were sliced at 20 and 100 µm using a cryostat with a −24°C temperature setting. The sections were placed in a positively charged glass slide (Superfrost Plus, Thermo Fisher Scientific, Waltham, MA, United States) and allowed to air-dry 15 min before being stored at −80°C until needed.

2.2 Lung decellularization

The lung slices were decellularized by using SDS followed by DNase leading to minimal alterations to ECM composition and mechanics in comparison with other methods (Narciso et al., 2021; Narciso et al., 2022a; Narciso et al., 2022b). In brief, acellular sections were created through a series of sequential washes while the lung sections remained attached to the glass slides, allowing us to maintain the physiological stretch (FV) at functional residual capacity (FRC) +1/2 tidal volume

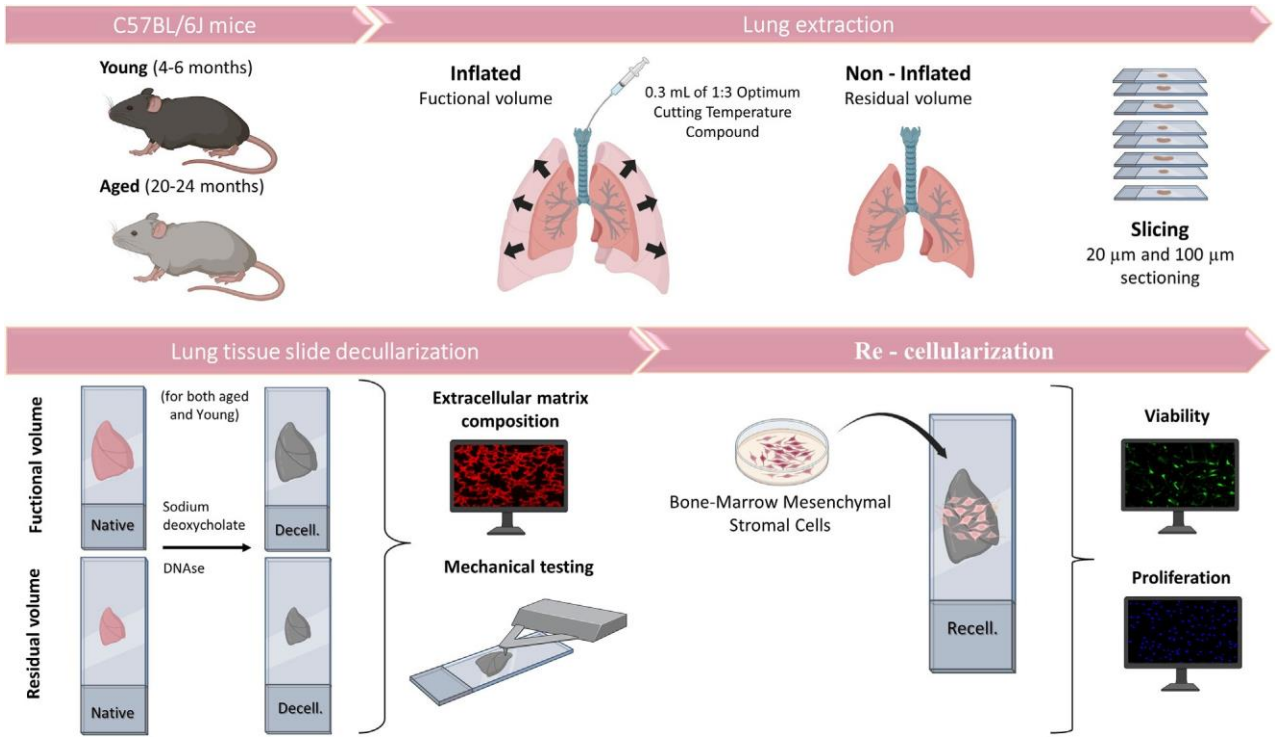

FIGURE 1
Schematic representation of the methodology.

(Rojas-Ruiz et al., 2023) or non-inflated (RV). Before the decellularization process, the tissue sections were allowed to thaw at room temperature (RT) for 20 min. The OCT was removed by immersing the sections in PBS for 20 min. The cells were lysed through two successive 10-min rinses with ultrapure water, followed by two 15-min incubations with 2% sodium deoxycholate (SD). After removing SD with three PBS washes,a 20-min incubation ina DNAseI solution (0.3 mg/mL, 5 mM $MgCl_2$, 5 mM $CaCl_2$ in 1 mM Tris-HCl) was carried out and then it was removed through three consecutive 5-min PBS washes. Decellularization was assessed by DNA immunostaining (Hoechst, Thermo Fisher Scientific).

2.3 Atomic force microscopy measurementsand data analysis

The lung ECM from eight young (n = 4 RV/FV conditions) and 16 aged animals (n = 8 RV/FV conditions) was mechanically probed in 20 µm-thick scaffolds immediately after decellularization by using cantilevers with a nominal spring constant (k) of 0.03 N/m and featuring a silicon oxide bead (5 µm in diameter) attached to their end (Novascan Technologies, IA) (Narciso et al., 2022a; Narciso et al., 2022c).

For each measurement point, the sample underwent five indentations to minimize measurement-to-measurement variability using 15 µ/s ramping speeds. Within each region, measurement points were separated by a minimum of 20 µm. We measured 3-5 points in each region and performed measurements in 3-5 different regions within the sample.

Considering that a spherical tip was used in this study, we deemed the Hertz contact model for a sphere indenting a semi-infinite half-space as the most suitable approach, in alignment with prior research in the field (Liu et al., 2010; Jorba et al., 2019; Júnior et al., 2021).

To determine the model's parameters, we employed a custom MATLAB code to fit each force-deflection curve (Jorba et al., 2019). Cellular viscosity was determined from force–distance curves using the method described by (Rebelo et al., 2014). Unspecific adhesion force was estimated as the most negative force value within the withdrawal part of the force-indentation curve.

2.4 Extracellular matrix immunofluorescence assay anddata analysis

Both decellularized and native non-inflated (RV) lungs ~20 µm-thick sections (n = 3) were stained for laminin, fibronectin, collagen I to characterize the matrix proteins. For native sections, immunofluorescence staining was performed after consecutive washes with PBS to remove the OCT. For decellularized sections, the staining protocol was performed immediately after the decellularization procedure. The tissue was fixed using 4% paraformaldehyde for 10 min at room temperature. Samples were then blocked using a buffer composed of 10% fetal bovine serum (FBS) and supplemented with 3% bovine serum albumin (BSA) for 1 h at RT. Primary antibodies against fibronectin (1:100, rabbit anti-fibronectin, ab2413, Abcam), laminin (1:100, rabbit anti-laminin,

Thermo Fisher Scientific) and type I collagen (rabbit anti-collagen type I, Abcam, 1:100) were incubated overnight at 4°C and constant agitation (80 rpm). Sections were then rinsed three times with the blocking buffer. The secondary antibody (goat anti-rabbit Cy3, Thermo Fisher Scientific, 1:200) was incubated for 2 h, at 37°C and constant agitation (80 rpm). Three 15-min rinses with PBS were performed. DNA of cellular and acellular samples was stained by incubation with Hoechst 33342 (Thermo Fisher Scientific) for 20 min at 80 rpm in an orbital shaker followed by three 5-min PBS washes. Finally, samples were mounted in Fluoromount mounting media (Thermo Fisher Scientific) and stored at 4°C. Epifluorescent images were acquired with a Leica SP5 inverted microscope equipped with a CCD camera (C9100, Hamamatsu Photonics K.K. Hamamatsu, Japan) and using a ×10 and ×20 Plan Fluor objective (Nikon).

Multi-channel TIFF images of the ECM stained with fibronectin, laminin and type I collagen were analyzed. The images were subjected to kernel density estimation using a custom MATLAB (MATLAB, The MathWorks Inc., MA, United States) script to evaluate the pixel intensity distribution across the image. Briefly, a lower and upper threshold for pixel intensity was applied to isolate the regions of interest. Both weak and intense light areas were quantified by calculating the area under the intensity distribution curve before and after the peak intensity. The results were normalized by the total area to account for variations in ECM deposition across samples. Comparisons between both groups were made based on the distribution of pixel intensities. The percentage of activated pixels was computed for each image.

2.5 Mesenchymal stromal cells repopulation, cell viability and proliferation assays

Primary human Bone Marrow-Derived MSCs (PCS-500–012, ATCC) were cultured in MSCs Basal Medium (PCS-500–030, ATCC) following manufacturer's instructions at 37°C, 5% CO_2 and 95% relative humidity.

Lungs from 20 animals (n = 5, young/aged and RV/FV) were decellularized. Then, ~100 µm-thick scaffolds were washed with PBS and $5{\cdot}10^4$ cells/cm^2 MSCs were seeded on top of the lung scaffolds. Control cultures were seeded on traditional culture plates (TCP). After 72 h, samples were stained using the LIVE/DEAD Viability/Cytotoxicity kit (L-3224, Invitrogen) (Bonenfant et al., 2013; ONeill et al., 2013; Syed et al., 2014). F-Actin (phalloidin, Thermo Fisher Scientific) and Ki67 (Thermo Fisher Scientific) were stained and visualized by a Nikon D-Eclipse Ci confocal microscope with a ×20 Plan Apo immersion oil objective (Nikon). Image quantification was performed using a custom MATLAB script. Initially, images in both Hoechst and Ki67 channels were converted to grayscale. User-defined thresholds were applied to distinguish cellular regions based on pixel intensity. Following the thresholding, region properties such as area, major axis length, and centroid were computed for individual cellular regions. To exclude artifacts and non-cellular elements, a minimum diameter filter was applied, removing any identified regions smaller than a pre-defined pixel size. To compensate for potential positional differences between the Hoechst and Ki67 staining, a dilation operation was performed on the Hoechst image. Ki67-positive cells were identified by overlaying the dilated Hoechst image with the Ki67 image, ensuring colocalization. Finally, the percentage of Ki67-positive nuclei relative to the total Hoechst-stained nuclei was computed to determine cellular proliferation.

2.6 Statistical analysis

All values are expressed as mean ± standard error (SE). Comparison in the expression of ECM protein content between young and aged lung samples was carried out with a *t*-test. Two-way ANOVA was used to compare changes in biomechanical properties and MSCs viability and proliferation as induced by age (young/aged) and/or tissular stretch (RV vs. FV). Student t-tests were employed to ascertain differences among groups. Statistical significance was considered when $p < 0.05$.

3. Results

3.1 Aging modifies the composition of the extracellular matrix

Results obtained by the quantification of immunofluorescence images showed that the protein composition of the lung ECM is affected by aging. Specifically, a significantly decreased level of laminin (~15%, $p = 0.041$) and increased expressions of fibronectin (~15%, $p < 0.001$) and collagen (19%, $p < 0.001$) were observed in samples from aged animals (Figures 2A, B).

3.2 Extracellular matrix biomechanics depends on aging and tissue stretch

The experimental setting allowed us to measure the lung ECM biomechanics by AFM at RV (collapsed) and at FV (stretched) conditions (Figure 3A). Regarding lung ECM stiffness, the Young's modulus, measured at RV, was significantly lower ($p = 0.003$) in aged mice (0.26 ± 0.03 kPa) when compared to that assessed in younger animals (0.47 ± 0.04 kPa) (Figure 3B). Conversely to RV, the stiffness of the lung ECM, measured at FV, was significantly increased ($p = 0.002$) in aged mice (0.54 ± 0.06 kPa) with respect to the younger counterparts (0.36 ± 0.03 kPa). Thus, these findings reveal that the effects of aging on ECM stiffness strongly depend on lung volume ($p < 0.001$). In this context, when comparing RV and FV measurements, it is noteworthy that aged lungs manifest a significant ~ 2-fold increase in ECM stiffness under FV conditions ($p < 0.001$). Conversely, a noticeable trend towards a decrease ($p = 0.063$) is observed in their younger counterparts (Figure 3B). Regarding ECM viscosity, no changes were observed between young/aged and RV/FV conditions (Figure 3C).

The AFM measurements also allowed us to measure the unspecific adhesion forces exerted by the ECM. The adhesion forces were similar between young (1.35 ± 0.15 nN) and aged (1.65 ± 0.14 nN) lung acellular ECM at FV conditions. However, the adhesion measured in young lung ECM (2.29 ± 0.39 nN) was ~2-fold higher ($p = 0.001$) with respect to aged counterparts (1.02 ± 0.12 nN) at RV conditions (Figure 3D). In a similar fashion to ECM

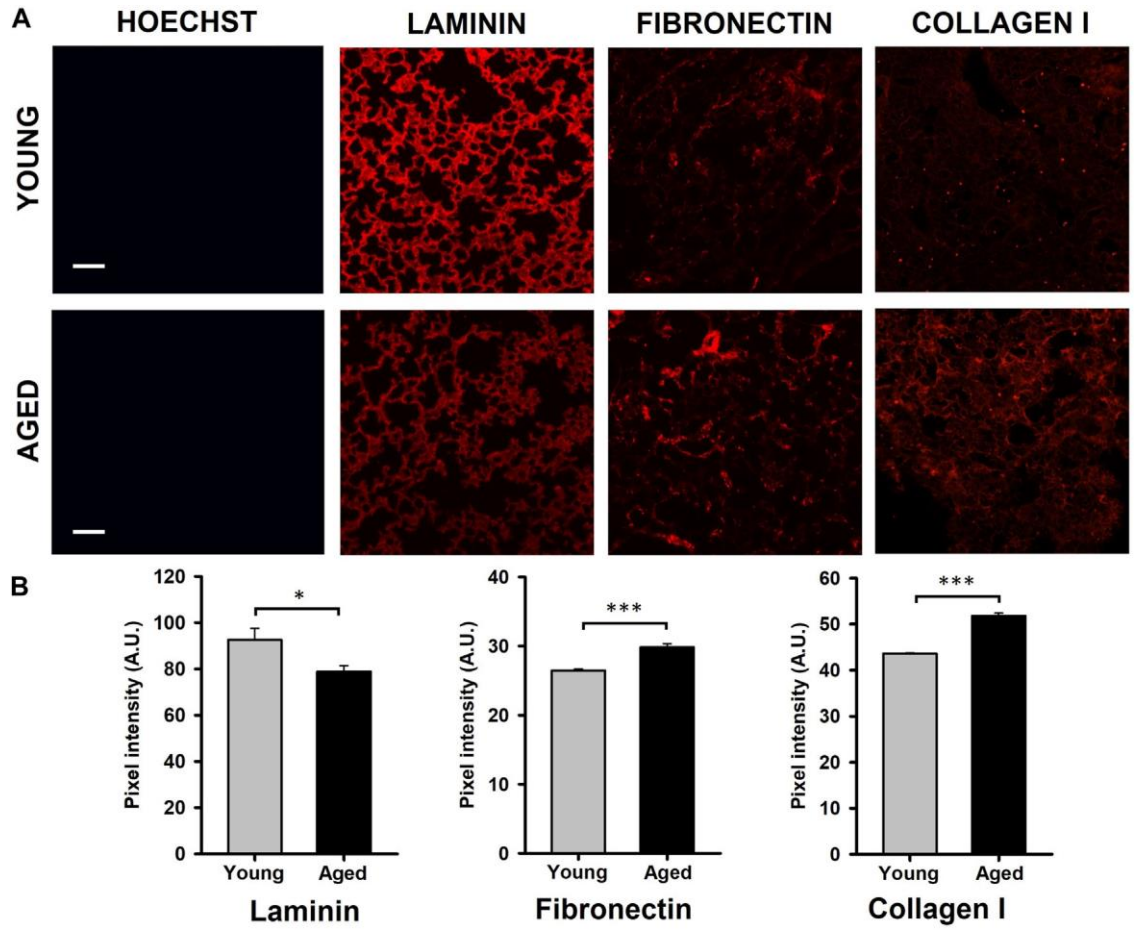

FIGURE 2
Quantification of ECM protein content. (A) Illustrative images of decellularized lung ECM stained for laminin, fibronectin, and collagen type I from young and aged mice. (B) Aging promotes a reduction of laminin and increases of fibronectin and collagen type I. Scale bar = 100 μm, values are represented as mean ± SE, *p < 0.05, **p < 0.01 and ***p < 0.001.

stiffness measurements, the lung ECM exerts different adhesion forces behavior between both lung volumes (RV and FV) (p = 0.006) only in young animals.

3.3 MSCs viability and proliferation on decellularized lung slices do not depend on the age and stretch of the lung

After 72 h of the lung scaffold repopulation with MSCs, they show a spread morphology indicative of their attachment to the scaffold. Additionally, no effects due to aging and lung volume were observed in cell viability presenting values higher than 96.5% in all groups (Figure 4A). In addition, the proliferation of MSCs, measured as a percentage of positive Ki67 cells, did not present significative differences in any condition (Figure 4B).

4. Discussion

This study provides novel insights into how age-induced alterations in the ECM composition are translated into biomechanical changes. Of particular interest is the discovery that variations in ECM stiffness and the adhesion forces exerted by aging are notably influenced by whether the lung is in a non-inflated or stretched state at RV and FV conditions, respectively. The model presented could provide novel insights in regenerative medicine, cancer, and other pulmonary chronic diseases during aging.

From rodent models, the studies that compared elderly to younger animals found a different biological response (Bos et al., 2018). In this regard, it is well established that there is a general pro-fibrotic response with aging in several organs and tissues, with particular relevance in the lungs. Specifically, it has been described that age-induced lung fibrosis is promoted by several factors, including genomic instability, telomere attrition, epigenetic alterations, mitochondrial dysfunction, cellular senescence, and stem cell exhaustion (Thannickal, 2013). For instance, decellularized lungs from aged rodents were reconstituted with bronchial epithelial cells and lung fibroblasts, exhibiting an altered gene expression of ECM proteins compared to young lungs (Godin et al., 2016). Even though ECM protein composition has been extensively studied in healthy lungs and in certain pulmonary diseases, the available data focused on ECM

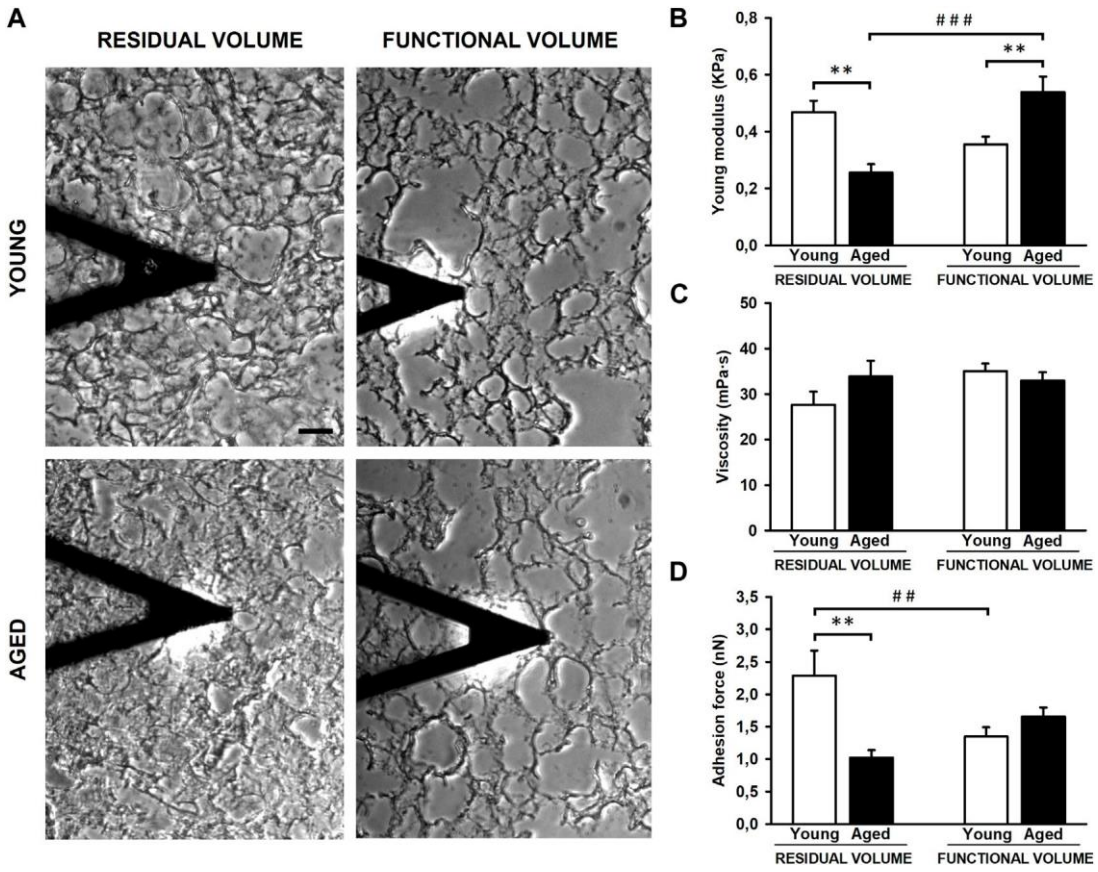

FIGURE 3
Mechanical properties of decellularized lung extracellular matrix (ECM). Atomic force microscopy images of lung samples from young and aged mice in residual (RV) and functional (FV) volumes (A). ECM stiffness of aged animals is softer compared to youngers at RV but stiffer at FV (B). No differences were observed in viscoelasticity (C) and unspecific adhesion forces are higher in young ECM only at RV (D). Scale bar = 50 µm, values are represented as mean ± SE, Comparisons between young/aged: $^{**}p < 0.01$ and between RV/FV: $^{\#\#}p < 0.01$ and $^{\#\#\#}p < 0.001$.

changes during aging is still very scarce. Collagens and fibronectin are considered two of the main ECM components and their dysregulation has been associated with the pathogenesis and progression of several chronic lung diseases, which predominantly occur in the elderly (Onursal et al., 2021). However, it is unknown whether ECM alterations induced by aging could lead to a predisposition to the development of such diseases. In this context, it has been reported that the synthesis and maturation of different types of collagens could be influenced by aging, resulting in distinct changes in collagen composition and in the collagen crosslinks (Sokocevica et al., 2011; Onursal et al., 2021). Interestingly, human bronchial epithelial cells and lung fibroblasts cultured on decellularized aged lung scaffolds showed a decreased expression of laminins α3 and α4, elastin and fibronectin, and elevated collagen, compared to young lungs (Godin et al., 2016). In contrast, Takubo Y. et al. reported increased total collagen content in lung ECM from 20-month-old mice, but no changes in collagen proportion and elastin content were found (Takubo et al., 1999). Furthermore, the degradation of collagen is also an essential process to resolve lung fibrosis. Podolsky MJ. et al. have shown that cell-mediated collagen uptake and degradation are diminished in the lungs of 10-month-old mice, suggesting that this impairment could contribute to age-related fibrosis (Podolsky et al., 2020). These results are also according to the findings observed by Huang K et al. showing a reduction of elastin fibers and increased density of collagen leading to an increased lung compliance during aging (Huang et al., 2007a; Huang et al., 2007b). The present study is focused on collagen I, laminin and fibronectin, two ECM components that contribute to ECM biomechanics of the static lung (Álvarez et al., 2015). As expected, all ECM components assessed in decellularized lung scaffolds were altered in a different manner by aging (Figure 2). According to previous results, collagen I and fibronectin were increased, and laminin expression was reduced in 2-year-old mice with respect to younger animals. Therefore, our results and prior data collectively suggest that aged lungs display unique ECM components, and those alterations could contribute to the onset of age-related lung diseases.

It may be expected that changes that occur in the composition of the ECM during aging may have an impact on its biomechanical properties. This information is crucial to better understand the physiology and pathophysiology of the lungs, considering thatcell-ECM interaction has been proposed to modify numerous cellular responses during development, aging and disease (Bonnans et al., 2014; Mebratu et al., 2023). In this context, numerous works have estimated the mechanical properties of

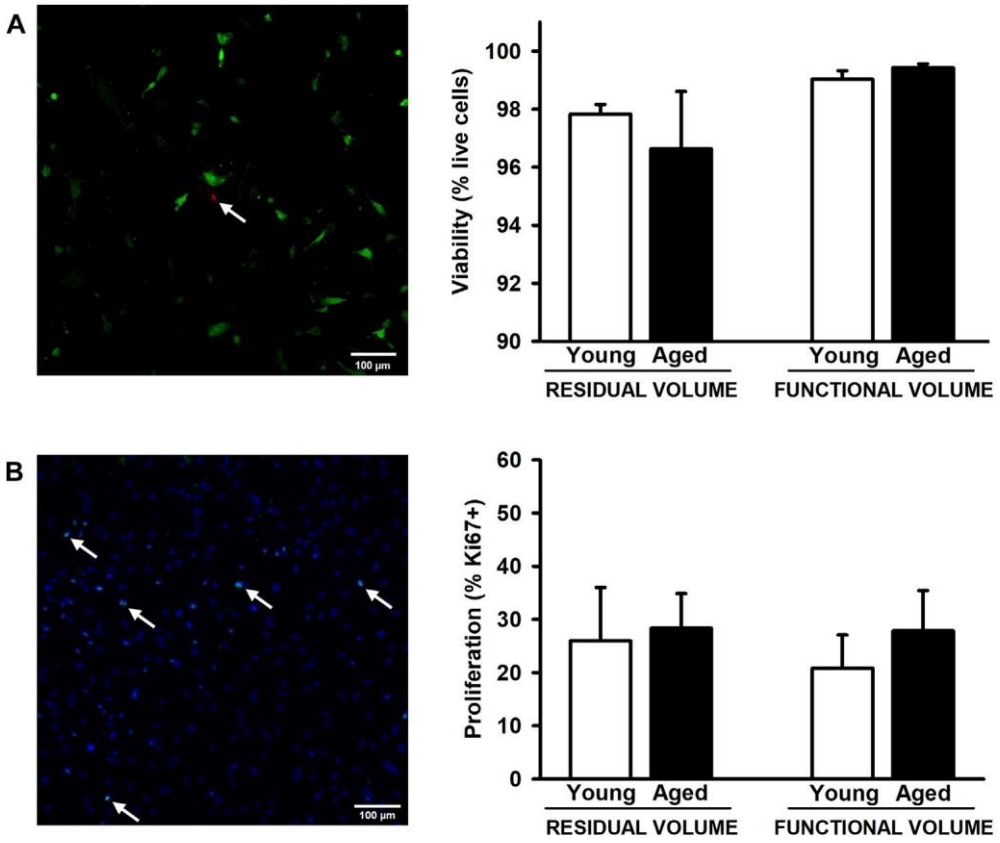

FIGURE 4
Proliferation and viability of mesenchymal stromal cells cultured on decellularized lung ECM. No changes were observed in viability (A) and proliferation (B) among all experimental groups. Arrows indicates some dead cells (A) and Ki67+ cells (B). Scale bar = 100 µm, values are represented as mean ± SE.

murine and human lungs at macroscale by indenting lung biopsies, stretching lung tissue strips, measuring whole lung compliance and elastance, and bulk modulus (Lai-Fook and Hyatt, 1985; Suki et al., 2022b). Although there are discrepancies on the Young's modulus values, all studies suggest an increased stiffness in the aged lung (Suki et al., 2022b). However, very limited data is currently available in the literature at nanoscale level. In accordance to our results, Melo et al. reported a tendence of increase on local stiffness in decellularized murine lungs at FV conditions (Melo et al., 2014). Sicard D et al. observed that non-decellularized lung tissues from 41 to 60 years/o subjects were stiffer than lung samples from 11 to 30 years/o subjects by using AFM in 10-µm thickness tissue slices from organ donors (Sicard et al., 2018). In contrast, Miura K suggests that lungs are gradually softening with age. The lung tissue stiffness from human samples was correlated to the speed of sound measured using a scanning acoustic microscope (Miura, 2022). Hence, the scarce existing data on lung biomechanics and aging appears to be contentious, likely due to variations in species, methodologies, and the use of native or decellularized samples across different studies. Another notable common characteristic in biomechanical studies of the lung is the absence of agreement regarding lung tissue stretch during measurements. Indeed, most studies relying on *ex vivo* experimental assessments use non-inflated lungs at RV (Sicard et al., 2018; Miura, 2022). However, recent observations highlight that alterations in tissue stretch during breathing can correlate with changes in ECM stiffness (Jorba et al., 2019). Given the variations in ECM content and the modifications in protein ECM crosslinks associated with certain lung diseases and aging, it is imperative to consider the level of tissue stretch during AFM measurements. In this manuscript, we describe for the first time how aging modifies some biomechanical properties of the lung at the microscale in non-inflated (RV) and physiologically inflated (FV) conditions. To reach the FV, the lungs were inflated with 0.3 mL of OCT solution (1:3 diluted) as previously reported (Mitzner et al., 2001; Uriarte et al., 2016). The amount instilled was the same in both groups considering the minimal change in lung volume (~20%) between young (4–6 months old) and aged (20–24 months old) mice (Elliott et al., 2016). As expected, changes in the ECM are correlated with alterations in ECM stiffness and adhesion forces exerted by the ECM during aging (Figure 3). Most importantly those changes are strongly dependent on the level of lung stretch. In this regard, it is noticeable that ECM during aging is softer when measured at RV but it becomes stiffer when measured at FV. A similar response was observed when unspecific adhesion forces were measured, being higher only in lung decellularized samples from young animals in RV. However, no changes in viscoelasticity were detected. Our findings may be related to the organization of collagen bundles at the microscale, as it has been reported that older collagen fibers display a straighter appearance and are less prone to waviness. In

this connection, these differences in straightness or waviness are likely related to differences in collagen fibrils crosslinking at the nanoscale (Sobin et al., 1988). A such, we speculate that collagen in older lungs may be crosslinked in a way to make it organize in a straighter manner, giving rise to a more compliant response in unstretched conditions (RV), but that such organization may lead to a strong strain-hardening response under stretched (FV) conditions. Conversely, the crosslinking of collagen fibrils in younger lungs may be more isotropic, giving rise to a less compliant unstretched lung but also less prone to strain-hardening. While these are interesting speculations, a nanoscale analysis of collagen fibrils and their crosslinks would be needed to confirm them, followed potentially by computational analysis to assess what would be the response to different stretch (thus inflation) levels.

As proof of concept, we employed these lung scaffolds from young and aged animals and at RV and FV conditions to repopulate MSCs. Despite the distinct biomechanical characteristics, we observed comparable cell attachment, viability, and proliferation across all conditions (Figure 4) in concordance with Sokocevika and Wagner et al. findings on aged lungs (Sokocevica et al., 2011; Wagner et al., 2014). These results suggest that the alterations in ECM composition and its mechanical properties are not enough to modulate MSCs proliferation as occurs in other diseases such pulmonary fibrosis with more relevant biomechanical alterations (Júnior et al., 2021; Qin et al., 2023). However, this model holds promise for advancing our comprehension of how aging and tissue stretch may alter other biological aspects which could be more susceptible such as cell differentiation and motility in MSCs and other pulmonary cells. Consequently, this work opens the opportunity to better understand the association of aging with regenerative medicine, lung cancer, and other chronic pulmonary diseases in more specifically designed studies.

5. Conclusion

This work provides novel insights into pulmonary ECM biomechanical alterations associated with aging at non-inflated (RV) and physiologically inflated (FV) lungs. Our findings indicate that aging induces changes in ECM protein composition, leading to ECM stiffness and adhesion force modifications depending on lung volume (RV and FV). The ECM biomechanical alterations caused by aging did not modify MSCs viability and proliferation. However, the use of decellularized lung scaffolds from aged and/or other lung disease murine/human under physiomimetic conditions (FV) is crucial for a comprehensive understanding of how biomechanical properties in the lung may contribute to susceptibility and progression of chronic lung diseases, lung development and cancer.

Data availability statement

The raw data supporting the conclusion of this article will be made available by the authors, without undue reservation.

Ethics statement

Ethical approval was not required for the studies on humans in accordance with the local legislation and institutional requirements because only commercially available established cell lines were used. The animal study was approved by the Ethical Committee of the University of Barcelona and Generalitat de Catalunya (OB 168/19 and 10972). The study was conducted in accordance with the local legislation and institutional requirements.

Author contributions

AU: Data curation, Formal Analysis, Investigation, Methodology, Supervision, Writing–original draft, Writing–review and editing. MN: Data curation, Formal Analysis, Investigation, Methodology, Supervision, Writing–review and editing. HS-F: Data curation, Investigation, Methodology, Supervision, Writing–review and editing. JO: Supervision, Writing–review and editing, Funding acquisition. RF: Funding acquisition, Supervision, Writing–review and editing, Project administration. NG: Funding acquisition, Project administration, Supervision, Writing–review and editing, Conceptualization, Data curation, Formal Analysis, Investigation, Methodology, Resources, Software. IA: Conceptualization, Data curation, Formal Analysis, Funding acquisition, Investigation, Methodology, Project administration, Resources, Supervision, Writing–review and editing, Writing–original draft.

Funding

The author(s) declare that financial support was received for the research, authorship, and/or publication of this article. The publication is part of the projects PID2019-108958RB-I00 and PID2020-113910RB-I00 funded by MICIU/AEI/10.13039/501100011033. The projects PID2022-140774OB-I00, PID2020-116808RB-I00, PID2021-128674OB-I00 funded by MICIU/AEI/10.13039/501100011033 and FEDER, UE and the project 900-2019 from SEPAR. MN was funded by the European Union's Horizon 2020 research and innovation programme under the Marie Sklodowska-Curie grant agreement No. 812772.

Acknowledgments

The authors acknowledge the use of Biorender.com.

Conflict of interest

The authors declare that the research was conducted in the absence of any commercial or financial relationships that could be construed as a potential conflict of interest.

The author(s) declared that they were an editorial board member of Frontiers, at the time of submission. This had no impact on the peer review process and the final decision.

Publisher's note

References

Álvarez, D., Levine, M., and Rojas, M. (2015). Regenerative medicine in the treatment of idiopathic pulmonary fibrosis: current position. *Stem Cells Cloning* 8, 61–65. doi:10.2147/SCCAA.S49801

Bonenfant, N. R., Sokocevic, D., Wagner, D. E., Borg, Z. D., Lathrop, M. J., Lam, Y. W., et al. (2013). The effects of storage and sterilization on de-cellularized and re-cellularized whole lung. *Biomaterials* 34 (13), 3231–3245. doi:10.1016/j.biomaterials.2013.01.031

Bonnans, C., Chou, J., and Werb, Z. (2014). Remodelling the extracellular matrix in development and disease. *Nat. Rev. Mol. Cell Biol.* 15 (12), 786–801. doi:10.1038/nrm3904

Bos, L. D., Martin-Loeches, I., and Schultz, M. J. (2018). ARDS: challenges in patient care and frontiers in research. *Eur Respir Rev Off J Eur Respir Soc* 27 (147), 170107. doi:10.1183/16000617.0107-2017

Burgess, J. K., and Harmsen, M. C. (2022). Chronic lung diseases: entangled in extracellular matrix. *Eur. Respir. Rev.* 31, 210202. doi:10.1183/16000617.0202-2021

Burgstaller, G., Oehrle, B., Gerckens, M., White, E. S., Schiller, H. B., and Eickelberg, O. (2017). The instructive extracellular matrix of the lung: basic composition and alterations in chronic lung disease. *Eur. Respir. J.* 50, 1601805. doi:10.1183/13993003.01805-2016

Cho, S. J., and Stout-Delgado, H. W. (2020). Aging and Lung Disease. *Annu. Rev. Physiol.* 82, 433–459. doi:10.1146/annurev-physiol-021119-034610

Elliott, J. E., Mantilla, C. B., Pabelick, C. M., Roden, A. C., and Sieck, G. C. (2016). Aging-related changes in respiratory system mechanics and morphometry in mice. *Am. J. Physiol. Lung Cell Mol. Physiol.* 311 (1), L167–L176. doi:10.1152/ajplung.00232.2016

Faner, R., Rojas, M., Macnee, W., and Agustí, A. (2012). Abnormal lung aging in chronic obstructive pulmonary disease and idiopathic pulmonary fibrosis. *Am. J. Respir. Crit. Care Med.* 186 (4), 306–313. doi:10.1164/rccm.201202-0282PP

Godin, L. M., Sandri, B. J., Wagner, D. E., Meyer, C. M., Price, A. P., Akinnola, I., et al. (2016). Decreased laminin expression by human lung epithelial cells and fibroblasts cultured in acellular lung scaffolds from aged mice. *PLoS One* 11 (3), 01509666–e151017. doi:10.1371/journal.pone.0150966

Hoffman, E. T., Uhl, F. E., Asarian, L., Deng, B., Becker, C., Uriarte, J. J., et al. (2023). Regional and disease specific human lung extracellular matrix composition. *Biomaterials* 293, 121960. doi:10.1016/j.biomaterials.2022.121960

Hopkins, E., and Sharma, S. (2022). Physiology, functional residual capacity. StatPearls. Available from https://www.ncbi.nlm.nih.gov/books/NBK500007/ (Accessed December 26, 2022).

Huang, K., Mitzner, W., Rabold, R., Schofield, B., Lee, H., Biswal, S., et al. (2007). Variation in senescent-dependent lung changes in inbred mouse strains. *J. Appl. Physiol.* 102 (4), 1632–1639. doi:10.1152/japplphysiol.00833.2006

Huang, K., Rabold, R., Schofield, B., Mitzner, W., and Tankersley, C. G. (2007). Age-dependent changes of airway and lung parenchyma in C57BL/6J mice. *J. Appl. Physiol.* 102 (1), 200–206. doi:10.1152/japplphysiol.00400.2006

Jorba, I., Beltrán, G., Falcones, B., Suki, B., Farré, R., García-Aznar, J. M., et al. (2019). Nonlinear elasticity of the lung extracellular microenvironment is regulated by macroscale tissue strain. *Acta Biomater.* 92, 265–276. doi:10.1016/j.actbio.2019.05.023

Júnior, C., Narciso, M., Marhuenda, E., Almendros, I., Farré, R., Navajas, D., et al. (2021). Baseline stiffness modulates the non-linear response to stretch of the extracellular matrix in pulmonary fibrosis. *Int. J. Mol. Sci.* 22 (23), 12928. doi:10.3390/ijms222312928

Júnior, C., Ulldemolins, A., Narciso, M., Almendros, I., Farré, R., Navajas, D., et al. (2023). Multi-step extracellular matrix remodelling and stiffening in the development of idiopathic pulmonary fibrosis. *Int. J. Mol. Sci.* 24 (2), 1708. doi:10.3390/ijms24021708

Lai-Fook, S. J., and Hyatt, R. E. (1985). Effects of age on elastic moduli of human lungs. *J. Appl. Physiol.* 89 (1), 163–168. doi:10.1152/jappl.2000.89.1.163

Liu, F., Mih, J. D., Shea, B. S., Kho, A. T., Sharif, A. S., Tager, A. M., et al. (2010). Feedback amplification of fibrosis through matrix stiffening and COX-2 suppression. *J. Cell Biol.* 190 (4), 693–706. doi:10.1083/jcb.201004082

Mebratu, Y. A., Soni, S., Rosas, L., Rojas, M., Horowitz, J. C., and Nho, R. (2023). The aged extracellular matrix and the profibrotic role of senescence-associated secretory phenotype. *Am. J. Physiol. Cell Physiol.* 325 (3), C565–C579. doi:10.1152/ajpcell.00124.2023

Melo, E., Cárdenes, N., Garreta, E., Luque, T., Rojas, M., Navajas, D., et al. (2014). Inhomogeneity of local stiffness in the extracellular matrix scaffold of fibrotic mouse lungs. *J. Mech. Behav. Biomed. Mater* 37, 186–195. doi:10.1016/j.jmbbm.2014.05.019

Mitzner, W., Brown, R., and Lee, W. (2001). *In vivo* measurement of lung volumes in mice. *Physiol. Genomics* 4 (3), 215–221. doi:10.1152/physiolgenomics.2001.4.3.215

Miura, K. (2022). Stiffness reduction and collagenase resistance of aging lungs measured using scanning acoustic microscopy. *PLoS One* 17 (2), e0263926. doi:10.1371/journal.pone.0263926

Narciso, M., Martínez, Á., Júnior, C., Díaz-valdivia, N., Ulldemolins, A., Neal, K., et al. (2022). Lung micrometastases display ECM depletion and softening while macrometastases are 30-fold stiffer and enriched in fi-bronectin. *Cancers* 43, 1–29. doi:10.3390/cancers15082404

Narciso, M., Otero, J., Navajas, D., Farré, R., Almendros, I., and Gavara, N. (2021). Image-based method to quantify decellularization of tissue sections. *Int. J. Mol. Sci.* 22 (16), 8399. doi:10.3390/ijms22168399

Narciso, M., Ulldemolins, A., Júnior, C., Otero, J., Navajas, D., Farré, R., et al. (2022). Novel decellularization method for tissue slices. *Front. Bioeng. Biotechnol.* 10, 832178–832213. doi:10.3389/fbioe.2022.832178

Narciso, M., Ulldemolins, A., Júnior, C., Otero, J., Navajas, D., Farré, R., et al. (2022). A fast and efficient decellularization method for tissue slices. *Bio-protocol* 12 (22), e4550. doi:10.21769/BioProtoc.4550

ONeill, J. D., Anfang, R., Anandappa, A., Costa, J., Javidfar, J. J., Wobma, H. M., et al. (2013). Decellularization of human and porcine lung tissues for pulmonary tissue engineering. *Bone* 96 (3), 1046–1055. doi:10.1016/j.athoracsur.2013.04.022

Onursal, C., Dick, E., Angelidis, I., Schiller, H. B., and Staab-Weijnitz, C. A. (2021). Collagen biosynthesis, processing, and maturation in lung ageing. *Front. Med.* 8, 593874. doi:10.3389/fmed.2021.593874

Podolsky, M. J., Yang, C. D., Valenzuela, C. L., Datta, R., Huang, S. K., Nishimura, S. L., et al. (2020). Age-dependent regulation of cell-mediated collagen turnover. *JCI insight* 5 (10), e137519. doi:10.1172/jci.insight.137519

Qin, L., Liu, N., Bao, C.-M., Yang, D.-Z., Ma, G.-X., Yi, W.-H., et al. (2023). Mesenchymal stem cells in fibrotic diseases-the two sides of the same coin. *Acta Pharmacol. Sin.* 44 (2), 268–287. doi:10.1038/s41401-022-00952-0

Rebelo, L. M., Cavalcante, P. N., de Sousa, J. S., Mendes Filho, J., Soares, S. A., and Soares, J. B. (2014). Micromorphology and microrheology of modified bitumen by atomic force microscopy. *Road. Mater Pavement Des.* 15 (2), 300–311. doi:10.1080/14680629.2013.869885

Rojas-Ruiz, A., Boucher, M., Gill, R., Gélinas, L., Tom, F.-Q., Fereydoonzad, L., et al. (2023). Lung stiffness of C57BL/6 versus BALB/c mice. *Sci. Rep.* 13 (1), 17481. doi:10.1038/s41598-023-44797-x

Sicard, D., Haak, A. J., Choi, K. M., Craig, A. R., Fredenburgh, L. E., and Tschumperlin, D. J. (2018). Aging and anatomical variations in lung tissue stiffness. *Am. J. Physiol. Lung Cell Mol. Physiol.* 314 (6), L946-L955. doi:10.1152/ajplung.00415.2017

Sobin, S. S., Fung, Y. C., and Tremer, H. M. (1988). Collagen and elastin fibers in human pulmonary alveolar walls. *J. Appl. Physiol.* 64 (4), 1659–1675. doi:10.1152/jappl.1988.64.4.1659

Sokocevica, D., Bonenfanta, N. R., Wagnera, D. E., Borga, Z. D., Lathropa, M. J., Lamb, Y. W., et al. (2011). The effect of age and emphysematous and fibrotic injury on the re-cellularization of de-cellularized lungs. *Biomaterials* 4 (164), 3256–3269. doi:10.1016/j.biomaterials.2013.01.028

Suki, B., and Bates, J. H. T. (2008). Extracellular matrix mechanics in lung parenchymal diseases. *Respir. Physiol. Neurobiol.* 163 (1–3), 33–43. doi:10.1016/j.resp.2008.03.015

Suki, B., Bates, J. H. T., and Bartolák-Suki, E. (2022). Remodeling of the aged and emphysematous lungs: roles of microenvironmental cues. *Compr. Physiol.* 12 (3), 3559–3574. doi:10.1002/cphy.c210033

Suki, B., Bates, J. H. T., and Bartolák-Suki, E. (2022). Remodeling of the aged and emphysematous lungs: roles of microenvironmental cues. *Compr. Physiol.* 12 (3), 3559–3574. doi:10.1002/cphy.c210033

Syed, O., Walters, N. J., Day, R. M., Kim, H. W., and Knowles, J. C. (2014). Evaluation of decellularization protocols for production of tubular small intestine submucosa scaffolds for use in oesophageal tissue engineering. *Acta Biomater.* 10 (12), 5043–5054. doi:10.1016/j.actbio.2014.08.024

Takubo, Y., Hirai, T., Muro, S., Kogishi, K., Hosokawa, M., and Mishima, M. (1999). Age-associated changes in elastin and collagen content and the proportion of types I and III collagen in the lungs of mice. *Exp. Gerontol.* 34 (3), 353–364. doi:10.1016/s0531-5565(99)00017-0

Thannickal, V. J. (2013). Mechanistic links between aging and lung fibrosis. *Biogerontology* 14 (6), 609–615. doi:10.1007/s10522-013-9451-6

Uriarte, J. J., Meirelles, T., Del Blanco, D. G., Nonaka, P. N., Campillo, N., Sarri, E., et al. (2016). Early impairment of lung mechanics in a murine model of marfan syndrome. *PLoS One* 11 (3), 1–19. doi:10.1371/journal.pone.0152124

Uriarte, J. J., Uhl, F. E., Rolandsson Enes, S. E., Pouliot, R. A., and Weiss, D. J. (2018). Lung bioengineering: advances and challenges in lung decellularization and recellularization. *Curr. Opin. Organ Transpl.* 23 (6), 673–678. doi:10.1097/MOT.0000000000000584

Wagner, D. E., Bonenfant, N. R., Parsons, C. S., Sokocevic, D., Brooks, E. M., Borg, Z. D., et al. (2014). Comparative decellularization and recellularization of normal versus emphysematous human lungs. *Biomaterials* 35 (10), 3281–3297. doi:10.1016/j.biomaterials.2013.12.103

Chapter VIII.

RESULTS SUMMARY

This thesis comprises three research articles and preliminary findings aimed at developing ECM-based models to understand respiratory diseases and explore their potential as ECM-based therapies.

In the first part of the thesis, L-HG and its released products were characterised by liquid mass spectrometry. The objective was to study how the use of L-HG as respiratory models can affect cells. Results obtained in the first study prompted the need of more clarification of the lung hydrogel when it is used as a model for acellular therapy. Therefore, L-HG release proteins were analysed, and their immunomodulatory and regenerative effects were assessed.

The detailed investigation performed in the first study provided us with novel insights regarding the products released from the L-HG, either trapped inside the mesh-like structure or because its degradation. Protein release peak was at 24 hours, with a decline by day 7. L-HG fibre diameter decreased by about 30% after 21 days, while the ECM structure remained intact. When alveolar epithelial cells were exposed to L-HG release products from day 1, IL-6 and TNF-α expression increased by 46-fold and 61-fold respectively, being higher than the induced by LPS. Pro-inflammatory cytokine expression was absent when alveolar epithelial cells were cultured with L-HG matrikines from day 7. Both day 1 and day 7 matrikines significantly increased wound closure in lung epithelial cell models (1.89 and 1.76 - fold increase respectively). Liquid mass spectrometry identified 181 proteins, mainly collagens and glycoproteins, with some non-ECM residuals (probably from decellularization). The comparison between days 1 and 7 revealed that 25 proteins were exclusively released at day 1, 8 proteins were released only at day 7, and 107 proteins were released at both times. ECM-related proteins were maintained during the different release times, while cell-related proteins were more prevalent at early stages. Variability was observed in the protein release over time since there was notably a decrease in the majority of collagens, laminins, and elastin release. Some proteins exhibited consistent release like collagen VI-α3 chain and laminin-α3, suggesting prolonged cellular interaction.

The second study showed that there is a combination of isolated vesicles and ECM-bound vesicles following the conventional EV's isolation protocol in the MSCs cultured on L-HG.

As expected, L-HG showed a higher release of ECM-bonded proteins (1250 µg/mL) that was decreased after consecutive daily washes (61.9 µg/mL after 7 days). The proportion corresponding to ECM-vesicles was 1/6 ratio with respect to the total protein release (227 µg/mL). Similarly with the ECM-bonded proteins, the ECM -vesicles were reduced reaching plateau after 3 daily washes (19 µg/mL). Even with the 3 days washes of the L-HG, nanoparticle tracking analysis showed a significant secretion of nanoparticles with similar physical characteristics to those released by MSCs. Both EVs isolated from MSCs cultured on conventional plastic and ECM-vesicles isolated from acellular L-HG exhibited a similar NTA profile, with a diameter of approximately 180 nm. Consequently, differentiating between EVs and ECM-vesicles from MSCs and L-HG, respectively, was not feasible when MSCs were cultured on L-HG. Moreover, the number of ECM-vesicles released from L-HG were still higher than EVs secreted by MSCs. Accordingly, the protein quantification from isolated vesicles showed a 3-fold increase in those from acellular L-HG (309 µg/mL, $p < 0.01$) and L-HG with MSCs (363 µg/mL, $p < 0.01$) compared to MSCs cultured on plastic (134 µg/mL). The administration of EVs and/or ECM-vesicles to a monolayer of epithelial cells led to increased wound closure percentages. Specifically, a notable increase in closure was observed when L-HG-derived vesicles were present (12.9% vs. 7.1% controls, $p < 0.05$). When wound closure was normalized by the total amount of protein applied, EVs derived from MSCs demonstrated the most efficient wound healing compared to other L-HG conditions.

Following the promising regenerative outcomes achieved in the preceding two research articles, the subsequent part of the thesis aimed to investigate the therapeutic potential of the L-HG as ECM-based therapies. Accordingly, the lung ECM-derived hydrogel was administered in an ALI rat model to study its regenerative capacity and immunomodulatory effects previously reported in vitro in rat lung epithelium (experiments 1 and 2). Preliminary findings presented here indicated that L-HG administration led to faster weight recovery. However, survival was lower compared to MSC treatment (75% vs. 100%) indicating that the ECM dosage should be still optimized. Rat lung weight was greater in ALI rats (1073.3 mg) compared to controls ($p < 0,001$) indicating increased lung edema. The use of conventional saline-MSCs resulted in reduction of lung weigh (750 mg) respect ALI rats ($p < 0.05$), while the use of L-HG showed

a non-significant reduction of lung weight (928.16 mg). Histological analysis revealed less inflammation, edema, and hemorrhage in treated lungs, with undamaged tissue and normal alveolar architecture. H&E staining showed infiltration of inflammatory cells in ALI (52.11 neutrophil count/image field) compared to controls ($p < 0.001$) with a reduction of the alveolar empty space in the ARDS rats compared to controls (18,30 %, $p < 0,001$). The instillation of MSCs (33.19%, $p = 0.06$ vs. ALI) and L-HG (38.02%, $p < 0.001$ vs. ALI) to the diseased rats produced a recovery of the alveolar empty space and a mitigation of neutrophil infiltration (16.91 neutrophil count/image field, $p < 0.001$ and 16.13 neutrophil count/image field, $p < 0.0001$, respectively). Regarding the expression of pro-inflammatory cytokines, MSC's instillation reduced the levels of IL-6 ($p < 0.05$) as IL-1 β ($p < 0.01$). The use of L-HG hindered the expression IL-6 ($p = 0.05$). However, L-HG did not affect the anti-inflammatory marker IL-1β. The MSCs were found engrafted in lung tissue 72 hours after instillation.

To better understand how ECM- based therapies could be used in ARDS treatment it is necessary to understand how aging affects the ECM, since ARDS is more prevalent in aged people. In the fourth research article of the thesis, age-driven changes in the ECM are characterized and how they can affect ECM – cell crosstalk. Protein composition of the lung ECM is affected by aging. Specifically, a decreased level of laminin (~15%, $p = 0.041$) and increased expressions of fibronectin (~15%, $p < 0.001$) and collagen type I (19%, $p < 0.001$) were observed in samples from aged animals. Lung ECM biomechanics were measured by AFM at RV (collapsed) and at FV (stretched) conditions. Regarding lung ECM stiffness, the Young's modulus, measured at RV, was significantly lower ($p = 0.003$) in aged mice (0.26 ± 0.03 kPa) when compared to that assessed in younger animals (0.47 ± 0.04 kPa). Conversely to RV, the stiffness of the lung ECM, measured at FV, was significantly increased ($p = 0.002$) in aged mice (0.54 ± 0.06 kPa) with respect to the younger counterparts (0.36 ± 0.03 kPa). Thus, these findings reveal that the effects of aging on ECM stiffness strongly depend on lung volume, aged lungs manifested a significant ~ 2-fold increase in ECM stiffness under FV conditions ($p < 0.001$). Conversely, a tendency of decrease ($p = 0.063$) was observed in their younger counterparts. Regarding ECM viscosity, it remained similar between young/aged and RV/FV conditions The unspecific adhesion forces exerted by the ECM showed no changes between young (1.35 ± 0.15 nN)

and aged (1.65 ± 0.14 nN) lung acellular ECM at FV conditions. However, the adhesion measured in young lung ECM (2.29 ± 0.39 nN) was ~2- fold higher ($p = 0.001$) with respect to aged counterparts (1.02 ± 0.12 nN) at RV conditions. In a similar way to ECM stiffness measurements, the lung ECM exerted different adhesion forces behaviour between both lung volumes (RV and FV) ($p = 0.006$) only in young animals. After 72 h of the lung scaffold repopulation with MSCs, they showed a spread morphology indicative of their attachment to the scaffold. Additionally, no effects due to aging and lung volume were observed in cell viability with values higher than 96.5% in all groups. In concordance with cell viability, the MSCs proliferation, quantified as a percentage of positive Ki67 cells, did not present significative differences in any condition.

Chapter IX.

DISCUSSION

While providing mechanical support to cells, the ECM modulates cellular behaviour through biochemical signalling and is involved in maintaining tissue homeostasis and organising responses to injury and disease.

Specifically, lung ECM has different functions including structural support and the regulation of pulmonary function and health. Additionally, the tissue integrity which is essential for cellular signalling, immune responses, and tissue repair mechanisms is maintained by the ECM composition. Alterations in the lung ECM composition are translated in a direct impact in lung physiology (i.e. aging or in pathological conditions such as ARDS). Understanding the collaboration between ECM based models and cells is of great importance for deciphering the pathophysiology of lung disorders and discovering effective therapeutic approaches. From the release of bioactive molecules and matrikines to the biomechanical properties, all these aspects can contribute individually to lung homeostasis.

The conventional lung *in vitro* models, that rely on traditional cell culture techniques, often fail to capture the detailed microenvironmental cues essential for replicate lung physiology. The presence of a complex scaffold composed of ECM proteins with realistic mechanical properties and under cyclical mechanical stretch are usually not represented in most available models. Consequently, there is a lack of translational significance in the findings from *in vitro* experiments to *in vivo* scenarios, particularly in the context of respiratory diseases. This inconsistency contributes to the insufficiency of correlation between preclinical studies and clinical outcomes in respiratory research (59,65,66). Addressing this issue, this thesis aims to develop and characterize novel models, like ECM – derived hydrogels and lung scaffolds, for respiratory research. Whereas scientific articles I and II are focused on the L-HG development and characterization, with complementary preliminary findings (article III) for their application in ARDS therapy, article IV studies two different ECM models for the assessment of age-related changes in composition and stiffness of the lung.

Recent studies have revealed the promising potential of physiomimetic ECM-derived hydrogels as advanced *in vitro* models, replicating the essential features of the cell environment (103). Hydrogels offer distinct advantages over conventional culture methods; they are easily tuneable for adjustment of biophysical characteristics and

facilitate MSCs engraftment and viability post-transplantation (110). MSCs therapy has gained attention as a potential treatment for respiratory diseases. However, clinical trials have not yet shown a therapeutic effect and other alternatives are still considered. In this sense, the paracrine activity of MSCs has emerged as a novel therapeutic alternative. The combination of ECM-derived hydrogels and MSCs paracrine approaches may have a synergistic effect in regenerative medicine, offering new possibilities for more effective treatment strategies.

In the first chapter of the present thesis, the composition of the L-HG and its released biomolecules have been characterized and studied in an *in vitro* monolayer of alveolar epithelial cells. The lung epithelium plays a critical role as a key regulator of innate responses to damage (166). It is constantly monitoring its environment for changes and initiating immune reactions when needed (49,166). Recent studies have highlighted the importance of the bioactive molecules released by lung hydrogels that interact with resident lung cells. Nevertheless, the information about these matrikines and their effect in the cells is still scarce.

In this work, the matrikines released by the L-HG triggered a significant inflammatory reaction. Among the pro-inflammatory cytokines, IL-6 plays a crucial role in transitioning to a reparative environment, which is essential for wound healing (167). Moreover, TNF-α induces the production of other cytokines promoting alveolar epithelial repair, spreading, and migrating on the edge of wounds (51). They also activate the expression of adhesion molecules and stimulate growth and migration. Our findings align with the second article presented in this thesis that demonstrated the L-HG's ability to promote epithelial migration. Surprisingly, rinsing L-HG prior to use reduced this inflammatory response, indicating a clear link between L-HG derived matrikines and tissue repair. When the L-HG was rinsed for 21 days there was a clear decrease in collagens fibre diameter suggesting that the proteins released must come from the hydrogel structure or were trapped inside of it in concordance with previous studies (101). The proteins released from the L-HG decreased significantly after day 7; therefore, the study was focused on comparing the released proteins at these two different times (day 1 and day 7). Even the significantly decrease of proteins after day 7, the L-HG release products still promoted cell migration.

The liquid spectrometry revealed that the L-HG was composed with a total of 181 proteins, mainly collagens and glycoproteins, as well as a big percentage of non-ECM proteins that were residuals of the decellularization process. The digestion step in L-HG formation gives rise to bioactive peptides, potentially the key players among the proteins secreted by the L-HG. Pepsin is a non-specific protease used in the synthesis of L-HG. It cleaves peptide bonds between aromatic aminoacids like tryptophan, tyrosine, and phenylalanine. This enzymatic activity is crucial due to the non-soluble nature of certain ECM proteins. However, since pepsin has non-specificity, it also leads to the breakdown of other ECM proteins. The hydrolysis of other components is influenced by the digestion time and particle size during the production of L-HG. Consequently, the site of digestion determines the types of peptides released, thereby influencing their physiological properties (168).

Comparing the composition of the released species at days 1 and 7, we found that there were 25 proteins exclusively released at day 1, only 8 proteins released exclusively at day 7, and 107 proteins that are being released at both times. When comparing the localization of exclusive proteins at both times, ECM-related proteins were maintained while cell-related proteins were much more present at early stages, as expected. By looking at the abundances of proteins that were released at both days 1 and 7 we can observe a huge heterogeneity in their release. When focusing on the proteins related to collagens, laminins, and elastin that are known to be sources of matrikines in the lung, there was a clear decrease in the release of most of them. For example, the collagen XIV-α1 chain was highly released at early stages but almost not present at day 7. Collagen XIV has been implicated in the regulation of fibrillogenesis, cell proliferation, and differentiation in the lung (169). When comparing all the proteomic data with all the already described matrikines found from lung ECM, the predominant bioactive matrikine emanating from lung collagen was PGP repeats. PGP may play an important role in facilitating wound repair and may restore demarcated airway epithelium in concordance with our results in the 1st and 2nd articles of this thesis. Moreover, PGP-induced signalling is considered a feed-forward inflammatory signal (17). These repeats were highly present in the protein sequence of all the collagen proteins released at day 1, which may explain the high inflammation cytokines expression from the epithelial cells when the released

proteins from the L-HG, without rinsing, were added. Among the collagens released there was collagen IV α5 chain, known as lamstatin. It is associated with decreased tumor cell invasion in breast, prostate, bronchoalveolar, and colorectal cancer (170). In fact, collagen IV matrikines have been implicated in inhibiting pathological angiogenesis and suppressing proliferating endothelial cells and tumor growth (30,171). Together, collagen and elastin-derived matrikines further stimulate the recruitment of inflammatory cells to the lungs (19,20).

Looking at the proteins that present almost no variation in the release over time, we can identify the proteins that will be acting on the cells even after 7 days of consecutive rinsing, explaining the persistent migratory effects. Collagen VI α3 chain showed sustained release. It is a peptide also called endotrophin, that functions as a hormone. Known to promote fibrosis and inflammation, endotrophin is released during ECM remodelling. Its effects include stimulating fibrosis, promoting endothelial cell migration, and enhancing macrophage infiltration into damaged tissue (172). Laminin-subunit α3 was also released equally at day 1 and day 7. This protein, known to safeguard alveolar epithelial cells from the detrimental effects of fibrosis, remains stable over time (173). By examining the sequence of peptides, various regions were identified as potential sites containing epidermal growth factor (EGF)-like domains linked to proliferation and migration (174,175). Moreover, it has been described that Laminin α3 contains angiogenic peptides (A13 an C16) that increase wound reepithelialisation (22,36). Altogether, these peptides contributed to the prolonged epithelial migration effect from the L-HG release components.

In the lungs, the signalling pathways activated by the action of matrikines match the signalling from the ECM proteins they originate from. Accordingly, structural proteins such as collagen and elastin can trigger leukocyte activation and inflammation, while the breakdown products of basement membrane components like laminin acts as signalling agents to the epithelial cells including epithelial proliferation, wound repair, alveologenesis and angiogenesis (121). These findings represent a new avenue for the utilization of lung-derived hydrogels in the treatment of respiratory diseases. In addition to the biomimetic substrate properties, the L-HG also includes the biological cues and ECM proteins released during both physiological and pathophysiological processes.

The second chapter of the thesis explores the effect of the EVs secreted from culturing MSCs on L-HG. This study uncovers that L-HG serves as a significant reservoir of vesicles, along with bioactive proteins, capable of influencing various cellular mechanisms, particularly in facilitating lung repair with the interaction of alveolar epithelial cells (15). Surprisingly, the therapeutic effects of the vesicles released by L-HG were comparable to those of MSCs-EVs in a wound healing assay, shedding light on a crucial aspect often overlooked in current studies which is the importance of considering hydrogel-derived vesicles in cell culture methodologies.

The EVs derived from MSCs play a role in maintaining tissue homeostasis. They are characterized by a lipid membrane bilayer and their content and release may depend on the surrounding environment. This study demonstrates the ability of MSC-derived EVs to enhance wound healing in a lung repair model. This result suggests their potential in the treatment of ARDS in patients requiring intervention. Surprisingly, MSC-derived EVs were a minor component among the ECM-vesicles released by the L-HG. The MSC-derived EVs may be masked by the greater amount of ECM-derived vesicles released. Yet, these EVs from MSCs exhibited a greater effect on epithelial repair when normalized by protein count, highlighting their specificity compared to the high heterogeneity of the lung hydrogel composition and release, as already seen in the first study of this thesis. These ECM-bound vesicles may participate in the modulation of the ECM remodelling and tissue regeneration, potentially offering immunomodulatory effects. Although their role remains unclear, our findings indicate the participation of L-HG-derived vesicles in tissue regeneration and repair, potentially explaining the protective role observed in a radiation-induced lung injury model (91).

Due to its natural biodegradability, the lung hydrogel releases a significant amount of proteins during the initial gelation period (101). While conventional EV isolation protocols apparently drastically reduce these proteins, transmission electron microscope images revealed the presence of ECM-bound vesicles attached to small protein fragments from ECM degradation. These degradation products may confer additional benefits, such as antibacterial activity and promoting cell migration and proliferation (176). However, their potential impact on alveolar epithelial wound healing requires further research.

Accordingly, to understand the response generated by different cell types in the presence of L-HG-released vesicles more immunomodulatory studies are needed.

Given the therapeutic potential of the L-HG, the third part of the present thesis is focused on the effect of L-HG in an LPS-induced ALI model. The inherent fluidity of the ECM-derived L-HG makes it suitable for administration via instillation. Since the first hydrogel used to treat lung disorders was synthesised (119), there has been total of 4 preclinical attempts to treat lung related conditions (91,118,119,133), and only 2 in cases of lung injury (91,118). More specifically, the administration of the L-HG has been performed via instillation and nebulization (91). The use of L-HG in this preliminary study revealed that early intervention with ECM-derived hydrogel could prevent ARDS in a rat lung injury model. Specifically, application of L-HG was able to reduce lung injury as assessed by histology, to reduce neutrophil infiltration and to reduce lung inflammation. Likewise, it has been reported that ECM- derived hydrogel promotes a reduction in oxidative stress and inflammation in lung injury caused by radiation exposure in rats (118). Specifically, L-HG and MSCs produced a notable suppression in the expression of proinflammatory cytokines IL-6 and IL-1β. Both cytokines are known for playing a pivotal role in the initiation of lung injury (25) and have been correlated with unfavourable prognoses in patients with ARDS (26,27). Xu Fet et al. also found a reduction of these inflammatory markers with the presence of MSCs (177). The preliminary results from this thesis shows a downregulation in the levels of IL-6 following treatment with ECM-derived hydrogel confirming its therapeutic potential in ARDS. These results are also similar to the latest preclinical study that uses L-HG as treatment for lung fibrosis in a rat model (133). In fact, L-HG therapeutic efficacy is in concordance with the previous chapters of the thesis, where the release bioactive peptides, nano-vesicles, chemokines, cytokines which the cells can interact with potentiate tissue repair (27). Ultimately, while several studies have presented preclinical indications of the therapeutic potential of ECM-derived hydrogel in animal models of lung diseases, up until now there is no clinic trial involving human participants employing lung hydrogels for the treatment of lung diseases. More information regarding the benefits of L-HG in respiratory diseases are still needed.

Unfortunately, our preliminary data also shows a low survival rate in ALI rats treated with L-HG. These negative results could be from a non-optimized dose or density of the L-HG

applied and more effort should be done on optimizing the administration process of the lung hydrogel. This could involve refining the delivery method to ensure proper distribution and retention of the hydrogel within the lung tissue and facilitate its use as vehicle of administration of other EVs or cells. Addressing these issues is essential for maximizing the therapeutic efficacy of lung hydrogel treatment and improving outcomes in animal models of ARDS.

To ensure the proper translation of L-HG and other ECM-based therapies into clinical use, it is of pivotal importance to understand how aging affects the lung ECM. The study of its effects is essential for comprehending the pathophysiology of lung disorders like ARDS, especially considering its higher prevalence in aged populations. The model presented in the last study of this thesis offers insights into the age-induced alterations in ECM biomechanics. This model elucidates how age-related ECM changes contribute to respiratory diseases and progression and opens the window for the development of new therapeutic strategies for mitigating the impact of aging on the lung.

This work also offers novel insights into the translation of age-induced alterations in ECM composition into biomechanical changes because age-related shifts in ECM components contribute to the static lung biomechanics (178). For example, it is known that, collagens and fibronectin dysregulation has been linked to the pathogenesis and progression of numerous chronic lung diseases, which are prevalent among the elderly (179). However, the specific ECM alterations during aging remain poorly understood. Additionally, it is unclear whether age-induced alterations in the ECM could predispose individuals to the development of such diseases. Studies have indicated that aging can influence the synthesis and maturation of various collagen types, resulting in distinct changes in collagen composition and crosslinks (179,180). Other experiments also using age decellularized lungs have shown reduced expression of laminins α3 and α4, elastin, and fibronectin, alongside increased collagen levels compared to young lungs (163). Moreover, collagen degradation is needed for the resolution of lung fibrosis, a process not found in elder mice lungs where there is diminished collagen uptake and, suggesting a potential contribution to age-related fibrosis (181). These findings are consistent with observations by Huang K et al., who noted a reduction in elastin fibres and increased collagen density, leading to increased lung compliance during aging (182,183). As

anticipated, the evaluation of ECM components in decellularized lung scaffolds in this thesis revealed varying alterations with aging consistent with earlier findings. Collagen I and fibronectin levels were elevated, while laminin content was diminished in 2-year-old mice compared to younger counterparts. Therefore, the results presented here combined with previous data, indicate that aging lungs exhibit distinctive ECM compositions, which may play a role in the development of age-related lung diseases.

The existing data regarding lung biomechanics and aging is inconclusive, Some studies show an increase of the stiffness on aged lungs (165,66) while others show a decrease (74). Moreover, there are different methodological variations and scarcity of studies in the literature at the nanoscale level. There is not a consensus on the lungs tissue measurements and stretch. Most of the studies performed the assessment using a RV approach (165,64). However, recent data have showed that changes in tissue stretch produced during spontaneous breathings has a relationship with alterations in ECM stiffness (184). Accordingly, the findings presented here demonstrate age-related alterations in ECM stiffness and adhesion forces that are strongly influenced by the level of lung stretch. Surprisingly, aged lungs showed softer ECM at RV but stiffer at FV, with varying adhesion forces. Even the methodological discrepancies, most of the studies agree with the increase of stiffness tendency as we age (185). In accordance to our results, Melo et al. reported a tendence of increase on local stiffness in decellularized murine lungs at FV conditions (66). These observations may be linked to the arrangement of collagen bundles on a microscale, as studies have indicated that aging collagen fibres tend to appear straighter and exhibit less waviness. These differences in straightness or waviness are likely attributed to variances in collagen fibril crosslinking at the nanoscale (186). Consequently, collagen in older lungs may undergo crosslinking that results in a straighter organization that leads to greater compliance in unstretched conditions. Nonetheless, this organization could contribute to a pronounced strain-hardening response under stretched conditions. In contrast, collagen fibril crosslinking in younger lungs may be more isotropic, resulting in a lung that is less compliant when unstretched but also less susceptible to strain-hardening.

Despite these biomechanical changes, cell behaviour (cell attachment, viability, and proliferation) remains consistent across conditions in concordance with (37,38).

These findings indicate that the changes in ECM composition and its mechanical properties do not appear to sufficiently influence MSC proliferation, unlike in conditions such as pulmonary fibrosis where biomechanical alterations play a more significant role (179,187). Nevertheless, this model shows potential for upgrade the understanding of how aging and tissue stretch may impact other biological processes, likes cell differentiation and motility in MSCs and other pulmonary cells. As a result, this research creates an opportunity to further investigate the relationship between aging and other conditions such as lung cancer and chronic pulmonary diseases.

Regardless the significant contributions made in this thesis, some limitations need to be acknowledged. The main limitation is the use of cells and ECM derived from animal sources. Although animal models provide valuable information of lung physiology and pathology, differences in anatomy, metabolism, physiology, and genetics could limit the translation of the results. In the future, further investigations with human-derived cells and ECM, may provide more clinically relevant data and increase the understanding of L-HG, ARDS, aging and potentially therapeutic approaches.

As a consequence of the scarcity of preclinical studies using L-HG as a therapy for lung diseases, there is a need for more *in vitro* and *in vivo* assays. However, the development of lung hydrogels from humans could be a promising starting point. New methodologies for the obtention of L-HG from humans are still under development (188,189). However, the challenges associated with obtaining healthy human lungs for hydrogel synthesis favour the use of porcine lung hydrogels. On the other hand, in the aging model presented in this thesis, future directions will involve utilizing human lung scaffolds from diseased donors (fibrosis, ALI, emphysema), which may provide valuable insights into how these diseases affect ECM content and biomechanical properties, and their crosstalk with cells. However, the obtention of a healthy lung donor, to be used as a control, without any pathology remains a challenge.

The work presented in this thesis represents a significant contribution to the growing field of physiomimetic modelling with the development and characterization of lung hydrogels and lung scaffolds. Thus, represents a significant advancement in the respiratory research with innovative approaches that replicate the microenvironment of the lung. Moreover,

it helps to move one step forward in the study of the active crosstalk between pulmonary cells and lung ECM. Finally, these models hold immense promise for enhancing the translational relevance of preclinical studies and therefore facilitate the development of more effective clinical treatments for respiratory pathologies.

Chapter X.

CONCLUSIONS

I. Matrikines generated during L-HG production and subsequently released exhibit an effect on alveolar epithelial cells.
   a. Products release from the L-HG produce an inflammatory effect can be mitigated by rinsing the L-HG for one week prior to cell seeding, highlighting a potential strategy to avoid unwanted cellular responses.
   b. Proteomic analysis reveals the ongoing release of various other matrikines even after the rinsing period, which may influence different cellular processes.
   c. Results from this study underscore the importance of not only characterizing the L-HG itself but also considering the substances released from these hydrogels.

II. The active involvement of ECM-vesicles should be considered, particularly when employing tissue-derived hydrogels for cell culture.
   a. The substantial quantity of ECM-vesicles released into supernatants may overshadow MSCs-derived EVs.
   b. ECM- vesicles and MSC-derived EVs promote alveolar epithelial repair.

III. Our study highlights the potential of ECM - lung hydrogels as an early intervention for addressing lung damage in a rat model of ALI.
   a. Treatment with ECM hydrogels significantly decreased lung inflammation, reduced lung edema, and improved histological signs of lung injury in the experimental model.
   b. Further experiments should focus on the optimization of the administration process of the L-HG.

IV. Aging induces alterations in ECM protein composition, resulting in modifications in ECM stiffness and adhesion forces, which vary depending on tissue stretch (RV and FV).
   a. The use of decellularized lung scaffolds from aged donors under FV is crucial for an accurate modelling.
   b. Aged lung becomes stiffer in FV indicating a strain-hardening response.

c. Despite ECM biomechanical changes induced by aging, MSCs viability and proliferation remained unaffected.

Chapter XI.

REFERENCES

1. Delgado BJ, Bajaj T. Physiology, Lung Capacity. In: StatPearls. Treasure Island (FL): StatPearls Publishing; July 24, 2023..

2. Weibel ER. Lung morphometry: the link between structure and function. Cell Tissue Res. 2017;367(3):413–26.

3. Scarpelli EM. The Alveolar Surface Network : A New Anatomy and Its Physiological Significance. 1998;527(December 1997):491–527.

4. Beers MF, Moodley Y. When Is an alveolar type 2 cell an alveolar type 2 cell?: A conundrum for lung stem cell biology and regenerative medicine. Am J Respir Cell Mol Biol. 2017;57(1):18–27.

5. Han SH, Mallampalli RK. The role of surfactant in lung disease and host defense against pulmonary infections. Ann Am Thorac Soc. 2015;12(5):765–74.

6. Roan E, Waters CM. What do we know about mechanical strain in lung alveoli? Am J Physiol - Lung Cell Mol Physiol. 2011;301(5):625–35.

7. Guillot L, Nathan N, Tabary O, Thouvenin G, Le Rouzic P, Corvol H, et al. Alveolar epithelial cells: Master regulators of lung homeostasis. Int J Biochem Cell Biol. 2013;45(11):2568–73.

8. Suki B, Bates JHT. Extracellular matrix mechanics in lung parenchymal diseases. Respir Physiol Neurobiol. 2008;163(1–3):33–43.

9. Burgstaller G, Oehrle B, Gerckens M, White ES, Schiller HB, Eickelberg O. The instructive extracellular matrix of the lung: Basic composition and alterations in chronic lung disease. Eur Respir J. 2017;50:1601805.

10. Zhou Y, Horowitz JC, Naba A, Ambalavanan N, Atabai K, Balestrini J, et al. Extracellular matrix in lung development, homeostasis and disease. Matrix Biol. 2018;73:77–104.

11. Wijsman PC, van Smoorenburg LH, de Bruin DM, Annema JT, Kerstjens HA, Mets OM, et al. Imaging the pulmonary extracellular matrix. Curr Opin Physiol. 2021;22.

12. Kadler KE, Baldock C, Bella J, Boot-Handford RP. Collagens at a glance. J Cell Sci. 2007;120(12):1955–8.

13. Ricard-blum S. The Collagen Family. 2011;1–20.

14. Rozario T, Desimone DW. The extracellular matrix in development and morphogenesis : A dynamic view. Dev Biol. 2010;341(1):126–40.

15. Wenger MPE, Bozec L, Horton MA, Mesquida P. Mechanical Properties of Collagen Fibrils. 2007;93(August):1255–63.

16. Bailey AJ, Macmillan J, Shrewry PR, Tatham AS, Gosline J, Lillie M, et al. Elastic proteins: biological roles and mechanical properties. Philos Trans R Soc London Ser B Biol Sci. 2002;357(1418):121–32.

17. Gosline JM, French CJ. Dynamic mechanical properties of elastin. Biopolymers. 1979 Aug 1;18(8):2091–103.

18. Hoeve CAJ, Flory PJ. The elastic properties of elastin. Biopolymers. 1974 Apr 1;13(4):677–86.

19. Schaefer L, Schaefer RM. Proteoglycans : from structural compounds to signaling molecules. 2010;237–46.

20. Frevert CW, Sannes PL. Matrix proteoglycans as effector molecules for epithelial cell function. Eur Respir Rev. 2005;14(97):137–44.

21. Roman J. Fibronectin and fibronectin receptors in lung development. Exp Lung Res. 1997;23(2):147–59.

22. Ponce ML, Kleinman HK. Identification of redundant angiogenic sites in laminin ⎵ 1 and ⍰1 chains. 2003;285:189–95.

23. Alcaraz J, Xu R, Mori H, Nelson CM, Mroue R, Spencer VA, et al. Laminin and biomimetic extracellular elasticity enhance functional differentiation in mammary epithelia. EMBO J. 2008;27(21):2829–38.

24. Jariwala N, Ozols M, Bell M, Bradley E, Gilmore A, Debelle L, et al. Matrikines as mediators of tissue remodelling. Adv Drug Deliv Rev. 2022;185:114240.

25. Patel DF, Snelgrove RJ. The multifaceted roles of the matrikine Pro-Gly-Pro in pulmonary health and disease. 2018;1–9.

26. Weathington NM, Houwelingen AH Van, Noerager BD, Jackson PL, Kraneveld AD, Galin FS, et al. A novel peptide CXCR ligand derived from extracellular matrix degradation during airway inflammation. 2006;12(3):317–23.

27. Xu X, Gaggar A, Akthar S, Patel DF, Beale RC, Peiro T, et al. Matrikines are key regulators in modulating the amplitude of lung inflammation in acute pulmonary infection. 2015;

28. Burgess JK, Boustany S, Moir LM, Weckmann M, Lau JY, Grafton K, et al. Reduction of Tumstatin in Asthmatic Airways Contributes to Angiogenesis , Inflammation , and Hyperresponsiveness. 2010;181:106–15.

29. Senior RM, Griffin GL, Mecham RP, Wrenn DS, Prasad KU, Urry DANW. Val-Gly-Val-Ala-Pro-Gly , a Repeating Peptide in Elastin , Is Chemotactic for Fibroblasts and Monocytes. 1984;99(September).

30. Taddese S, Weiss AS, Jahreis G, Neubert RHH, Schmelzer CEH. In vitro degradation of human tropoelastin by MMP-12 and the generation of matrikines from domain 24. Matrix Biol. 2009;28(2):84–91.

31. Scheibner KA, Lutz MA, Boodoo S, Fenton MJ, Powell JD, Horton MR. Hyaluronan Fragments Act as an Endogenous Danger Signal by Engaging TLR2 1. 2006;31–3.

32. BIX G, IOZZO R V. Novel Interactions of Perlecan: Unraveling Perlecan's Role in Angiogenesis. 2008;71(5):339–48.

33. Lhpez-moratalla N, Calonge M, Ldpez-zabalza MJ, Pcrez-mediavilla LA, Subir ML, Santiago E. Activation of human lymphomononuclear cells by peptides derived from extracellular matrix proteins. 1995;1265:181–8.

34. Koshikawa N, Schenk S, Moeckel G, Sharabi A, Miyazaki K, Gardner H, et al. Proteolytic processing of laminin-5 by MT1-MMP in tissues and its effects on epithelial cell morphology. 2003;(1).

35. Sadowski T, Dietrich S, Koschinsky F, Ludwig A, Proksch E, Titz B, et al. Matrix metalloproteinase 19 processes the laminin 5 gamma 2 chain and induces epithelial cell migration. 2005;62:870–80.

36. Biology C, Malinda KM, Wysocki AB, Koblinski JE, Kleinman HK, Ponce ML. Angiogenic laminin-derived peptides stimulate wound healing. 2008;40:2771–80.

37. Gaggar A, Weathington N. Bioactive extracellular matrix fragments in lung health and disease. 2016;126(9):3176–84.

38. Burgess JK, Harmsen MC. Chronic lung diseases : entangled in extracellular matrix. Eur Respir Rev. 2022;31:210202.

39. Rosmark O, Åhrman E, Müller C, Rendin LE, Malmström A, Hallgren O, et al. Quantifying extracellular matrix turnover in human lung scaffold cultures. 2018;1–13.

40. Burgess JK, Mauad T, Tjin G, Karlsson JC, Westergren-Thorsson G. The extracellular matrix – the under-recognized element in lung disease? J Pathol. 2016;240(4):397–409.

41. Tzotzos SJ, Fischer B, Fischer H, Zeitlinger M. Incidence of ARDS and outcomes in hospitalized patients with COVID-19 : a global literature survey. 2020;1–4.

42. Han S, Mallampalli RK. The acute respiratory distress syndrome: from mechanism to translation. J Immunol. 2015 Feb;194(3):855–60.

43. Ji H-L, Liu C, Zhao R-Z. Stem cell therapy for COVID-19 and other respiratory diseases: Global trends of clinical trials. World J Stem Cells. 2020 Jun;12(6):471–80.

44. Bos LDJ, Ware LB. Acute respiratory distress syndrome: causes, pathophysiology, and phenotypes. Lancet. 2022;400(10358):1145–56.

45. Swenson KE. Pathophysiology of Acute Respiratory Distress Syndrome and COVID-19 Lung Injury. 2020;(January).

46. Fujishima S. Pathophysiology and biomarkers of acute respiratory distress syndrome. 2014;1–6.

47. Matthay MA, Zemans RL. The Acute Respiratory Distress Syndrome : Pathogenesis and Treatment. 2011;

48. Ferreira DM, Gordon SB. Chapter 20 - Mechanisms Causing the Inflammatory Response to Streptococcus pneumoniae. In: Brown J, Hammerschmidt S, Orihuela CBT-SP, editors. Amsterdam: Academic Press; 2015. p. 383–400.

49. Ratner AJ, Hippe KR, Aguilar JL, Bender MH, Nelson AL, Weiser JN. Epithelial Cells are Sensitive Detectors of Bacterial Pore-Forming Toxins. 2006;281(18):12994–8.

50. Crestani B, Comillet P, Dehoux M, Rolland C, Guenounou M, Aubier M, et al. Alveolar Type II Epithelial Cells Produce Interleukin-6 In Vitro and In Vivo. Production. 1994;94(August):731–40.

51. Katsura H, Kobayashi Y, Tata PR, Hogan BLM. IL-1 and TNFα Contribute to the Inflammatory Niche to Enhance Alveolar Regeneration. Stem Cell Reports. 2019;12(4):657–66.

52. Thorley AJ, Grandolfo D, Lim E, Goldstraw P, Young A, Tetley TD. Innate immune responses to bacterial ligands in the peripheral human Lung - Role of alveolar epithelial TLR expression and signalling. PLoS One. 2011;6(7).

53. Stukas S, Hoiland RL, Cooper J, Thiara S, Griesdale DE, Thomas AD, et al. The Association of Inflammatory Cytokines in the Pulmonary Pathophysiology of Respiratory Failure in Critically Ill Patients With Coronavirus Disease 2019. Crit Care Explor. 2020;2(9):e0203.

54. Li Z, Mao Z, Lin Y, Liang W, Jiang F, Liu J, et al. Dynamic changes of tissue factor pathway inhibitor type 2 associated with IL-1beta; and TNF-alpha; in the development of murine acute lung injury. Thromb Res. 2008 Dec 1;123(2):361–6.

55. Matthay MA, Zemans RL, Zimmerman GA, Arabi YM, Beitler JR, Mercat A, et al. Acute respiratory distress syndrome. Nat Rev Dis Prim. 2018;5(1).

56. Griffiths MJD, Mcauley DF, Perkins GD, Barrett N, Blackwood B, Boyle A, et al. Guidelines on the management of acute respiratory distress syndrome. 2019;

57. Palakshappa JA, Krall JTW, Belfield LT, Files C. Long-Term Outcomes in Acute Respiratory Distress Syndrome. Crit Care Clin. 2021;37(January):895–911.

58. Gotzev R, Kenarov P. Acute Respiratory Distress Syndrome (ARDS). Anaesthesiol

Intensive Care. 2013;42(1):43–9.

59. Urbanczyk M, Layland SL, Schenke-Layland K. The role of extracellular matrix in biomechanics and its impact on bioengineering of cells and 3D tissues. Matrix Biol. 2020;85–86:1–14.

60. Chaudhuri O, Cooper-White J, Janmey PA, Mooney DJ, Shenoy VB. Effects of extracellular matrix viscoelasticity on cellular behaviour. Nature. 2020;584(7822):535–46.

61. Gong F, Yang Y, Wen L, Wang C, Li J, Dai J. An Overview of the Role of Mechanical Stretching in the Progression of Lung Cancer. Front Cell Dev Biol. 2021;9(December):1–10.

62. Lutfi MF. The physiological basis and clinical significance of lung volume measurements. Multidiscip Respir Med . 2017;12(1):1–12.

63. Sicard D, Haak AJ, Choi KM, Craig AR, Fredenburgh LE, Tschumperlin DJ. Aging and anatomical variations in lung tissue stiffness. Am J Physiol Lung Cell Mol Physiol. 2018 Jun;314(6):L946–55.

64. Miura K. Stiffness reduction and collagenase resistance of aging lungs measured using scanning acoustic microscopy. PLoS One. 2022;17(2):e0263926.

65. Uriarte JJ, Meirelles T, Del Blanco DG, Nonaka PN, Campillo N, Sarri E, et al. Early impairment of lung mechanics in a murine model of marfan syndrome. PLoS One. 2016;11(3):1–19.

66. Melo E, Cardenes N, Garreta E, Luque T, Rojas M, Navajas D, et al. Inhomogeneity of local stiffness in the extracellular matrix scaffold of fi brotic mouse lungs. 2014;37:186–95.

67. Laffey JG, Matthay MA. Fifty Years of Research in ARDS. Cell-based Therapy for Acute Respiratory Distress Syndrome. Biology and Potential Therapeutic Value. Am J Respir Crit Care Med. 2017 Aug;196(3):266–73.

68. Huang K, Kang X, Wang X, Wu S, Xiao J, Li Z, et al. Conversion of bone marrow mesenchymal stem cells into type II alveolar epithelial cells reduces pulmonary

fibrosis by decreasing oxidative stress in rats. Mol Med Rep. 2015;11(3):1685–92.

69. Wang F, Fang B, Qiang X, Shao J, Zhou L. The efficacy of mesenchymal stromal cell-derived therapies for acute respiratory distress syndrome—a meta-analysis of preclinical trials. Respir Res. 2020;21(1):307.

70. Matthay MA. Therapeutic Potential of Mesenchymal Stromal Cells for Acute Respiratory Distress Syndrome. 2015;12(March).

71. Wang F, Li Y, Wang B, Li J, Peng Z. The safety and efficacy of mesenchymal stromal cells in ARDS : a meta - analysis of randomized controlled trials. Crit Care. 2023;1–11.

72. Zhang X, Wei X, Deng Y, Yuan X, Shi J, Huang W, et al. Mesenchymal stromal cells alleviate acute respiratory distress syndrome through the cholinergic anti-in fl ammatory pathway. 2022;(August 2021).

73. Wilson JG, Liu KD, Zhuo H, Caballero L, McMillan M, Fang X, et al. Phase 1 Clinical Trial Designs Phase 1 Designs. Lancet Respir Med. 2015;3(1):24–32.

74. Qin H. Mesenchymal stem cell therapy for acute respiratory distress syndrome : from basic to clinics. Protein Cell. 2020;11(10):707–22.

75. Matthay MA, Calfee CS, Zhuo H, Thompson BT, Wilson JG, Levitt JE, et al. Treatment with allogeneic mesenchymal stromal cells for moderate to severe acute respiratory distress syndrome (START study): a randomised phase 2a safety trial. Lancet Respir Med. 2019 Feb 1;7(2):154–62.

76. Nagpal A, Choy FC, Howell S, Hillier S, Chan F, Hamilton-Bruce MA, et al. Safety and effectiveness of stem cell therapies in early-phase clinical trials in stroke: a systematic review and meta-analysis. Stem Cell Res Ther. 2017 Aug;8(1):191.

77. Schmitt S, Hendricks P, Weir J, Somasundaram R, Sittampalam GS, Nirmalanandhan VS. Stretching mechanotransduction from the lung to the lab: approaches and physiological relevance in drug discovery. Assay Drug Dev Technol. 2012 Apr;10(2):137–47.

78. Humphrey JD, Dufresne ER, Schwartz MA, Haven N, Haven N, Haven N, et al.

Mechanotransduction and extracellular matrix homeostasis. 2015;15(12):802–12.

79. Jhala D, Vasita R. A Review on Extracellular Matrix Mimicking Strategies for an Artificial Stem Cell Niche. Polym Rev. 2015 Oct 2;55(4):561–95.

80. Kular JK, Basu S, Sharma RI. The extracellular matrix: Structure, composition, age-related differences, tools for analysis and applications for tissue engineering. J Tissue Eng. 2014;5.

81. Blatchley M, Bader JS, Pandey A, Pardoll D. Tissue matrix arrays for high throughput screening and systems analysis of cell function Vince. 2016;12(12):1197–204.

82. Urbanczyk M, Layland SL, Schenke-layland K. The role of extracellular matrix in biomechanics and its impact on bioengineering of cells and 3D tissues. Matrix Biol . 2020;85–86:1–14.

83. Chen CS. Mechanotransduction - A field pulling together? J Cell Sci. 2008;121(20):3285–92.

84. Trubelja A, Bao G. Molecular mechanisms of mechanosensing and mechanotransduction in living cells. Extrem Mech Lett. 2018;20:91–8.

85. Engler AJ, Sen S, Sweeney HL, Discher DE. Matrix elasticity directs stem cell lineage specification. Cell. 2006 Aug;126(4):677–89.

86. Sun Z, Guo SS, Fässler R. Integrin-mediated mechanotransduction. 2016;215(4).

87. Cai X, Wang KC, Meng Z. Mechanoregulation of YAP and TAZ in Cellular Homeostasis and Disease Progression. Front Cell Dev Biol. 2021;9(May):1–12.

88. DuFort CC, Paszek MJ, Weaver VM. Balancing forces: architectural control of mechanotransduction. Nat Rev Mol Cell Biol. 2011 May;12(5):308–19.

89. Park JS, Chu JS, Tsou AD, Diop R, Tang Z, Wang A, et al. The effect of matrix stiffness on the differentiation of mesenchymal stem cells in response to TGF-β. Biomaterials. 2011;32(16):3921–30.

90. Melo E, Garreta E, Luque T, Cortiella J, Nichols J, Navajas D, et al. Effects of the decellularization method on the local stiffness of acellular lungs. Tissue Eng Part C

Methods. 2014 May;20(5):412–22.

91. Wu J, Ravikumar P, Nguyen KT, Hsia CCW, Hong Y. Lung protection by inhalation of exogenous solubilized extracellular matrix. PLoS One. 2017;12(2):1–15.

92. Darnell M, Neil AO, Mao A, Gu L, Rubin LL, Mooney DJ. Material microenvironmental properties couple to induce distinct transcriptional programs in mammalian stem cells. 2018;115(36).

93. Dan P, Velot É, Decot V, Menu P. The role of mechanical stimuli in the vascular differentiation of mesenchymal stem cells. 2015;2415–22.

94. Max D, Alison O, Angelo M, Luo G, L. RL, J. MD. Material microenvironmental properties couple to induce distinct transcriptional programs in mammalian stem cells. Proc Natl Acad Sci. 2018 Sep 4;115(36):E8368–77.

95. Cesarz Z, Tamama K. Spheroid Culture of Mesenchymal Stem Cells. 2016;2016.

96. Nonaka PN, Falcones B, Farre R, Artigas A, Almendros I, Navajas D. Biophysically Preconditioning Mesenchymal Stem Cells Improves Treatment of Ventilator-Induced Lung Injury. Arch Bronconeumol. 2020 Mar;56(3):179–81.

97. Badylak SF, Taylor D, Uygun K. Whole-organ tissue engineering: decellularization and recellularization of three-dimensional matrix scaffolds. Annu Rev Biomed Eng. 2011 Aug;13:27–53.

98. Edgar L, Pu T, Porter B, Aziz JM, La Pointe C, Asthana A, et al. Regenerative medicine, organ bioengineering and transplantation. Br J Surg. 2020 Jun;107(7):793–800.

99. Crapo PM, Gilbert TW, Badylak SF. An overview of tissue and whole organ decellularization processes. Biomaterials. 2011 Apr;32(12):3233–43.

100. Narciso M, Ulldemolins A, Júnior C, Otero J, Navajas D, Farré R, et al. Novel Decellularization Method for Tissue Slices. Front Bioeng Biotechnol. 2022;10(March):1–13.

101. Pouliot RA, Link PA, Mikhaiel NS, Schneck MB, Valentine MS, Kamga Gninzeko FJ, et al. Development and characterization of a naturally derived lung extracellular

matrix hydrogel. J Biomed Mater Res - Part A. 2016;104(8):1922–35.

102. Marhuenda E, Villarino A, Narciso ML, Camprubí-Rimblas M, Farré R, Gavara N, et al. Lung Extracellular Matrix Hydrogels Enhance Preservation of Type II Phenotype in Primary Alveolar Epithelial Cells. Int J Mol Sci. 2022 Apr;23(9).

103. Marhuenda E, Villarino A, Narciso M, Elowsson L, Almendros I, Westergren-Thorsson G, et al. Development of a physiomimetic model of acute respiratory distress syndrome by using ECM hydrogels and organ-on-a-chip devices. Front Pharmacol. 2022;13(September):1–15.

104. Martinez-garcia FD, de Hilster RHJ, Sharma PK, Borghuis T, Hylkema MN, Burgess JK, et al. Architecture and composition dictate viscoelastic properties of organ-derived extracellular matrix hydrogels. Polymers (Basel). 2021;13(18).

105. Nizamoglu M, de Hilster RHJ, Zhao F, Sharma PK, Borghuis T, Harmsen MC, et al. An in vitro model of fibrosis using crosslinked native extracellular matrix-derived hydrogels to modulate biomechanics without changing composition. Acta Biomater. 2022;147:50–62.

106. Pouliot RA, Young BM, Link PA, Park HE, Kahn AR, Shankar K, et al. Porcine Lung-Derived Extracellular Matrix Hydrogel Properties Are Dependent on Pepsin Digestion Time. Tissue Eng - Part C Methods. 2020;26(6):332–46.

107. Hoffman ET, Uriarte JJ, Uhl FE, Eckstrom K, Tanneberger AE, Becker C, et al. Human alveolar hydrogels promote morphological and transcriptional differentiation in iPSC - derived alveolar type 2 epithelial cells. Sci Rep. 2023;1–16.

108. Park S, Kim TH, Kim SH, You S, Jung Y. Three-Dimensional Vascularized Lung Cancer-on-a-Chip with Lung Extracellular Matrix Hydrogels for In Vitro Screening. 2021;1–17.

109. Tang G, Zhou B, Li F, Wang W, Liu Y, Wang X, et al. Advances of Naturally Derived and Synthetic Hydrogels for Intervertebral Disk Regeneration. 2020;8(June):1–13.

110. Falcones B, Sanz-Fraile H, Marhuenda E, Mendizábal I, Cabrera-Aguilera I, Malandain N, et al. Bioprintable Lung Extracellular Matrix Hydrogel Scaffolds for

3D Culture of Mesenchymal Stromal Cells. Vol. 13, Polymers . 2021.

111. Zhu Y-G, Feng X-M, Abbott J, Fang X-H, Hao Q, Monsel A, et al. Human mesenchymal stem cell microvesicles for treatment of Escherichia coli endotoxin-induced acute lung injury in mice. Stem Cells. 2014 Jan;32(1):116–25.

112. Saldin LT, Cramer MC, Velankar SS, White LJ, Badylak SF. Extracellular matrix hydrogels from decellularized tissues: Structure and function. Acta Biomater. 2017;49:1–15. Available from:

113. Hoffman ET, Pouliot R, Alysandratos K, Ikonomou L, Kotton D, Weiss DJ. Alveolar Extracellular Matrix Hydrogels Facilitate Proliferation of Induced Pluripotent Stem Cell-Derived Alveolar Epithelial Spheroids. Cytotherapy. 2020;22(5):S204.

114. Huleihel L, Bartolacci JG, Dziki JL, Vorobyov T, Arnold B, Scarritt ME, et al. Matrix-Bound Nanovesicles Recapitulate Extracellular Matrix Effects on Macrophage Phenotype. Tissue Eng Part A. 2017 Nov;23(21–22):1283–94.

115. van der Merwe Y, Faust AE, Sakalli ET, Westrick CC, Hussey G, Conner IP, et al. Matrix-bound nanovesicles prevent ischemia-induced retinal ganglion cell axon degeneration and death and preserve visual function. Sci Rep. 2019;9(1):1–15.

116. Li Q, Uygun BE, Geerts S, Ozer S, Scalf M, Gilpin SE, et al. Proteomic analysis of naturally-sourced biological scaffolds. Biomaterials. 2016 Jan;75:37–46.

117. Calle EA, Hill RC, Leiby KL, Le A V, Gard AL, Madri JA, et al. Targeted proteomics effectively quantifies differences between native lung and detergent-decellularized lung extracellular matrices. Acta Biomater. 2016 Dec;46:91–100.

118. Zhou J, Wu P, Sun H, Zhou H, Zhang Y, Xiao Z. Lung tissue extracellular matrix-derived hydrogels protect against radiation-induced lung injury by suppressing epithelial–mesenchymal transition. J Cell Physiol. 2020;235(3):2377–88.

119. Manni ML, Czajka CA, Oury TD, Gilbert TW. Extracellular matrix powder protects against bleomycin-induced pulmonary fibrosis. Tissue Eng - Part A. 2011;17(21–22):2795–804.

120. Badylak SF. The extracellular matrix as a scaffold for tissue reconstruction. Semin

Cell Dev Biol. 2002 Oct;13(5):377–83.

121. Gaggar A, Weathington N. Bioactive extracellular matrix fragments in lung health and disease. J Clin Invest. 2016 Sep;126(9):3176–84.

122. Horejs C-M, St-Pierre J-P, Ojala JRM, Steele JAM, da Silva PB, Rynne-Vidal A, et al. Preventing tissue fibrosis by local biomaterials interfacing of specific cryptic extracellular matrix information. Nat Commun. 2017;8(1):15509.

123. Lee JS, Shin J, Park H-M, Kim Y-G, Kim B-G, Oh J-W, et al. Liver extracellular matrix providing dual functions of two-dimensional substrate coating and three-dimensional injectable hydrogel platform for liver tissue engineering. Biomacromolecules. 2014 Jan;15(1):206–18.

124. DeQuach JA, Mezzano V, Miglani A, Lange S, Keller GM, Sheikh F, et al. Simple and high yielding method for preparing tissue specific extracellular matrix coatings for cell culture. PLoS One. 2010 Sep;5(9):e13039.

125. Farnebo S, Woon CYL, Schmitt T, Joubert L-M, Kim M, Pham H, et al. Design and characterization of an injectable tendon hydrogel: a novel scaffold for guided tissue regeneration in the musculoskeletal system. Tissue Eng Part A. 2014 May;20(9–10):1550–61.

126. Johnson TD, Dequach JA, Gaetani R, Ungerleider J, Elhag D, Nigam V, et al. Human versus porcine tissue sourcing for an injectable myocardial matrix hydrogel. Biomater Sci. 2014;2014:60283D.

127. Nagao RJ, Xu J, Luo P, Xue J, Wang Y, Kotha S, et al. Decellularized Human Kidney Cortex Hydrogels Enhance Kidney Microvascular Endothelial Cell Maturation and Quiescence. Tissue Eng Part A. 2016 Oct;22(19–20):1140–50.

128. Chaimov D, Baruch L, Krishtul S, Meivar-Levy I, Ferber S, Machluf M. Innovative encapsulation platform based on pancreatic extracellular matrix achieve substantial insulin delivery. J Control Release Soc. 2017 Jul;257:91–101.

129. Ungerleider JL, Johnson TD, Hernandez MJ, Elhag DI, Braden RL, Dzieciatkowska M, et al. Extracellular Matrix Hydrogel Promotes Tissue Remodeling, Arteriogenesis,

and Perfusion in a Rat Hindlimb Ischemia Model. JACC Basic to Transl Sci. 2016;1(1–2):32–44.

130. Fernández-Pérez J, Ahearne M. The impact of decellularization methods on extracellular matrix derived hydrogels. Sci Rep. 2019;9(1):14933.

131. Hernandez MJ, Yakutis GE, Zelus EI, Hill RC, Dzieciatkowska M, Hansen KC, et al. Manufacturing considerations for producing and assessing decellularized extracellular matrix hydrogels. Methods. 2020 Jan;171:20–7.

132. Evangelista-Leite D, Carreira ACO, Gilpin SE, Miglino MA. Protective Effects of Extracellular Matrix-Derived Hydrogels in Idiopathic Pulmonary Fibrosis. Tissue Eng - Part B Rev. 2022;28(3):517–30.

133. Evangelista-Leite D, Carreira ACO, Nishiyama MY, Gilpin SE, Miglino MA. The molecular mechanisms of extracellular matrix-derived hydrogel therapy in idiopathic pulmonary fibrosis models. Biomaterials. 2023;302(August).

134. Cruz FF, Rocco PRM. Stem-cell extracellular vesicles and lung repair. Stem cell Investig. 2017;4:78.

135. Mianehsaz E, Mirzaei HR, Mahjoubin-Tehran M, Rezaee A, Sahebnasagh R, Pourhanifeh MH, et al. Mesenchymal stem cell-derived exosomes: a new therapeutic approach to osteoarthritis? Stem Cell Res Ther. 2019;10(1):340.

136. Lamichhane TN, Sokic S, Schardt JS, Raiker RS, Lin JW, Jay SM. Emerging Roles for Extracellular Vesicles in Tissue Engineering and Regenerative Medicine. Tissue Eng Part B Rev. 2014 Jun 23;21(1):45–54.

137. Yi X, Wei X, Lv H, An Y, Li L, Lu P, et al. Exosomes derived from microRNA-30b-3p-overexpressing mesenchymal stem cells protect against lipopolysaccharide-induced acute lung injury by inhibiting SAA3. Exp Cell Res. 2019;383(2):111454.

138. Wu Y, Li J, Yuan R, Deng Z, Wu X. Bone marrow mesenchymal stem cell-derived exosomes alleviate hyperoxia-induced lung injury via the manipulation of microRNA-425. Arch Biochem Biophys. 2021;697:108712.

139. Li J wei, Wei L, Han Z, Chen Z. Mesenchymal stromal cells-derived exosomes

alleviate ischemia/reperfusion injury in mouse lung by transporting anti-apoptotic miR-21-5p. Eur J Pharmacol. 2019;852:68–76.

140. Gurunathan S. Biogenesis , Composition and Potential Therapeutic Applications of Mesenchymal Stem Cells Derived Exosomes in Various Diseases. 2023;(May):3177–210.

141. Zou J, Yang W, Cui W, Li C, Ma C, Ji X, et al. Therapeutic potential and mechanisms of mesenchymal stem cell-derived exosomes as bioactive materials in tendon-bone healing. J Nanobiotechnology. 2023 Jan;21(1):14.

142. Ionescu L, Byrne RN, Haaften T Van, Vadivel A, Alphonse RS, Rey-parra GJ, et al. Stem cell conditioned medium improves acute lung injury in mice : in vivo evidence for stem cell paracrine action. 2012;45:967–77.

143. Feng Y, Guo K, Jiang J, Lin S. Mesenchymal stem cell-derived exosomes as delivery vehicles for non-coding RNAs in lung diseases. Biomed Pharmacother. 2024;170:116008.

144. Shah T, Qin S, Vashi M, Predescu DN, Jeganathan N, Bardita C, et al. Alk5/Runx1 signaling mediated by extracellular vesicles promotes vascular repair in acute respiratory distress syndrome. Clin Transl Med. 2018 Jun;7(1):19.

145. Tang X, Shi L, Monsel A, Li X, Zhu H, Zhu Y. Mesenchymal Stem Cell Microvesicles Attenuate Acute Lung Injury in Mice Partly Mediated by Ang-1 mRNA.

146. Shah T, Qin S, Vashi M, Predescu DN, Jeganathan N, Bardita C, et al. Alk5/Runx1 signaling mediated by extracellular vesicles promotes vascular repair in acute respiratory distress syndrome. Clin Transl Med. 2018;7(1):1–18.

147. Li J, Deng X, Ji X, Shi X, Ying Z, Shen K, et al. Mesenchymal stem cell exosomes reverse acute lung injury through Nrf-2/ARE and NF-κB signaling pathways. PeerJ. 2020;8:1–10.

148. Kaspi H, Semo J, Abramov N, Dekel C, Lindborg S, Kern R, et al. MSC-NTF (NurOwn®) exosomes: a novel therapeutic modality in the mouse LPS-induced ARDS model. Stem Cell Res Ther. 2021;12(1):1–10.

149. Park J, Kim S, Lim H, Liu A, Hu S, Lee J, et al. Therapeutic effects of human mesenchymal stem cell microvesicles in an ex vivo perfused human lung injured with severe E. coli pneumonia. Thorax. 2019 Jan;74(1):43–50.

150. Chang C Lo, Sung PH, Chen KH, Shao PL, Yang CC, Cheng BC, et al. Adipose-derived mesenchymal stem cell-derived exosomes alleviate overwhelming systemic inflammatory reaction and organ damage and improve outcome in rat sepsis syndrome. Am J Transl Res. 2018;10(4):1053–70.

151. Hu S, Park J, Liu A, Lee J, Zhang X, Hao Q, et al. Mesenchymal Stem Cell Microvesicles Restore Protein Permeability Across Primary Cultures of Injured Human Lung Microvascular Endothelial Cells. Stem Cells Transl Med. 2018 Aug;7(8):615–24.

152. Sengupta V, Sengupta S, Lazo A, Woods P, Nolan A, Bremer N. Exosomes Derived from Bone Marrow Mesenchymal Stem Cells as Treatment for Severe COVID-19. Stem Cells Dev. 2020 Jun;29(12):747–54.

153. Monsel A, Zhu Y, Gennai S, Hao Q, Hu S, Rouby J, et al. Therapeutic Effects of Human Mesenchymal Stem Cell – derived Microvesicles in Severe Pneumonia in Mice. 2015;192(3):324–36.

154. Song Y, Dou H, Li X, Zhao X, Li Y, Liu D, et al. Exosomal miR-146a Contributes to the Enhanced Therapeutic Efficacy of Interleukin-1-Primed Mesenchymal Stem Cells Against Sepsis Exosomal miR-146a Contributes to the Enhanced Therapeutic Efficacy of Interleukin-1 b -Primed Mesenchymal Stem Cells Against S. Stem Cells. 2017;35:1208–21.

155. Park J, Kim S, Lim H, Liu A, Hu S, Lee J, et al. Therapeutic Effects of Human Mesenchymal Stem Cell Microvesicles in an Ex Vivo Perfused Human Lung Injured with Severe E.coli Pneumonia. Thorax. 2019;72(23):2964–79.

156. Beaty TH, Cohen BH, Newill CA, Menkes HA, Diamond EL, Chen CJ. Impaired pulmonary function as a risk factor for mortality. Am J Epidemiol. 1982 Jul;116(1):102–13.

157. Fain SB, Altes TA, Panth SR, Evans MD, Waters B, Mugler JP, et al. Detection of Age-

Dependent Changes in Healthy Adult Lungs With Diffusion-Weighted 3He MRI. Acad Radiol. 2005;12(11):1385–93.

158. Koff WC, Williams MA. Covid-19 and Immunity in Aging Populations — A New Research Agenda. N Engl J Med. 2020 Apr 17;383(9):804–5.

159. Williamson EJ, Walker AJ, Bhaskaran K, Bacon S, Bates C, Morton CE, et al. Factors associated with COVID-19-related death using OpenSAFELY. Nature. 2020;584(7821):430–6.

160. Budinger GRS, Kohanski RA, Gan W, Kobor MS, Amaral LA, Armanios M, et al. The Intersection of Aging Biology and the Pathobiology of Lung Diseases: A Joint NHLBI/NIA Workshop. Journals Gerontol Ser A. 2017 Oct 12;72(11):1492–500.

161. Gruber MP, Coldren CD, Woolum MD, Cosgrove GP, Zeng C, Barón AE, et al. Human lung project: evaluating variance of gene expression in the human lung. Am J Respir Cell Mol Biol. 2006 Jul;35(1):65–71.

162. Misra V, Lee H, Singh A, Huang K, Thimmulappa RK, Mitzner W, et al. Global expression profiles from C57BL/6J and DBA/2J mouse lungs to determine aging-related genes. Physiol Genomics. 2007 Nov 1;31(3):429–40.

163. Schneider JL, Rowe JH, Garcia-de-Alba C, Kim CF, Sharpe AH, Haigis MC. The aging lung: Physiology, disease, and immunity. Cell. 2021;184(8):1990–2019.

164. Godin LM, Sandri BJ, Wagner DE, Meyer CM, Price AP, Akinnola I, et al. Decreased laminin expression by human lung epithelial cells and fibroblasts cultured in acellular lung scaffolds from aged mice. PLoS One. 2016;11(3):1–17.

165. Júnior C, Narciso M, Marhuenda E, Almendros I, Farré R, Navajas D, et al. Baseline stiffness modulates the non-linear response to stretch of the extracellular matrix in pulmonary fibrosis. Int J Mol Sci. 2021;22(23).

166. Waters CM, Roan E, Navajas D. Mechanobiology in lung epithelial cells: Measurements, perturbations, and responses. Compr Physiol. 2012;2(1):1–29.

167. Johnson, B. Z., Stevenson, A. W., Prêle, C. M., Fear, M. W. and Wood, F. M. (2020) 'The Role of IL-6 in Skin Fibrosis and Cutaneous Wound Healing', Biomedicines, 8(5).

168. Amigo L, Hernández-Ledesma B. Current Evidence on the Bioavailability of Food Bioactive Peptides. Molecules. 2020 Sep;25(19).

169. Nizamoglu M, Koloko Ngassie ML, Meuleman RA, Banchero M, Borghuis T, Timens W, et al. Collagen type XIV is proportionally lower in the lung tissue of patients with IPF. Sci Rep. 2023;13(1):19393.

170. Weckmann M, Moir LM, Heckman CA, Black JL, Oliver BG, Burgess JK. Lamstatin – a novel inhibitor of lymphangiogenesis derived from collagen IV. J Cell Mol Med. 2012 Dec 1;16(12):3062–73.

171. Hamano Y, Kalluri R. Tumstatin, the NC1 domain of α3 chain of type IV collagen, is an endogenous inhibitor of pathological angiogenesis and suppresses tumor growth. Biochem Biophys Res Commun. 2005;333(2):292–8.

172. Rønnow SR, Langholm LL, Karsdal MA, Manon-Jensen T, Tal-Singer R, Miller BE, et al. Endotrophin, an extracellular hormone, in combination with neoepitope markers of von Willebrand factor improves prediction of mortality in the ECLIPSE COPD cohort. Vol. 21, Respiratory research. England; 2020. p. 202.

173. Morales-Nebreda LI, Rogel MR, Eisenberg JL, Hamill KJ, Soberanes S, Nigdelioglu R, et al. Lung-specific loss of α3 laminin worsens bleomycin-induced pulmonary fibrosis. Am J Respir Cell Mol Biol. 2015 Apr;52(4):503–12.

174. Hamill KJ, Paller AS, Jones JCR. Adhesion and migration, the diverse functions of the laminin alpha3 subunit. Dermatol Clin. 2010 Jan;28(1):79–87.

175. Engel J. EGF-like domains in extracellular matrix proteins: Localized signals for growth and differentiation? FEBS Lett. 1989 Jul 17;251(1–2):1–7.

176. Reing JE, Zhang L, Myers-Irvin J, Cordero KE, Freytes DO, Heber-Katz E, et al. Degradation products of extracellular matrix affect cell migration and proliferation. Tissue Eng Part A. 2009 Mar;15(3):605–14.

177. Xu F, Hu Y, Zhou J, Wang X. Mesenchymal stem cells in acute lung injury: are they ready for translational medicine? J Cell Mol Med. 2013 Aug 1;17(8):927–35.

178. Álvarez D, Levine M, Rojas M. Regenerative medicine in the treatment of idiopathic pulmonary fibrosis : current position. 2015;61–5.

179. Onursal C, Dick E, Angelidis I, Schiller HB, Staab-Weijnitz CA. Collagen Biosynthesis, Processing, and Maturation in Lung Ageing. Front Med. 2021;8:593874.

180. Sokocevica D, Bonenfanta NR, Wagnera DE, Borga ZD, Lathropa MJ, Lamb YW, et al. The effect of age and emphysematous and fibrotic injury on the re-cellularization of de-cellularized lungs. 2011;4(164):3256–69.

181. Podolsky MJ, Yang CD, Valenzuela CL, Datta R, Huang SK, Nishimura SL, et al. Age-dependent regulation of cell-mediated collagen turnover. JCI insight. 2020 May;5(10).

182. Huang K, Mitzner W, Rabold R, Schofield B, Lee H, Biswal S, et al. Variation in senescent-dependent lung changes in inbred mouse strains. J Appl Physiol. 2007 Apr;102(4):1632–9.

183. Huang K, Rabold R, Schofield B, Mitzner W, Tankersley CG. Age-dependent changes of airway and lung parenchyma in C57BL/6J mice. J Appl Physiol. 2007 Jan;102(1):200–6.

184. Jorba, I., Beltrán, G., Falcones, B., Suki, B., Farré, R., García-Aznar, J. M., et al. (2019). Nonlinear elasticity of the lung extracellular microenvironment is regulated by macroscale tissue strain. *Acta Biomater.* 92, 265–276.

185. Suki, B., Bates, J. H. T., and Bartolák-Suki, E. (2022). Remodeling of the aged and emphysematous lungs: roles of microenvironmental cues. *Compr. Physiol.* 12 (3), 3559–3574.

186. Sobin SS, Fung YC, Tremer HM. Collagen and elastin fibers in human pulmonary alveolar walls. J Appl Physiol. 1988 Apr;64(4):1659–75.

187. Qin L, Liu N, Bao C-M, Yang D-Z, Ma G-X, Yi W-H, et al. Mesenchymal stem cells in fibrotic diseases-the two sides of the same coin. Acta Pharmacol Sin. 2023

Feb;44(2):268–87.

188. de Hilster RHJ, Sharma PK, Jonker MR, White ES, Gercama EA, Roobeek M, et al. Human lung extracellular matrix hydrogels resemble the stiffness and viscoelasticity of native lung tissue. Am J Physiol Lung Cell Mol Physiol. 2020 Apr;318(4):L698–704.

189. Hoffman ET, Uriarte JJ, Uhl FE, Eckstrom K, Tanneberger AE, Becker C, et al. Human alveolar hydrogels promote morphological and transcriptional differentiation in iPSC-derived alveolar type 2 epithelial cells. Sci Rep. 2023 Jul;13(1):12057.

Chapter XII.

CONTRIBUTION TO OTHER RESEARCH PROJECTS

The PhD candidate has participated in other research projects related to lung bioengineering as well as other scaffolds for MSCs culturing. She also has been offered to defend some of her scientific works in national and international conferences listed below.

Scientific papers

1. Sanz-Fraile, H.; Herranz-Diez, C.; **Ulldemolins, A.**; Falcones, B.; Almendros, I.; Gavara, N.; Sunyer, R.; Farré, R.; Otero, J. Characterization of Bioinks Prepared via Gelifying Extracellular Matrix from Decellularized Porcine Myocardia. Gels 2023, 9, 745. https://doi.org/10.3390/gels9090745

The candidate has performed the culturing of human bone marrow mesenchymal stem cells on cardiac hydrogels and carried out the immunostainings of the cardiac biomarkers.

2. Narciso, M.; Martínez, Á.; Júnior, C.; Díaz-Valdivia, N.; **Ulldemolins, A**.; Berardi, M.; Neal, K.; Navajas, D.; Farré, R.; Alcaraz, J.; et al. Lung Micrometastases Display ECM Depletion and Softening While Macrometastases Are 30-Fold Stiffer and Enriched in Fibronectin. Cancers 2023, 15, 2404. https://doi.org/10.3390/cancers15082404

The candidate contributed to the animal procedures, specifically in the metastasic murine C57BL/6J model injected trough the tail vein with murine melanoma cells B16-F10. The lung excision and sampling were also performed by the candidate.

3. Júnior, C.; **Ulldemolins, A**.; Narciso, M.; Almendros, I.; Farré, R.; Navajas, D.; López, J.; Eroles, M.; Rico, F.; Gavara, N. Multi-Step Extracellular Matrix Remodelling and Stiffening in the Development of Idiopathic Pulmonary Fibrosis. Int. J. Mol. Sci. 2023, 24, 1708. https://doi.org/10.3390/ijms24021708

The candidate carried out the bleomycin- induced fibrosis model in 30 Sprague Dawley rats and excised the lungs. Blood samples were also and collected by the candidate.

4. Jurado A, **Ulldemolins A**, Lluís H, Gasull X, Gavara N, Sunyer R, Otero J, Gozal D, Almendros I and Farré R (2023) Fast cycling of intermittent hypoxia in a physiomimetic 3D environment: A novel tool for the study of the parenchymal

effects of sleep apnea. Front. Pharmacol. 13:1081345. doi: 10.3389/fphar.2022.1081345

The oxygen sensor set up and calibration was executed by the candidate. She also provided guidance and insight in the lung hydrogel encapsulation of MSCs.

5. Narciso M, **Ulldemolins A**, Júnior C, et al. A Fast and Efficient Decellularization Method for Tissue Slices. Bio Protoc. 2022;12(22):e4550. Published 2022 Nov 20. doi:10.21769/BioProtoc.4550

The protocol for culturing cells on decellularized tissue slide was settled by the candidate, and the viability assay and immunostaining were performed by her.

6. Buj-Corral I, Sanz-Fraile H, **Ulldemolins A**, et al. Characterization of 3D Printed Metal-PLA Composite Scaffolds for Biomedical Applications. Polymers (Basel). 2022;14(13):2754. Published 2022 Jul 5. doi:10.3390/polym14132754

The candidate executed the culturing of human bone marrow mesenchymal stem cells on the Metal-PLA composite scaffolds. The viability and differentiation of the cells on the scaffolds was also assessed by the candidate.

7. Narciso M, **Ulldemolins A**, Júnior C, et al. Novel Decellularization Method for Tissue Slices. Front Bioeng Biotechnol. 2022;10:832178. Published 2022 Mar 9. doi:10.3389/fbioe.2022.832178

The protocol for culturing cells on decellularized tissue slide was settled by the candidate, and the viability assay and immunostaining were performed by her.

8. Otero J, **Ulldemolins A**, Farré R, Almendros I. Oxygen Biosensors and Control in 3D Physiomimetic Experimental Models. Antioxidants (Basel). 2021;10(8):1165. Published 2021 Jul 22. doi:10.3390/antiox10081165

The candidate summarized and described the available bioreactors with real-time oxygen monitoring in the literature.

9. Osuna A, **Ulldemolins A,** Sanz-Fraile H, et al. Experimental Setting for Applying Mechanical Stimuli to Study the Endothelial Response of Ex Vivo Vessels under

Realistic Pathophysiological Environments. Life (Basel). 2021;11(7):671. Published 2021 Jul 8. doi:10.3390/life11070671

The oxygen sensor set up on the bioreactor was performed by the candidate and the oxygen measurements were also carried out by her.

Congress communications

International American Thoracic Society Conference, 19- 24 May 2024 | San Diego, USA

I. *Secretion of mesenchymal stem cells-derived exosomes is enhanced by culturing on lung extracellular matrix hydrogels*
A. Jurado, A. Ulldemolins, J. Otero, R. Farre, A. Lu and I. Almendros

II. *Changes In Lung Extracellular Matrix Stiffness Caused By Aging: Dependence On Whether Measured At Functional Or Residual Volumes*
I. Almendros, A. Ulldemolins, M. Narciso, D. Navajas, R. Farre, N. Gavara

III. *Lung Derived-Extracellular Matrix Hydrogels Promote Inflammation And Migration In Alveolar Epithelial Type 2 Cells*
Almendros, C. Herranz-Díez, A. Ulldemolins, R. Sunyer, N. Gavara, R. Farre, J. Otero.

European Respiratory Society International Congress, 9 – 13 September 2023 | Milan, Italy

IV. *Lung Extracellular Matrix Hydrogels-Derived Vesicles Contribute to Epithelial Lung Repair*
A. Ulldemolins, A. Jurado, C. Herranz-Diez, N. Gavara, J. Otero, R. Farré, Almendros

V. *Age related changes of the lung extracellular matrix stiffness and stem cell viability*

M. Narciso, A. Ulldemolins, A. Jurado, D. Navajas, R. Farré , N. Gavara and I. Almendros

VI. *Application of intermittent hypoxia to precisely cut tissue slices: a novel ex vivo model for studying the parenchymal effects of obstructive sleep apnea (OSA)*
A. Jurado, A. Ulldemolins, H. Lluis, X. Gasull , N. Gavara, R. Sunyer, J. Otero , D. Gozal , R. Farré Ventura , I. Almendros

Jornadas CIBERES-CIBERINFEC, 15- 16 June 2023 | Madrid, Spain

VII. *Lung Extracellular Matrix Hydrogels derived matrikines contribute to inflammatory cell response*
A. Ulldemolins, C. Herranz-Diez, R. Farré, N. Gavara, I. Almendros, R. Sunyer and J. Otero.

International American Thoracic Society Conference, 19- 24 May 2023 | Washington DC, USA

VIII. Lung Extracellular Matrix Hydrogels - Derived Nanoparticles Contribute To Epithelial Lung Repair
A. Ulldemolins, A. Jurado, C. Herranz-Diez, N. Gavara, J. Otero, R. Farre, I. Almendros

Jornadas de formación CIBERES, 24- 25 November 2022 | Madrid, Spain

IX. *Lung Extracellular Matrix Hydrogels – derived nanoparticles contribute to epithelial lung repair*
A. Ulldemolins , A. Jurado, J. Otero, R. Farré and I. Almendros

X. New model for subjecting 3D-Cultured Cells To Intermittent Hypoxia Mimicking Sleep Apnea.
A. Jurado, A. Ulldemolins, J. Otero, R. Farré and I. Almendros

European Respiratory Society International Congress, 4-6 September 2022 | Barcelona, Spain

XI. *Aging induces stiffening of the lung extracellular matrix*
M. Narciso, A. Ulldemolins, D. Navajas, R. Farré, N. Gavara and I. Almendros

International American Thoracic Society Conference, 13-18 May 2022| San Francisco, USA

XII. Novel Method for Fast Decellularization of Lung Slices
I. Almendros, M. Narciso, A. Ulldemolins, C. Júnior, J. Otero, D. Navajas, R. Farre and N.Gavara

European Respiratory Society Research Seminar: Innovative 3D models for understanding mechanisms underlying lung diseases: powerful tools for translational research, 7–8 April 2022 | Lisbon, Portugal.

XIII. *Lung Tumor Decellularization Mechanics*
M. Narciso, A. Ulldemolins, C. Junior, J. Otero, D. Navajas, R. Farré, N. Gavara, and I. Almendros

Awards

1. **CIBERES 2022 - ACCION FORMATIVA 2022 | Best abstract award:**
   Lung Extracellular Matrix Hydrogels – derived nanoparticles contribute to epithelial lung repair. Ulldemolins, A. Jurado, J. Otero, R. Farré and I. Almendros

Chapter XIII.
APPENDICES

APPENDIX A. RAT BONE MARROW MESENCHYMAL STROMAL CELL ISOLATION AND CULTURE PROTOCOL

The study of primary MSCs is crucial for the treatment of many respiratory diseases. Here I explain the process to isolate primary BM-MSCs required in order to carry out every replicate of the EV's isolation model.

o Isolation of Rat Bone Marrow- Mesenchymal Stem Cells

MATERIALS

- Sprague-Dawley rat
- Needle 19G (BD, cat no 400925)
- Scalpel (Swann Morton, cat. no. 0206)
- 10 mL syringe (BD, cat no 305959
- Petri dishes (TPP, Switzerland, cat. no. 93100)
- 5 ml sterile serological pipettes (Greiner Bio-One, cat. no. 606180)
- 10 ml sterile serological pipettes (Greiner Bio-One, cat. no. 607180)
- Pipettor (Pipet-Aid, XP model)
- 50 ml falcon tube (Corning, cat. no. 352070)
- 100-1000 µl micropipette (Eppendorf, cat. no., ES-1000)
- 1000 µl pipette tips (Eppendorf, cat. no 0030000927)
- Sterile Pasteur pipettes (Deltalab, cat. no. 200006C)
- Glass Pasteur pipettes (VWR, Pensilvania, cat. no. 612-3814)
- 100 µm cell strainer (Thermo Scientific; 22-363-549)
- 75 cm2 flasks (Techno Plastic Products, cat no. 90025)
- Ice

REAGENTS

- DMEM (Gibco, cat no 10313021)
- α-MEM (Gibco, cat no 12561056)
- Amphotericin B solution (Sigma, cat. no. A2942)
- Fetal Bovine Serum (Gibco, cat. no. 10270106)
- Penicillin/streptomycinin solution (Sigma, cat. no P4333)

- PBS 1X (Gibco, Massachusetts, cat. no. 10010-015)
- Ethanol 70% (Sigma Aldrich, Misuri)
- TrypLE Express Enzyme (1X) (Gibco, 11558856)
- DMEM complete medium: DMEM medium is supplemented with a 10% FBS and 1% of antibiotics mix (streptomycin, penicillin and amphotericin
- αMEM complete medium: αMEM medium is supplemented with a 10% FBS and 1% of antibiotics mix (streptomycin, penicillin and amphotericin).

EQUIPMENTS

- Centrifuge (Heraeus Instruments, Labofuge 400R model)
- Cell culture incubator (Thermo Scientific Heracell 150i CO2 incubator)
- Laminar flow cabinet for cell culture (Scanlaf Mars Safety Class 2)
- Optical microscope (Olympus Life Science, CKX31 model)

PROCEDURE

1. Euthanize the rat with isoflurane overdose.
2. Shave both legs of the animal.
3. Remove the peripheral muscle tissue.
4. Obtain the tibia and the femur dislocating the leg from the hip without breaking the femur.

NOTE: Keep the bones on ice or in cold reagents during the procedure

5. Clean the bones with gauzes to separate the remaining muscle from the bone.
6. Held the bones in a falcon with cold sterile PBS 1X at 4ºC.
7. Enter the bones in the culture hood and soak the femur and tibia with ethanol 70% during 1 min in a petri dish.
8. Wash again with cold PBS 1X and place it on a petri dish.
9. Separate the tibia and the femur carefully with a scalpel.

10. Cut the caps of the bones and flush trough the bone with a 19G needle and a syringe with cold supplemented medium (DMEM 10% FBS, 1% PSA) until the bone turns completely white.

NOTE: Usually flush 10 mL trough every bone, but sometimes is difficult to detach the bone marrow and it will require more volume of medium.

11. Collect the whole mesh in a clean petri dish and pass again trough the 19G needle until the bone marrow is desegregated.
12. Filter the bone marrow suspension with a 200-mesh filter and place it in a 50 mL falcon.
13. Centrifuge at 250G 5 min.
14. Resuspend the pellet in prewarmed DMEM supplemented medium with a plastic Pasteur pipette.
15. Plate the cells in T75 flasks and incubate them at 37ºC and 5% CO_2.
16. After 24h, change the medium from DMEM to a α-MEM complete medium and change the media every 2 days until 80-90% confluence.

NOTE: After a week some MSC colonies start to being visible and grow

17. After 2 weeks proceed with a passage.
18. Cells on passage 3 can be used for experiments.

APPENDIX B. CELL CULTURE ON LUNG HYDROGELS PROTOCOL

The study of the release products from MSCs is crucial for the treatment of many respiratory diseases. Here I explain the process to culture MSCs in L-HG and the isolation of EV's in order to carry out every replicate of the experiment.

MATERIALS:

- Decellularized lung ECM powder
- Isolated BM-MSCs
- Weighting boats (VWR International, cat. no. 611-0094)

- Spoon (DD BioLab, cat. no. 442195)
- 10 mL syringe (BD, cat no 305959
- 5 ml sterile serological pipettes (Greiner Bio-One, cat. no. 606180)
- 10 ml sterile serological pipettes (Greiner Bio-One, cat. no. 607180)
- Pipettor (Pipet-Aid, XP model)
- 50 ml falcon tube (Corning, cat. no. 352070)
- 100-1000 µl micropipette (Eppendorf, cat. no., ES-1000)
- 1000 µl pipette tips (Eppendorf, cat. no 0030000927)
- Sterile Pasteur pipettes (Deltalab, cat. no. 200006C)
- Glass Pasteur pipettes (VWR, Pensilvania, cat. no. 612-3814)
- 100 µm cell strainer (Thermo Scientific; 22-363-549)
- 75 cm2 flasks (Techno Plastic Products, cat no. 90025)
- Hemocytometer (VWR, MARI0640011)
- Tissue culture plates (Sigma, cat. No. Z707783)
- Vacuum filters (Nalgene, cat no Z358207-1CS)
- Ice

REAGENTS:

- DMEM (Gibco, cat no 10313021)
- α-MEM (Gibco, cat no 12561056)
- Amphotericin B solution (Sigma, cat. no. A2942)
- Fetal Bovine Serum (Gibco, cat. no. 10270106)
- Penicillin/streptomycinin solution (Sigma, cat. no P4333)
- PBS 1X (Gibco, Massachusetts, cat. no. 10010-015)
- Ethanol 70% (Sigma Aldrich, Misuri)
- TrypLE Express Enzyme (1X) (Gibco, 11558856)
- Trypan Blue (Sigma, cat. no. T8154)
- NaOH (Sigma, cat no 1310-73-2)
- HCl (Sigma, cat no 320331)
- Total Exosome Isolation Reagent (from cell culture media) (Invitrogen, cat. No. 4478359)
- DMEM complete medium: DMEM medium is supplemented with a 10% FBS and 1% of

antibiotics mix (streptomycin, penicillin and amphotericin

- αMEM complete medium: αMEM medium is supplemented with a 10% FBS and 1% of antibiotics mix (streptomycin, penicillin and amphotericin).

EQUIPMENT:

- Centrifuge (Heraeus Instruments, Labofuge 400R model)
- Laminar flow cabinet for cell culture (Scanlaf Mars Safety Class 2)
- Optical microscope (Olympus Life Science, CKX31 model)
- Cell culture incubator (Thermo Scientific Heracell 150i CO2 incubator)
- Precision balance scale (PCE Instruments, Germany, PCE-BSK 310)
- Vortex (Scientific Industries, Vortex Genie 2 model)

PROCEDURE:

○ Lung hydrogel preparation

1. Weight the lyophilized lung powder (100mg) to the desired concentration (20 mg/ml) and the pepsin (10 mg) at a 10% (w/w) proportion.

From now on the whole procedure will be at sterile conditions, therefore all the reagents must be filtered through 0.20µm filters.

2. Add the HCL 0.01 M until reaching the total volume of wanted hydrogel (5mL).
3. Mix the acid with the powder with a Pasteur pipette until obtaining a homogeneous solution.
4. Add a sterile magnetic stirrer at the solution at 400 rpm at room temperature for 16h.
5. Put the viscous mixture (pregel solution) on ice to avoid jellification. Mix 1/9 of the volume of the ECM solution of cool PBS 10x (*555 µL)* with the pregel and vortex vigorously.

From now on the pregel solution is going to be kept in ice to avoid jellification

6. Add 1/10 of the volume of the acid added of cold NaOH 0.1 M (*500 µL)*, mix vigorously and check pH with a stripe. If necessary, add more NaOH to the pregel until reaching a pH ~7.4.
7. Aliquot the neutralized solution on cooled 1 mL Eppendorf and immediately freeze at-80° C (The aliquots can be storage at that temperature until usage) Or keep them on ice for subsequently use.

o Mesenchymal Stem Cell culture on lung hydrogel

8. Once the pregel looks viscous centrifuge per 2 minutes at 1000g and 4° C to avoid bubbles.
9. Add the pregel solution into the desired well-plate.
10. Let it jellify for 30 min in the incubator at 37ºC
11. Trypsin the cells:
    a. Remove the medium with a sterile glass Pasteur pipette.
    b. Add 5 mL of PBS1X to completely remove the medium
    c. Add 2mL of Tryple Trypsin and leave it for 5 minutes in the cell incubator at 37ºC.
    d. Add 5mL of TNS to stop the solution (check first that the cells are completely detached from the glass)
    e. Transfer the content to a falcon and centrifuge during 5 minutes at 250G.
    f. Aspirate the TNS and resuspend in 1mL of complete medium.
12. Count the cells:
    a. Take a small aliquot of the cell suspension and dilute it in 1:10 v/v with trypan blue. Mix it well with micropipette. ´
    b. Place 10 µL of the solution and place it carefully in the hemocytometer chamber.
    c. Count the cells and calculate the cell concentration.
13. Add the desired amount of cells according to the experimental design on top of the lung hydrogel and complete with the supplemented medium to reach the medium well volume.

Is recommended to pipette the medium slowly and through the wall of the well to avoid the detaching of the hydrogel to the bottom of the well.

○ Extracellular vesicle isolation

PROCEDURE

14. The medium from the cells cultured without FBS for 48h is collected and centrifuged at 2000G for 30 minutes.

For culturing without FBS, culture the cells with your medium supplemented with FBS till reach confluence, then wash 3 times with PBS 1X and add to medium without FBS.

15. The supernatant is centrifuged again at 10000G for 20 minutes.
16. The supernatant is filtered through a 20 μm filter with a syringe.
17. Total Exosome Isolation Reagent is added to the filtered supernatant and well mixed by pipetting.
18. The mix is incubated overnight at 4ºC.
19. After that is centrifuged at 10000G for 1 hour.
20. The pellet is resuspended in PBS 1X and stored at-80ºC.

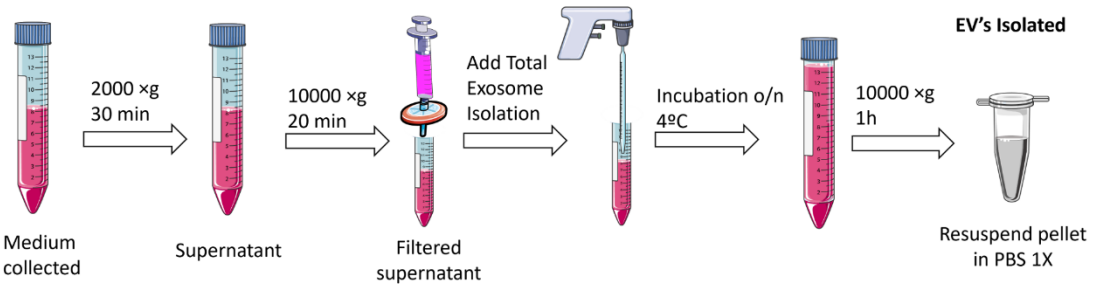

Figure A1. *Schematic representation of the EV's isolation protocol protocol.*

APPENDIX C. INTRATRACHEAL INSTILLATION OF LUNG HYDROGEL IN RATS PROTOCOL

The use of a reliable model is crucial for test the effectiveness of the lung hydrogel to be used as therapy. Here I explain the ALI model of aspiration pneumonia used for every replicate in the intratracheall instillation of L-HG study.

o LPS- Induced Acute Lung Injury

MATERIALS:

- Sprague-Dawley rat
- Isofluorane chamber (SomnoFlo Anesthesia Systems, Catalog no: SOMNO-0530SM)
- Isolated BM-MSCs
- Tweezers (rubisTech, catalog number: 1-SA)
- Ice
- Hemocytometer (VWR, MARI0640011)
- Custom-made glass tubes for animal exposure

REAGENTS:

- HCl (Sigma, cat no. 320331)
- LPS from E.Coli (Sigma, cat no. O128:B12)
- Isofluorane (Sigma, cat no. 26675-46-7)
- PBS 1X (Gibco, Massachusetts, cat. no. 10010-015)
- Urethane (Sigma, cat. no. 51-79-6)

EQUIPMENT:

- Centrifuge (Heraeus Instruments, Labofuge 400R model)
- Cell culture incubator (Thermo Scientific Heracell 150i CO2 incubator)
- Optical microscope (Olympus Life Science, CKX31 model)
- 5 ml sterile serological pipettes (Greiner Bio-One, cat. no. 606180)
- 10 ml sterile serological pipettes (Greiner Bio-One, cat. no. 607180)
- Pipettor (Pipet-Aid, XP model)
- 15 ml sterile Falcon tube (Corning, cat. no. 652095)
- 0.5 ml sterile tube (Eppendorf, cat. no 022363611)
- 0.5-10 µl micropipette (Eppendorf, cat. no. ES-10)
- 20-200 µl micropipette (Eppendorf, cat. no., ES-200)
- 100-1000 µl micropipette (Eppendorf, cat. no., ES-1000)
- 10 µl pipette tips (Eppendorf, cat. no 0030000854)

- 200 µl pipette tips (Eppendorf, cat. no 0030000897)
- 1000 µl pipette tips (Eppendorf, cat. no 0030000927)
- 1 mL syringe (BD, cat no 309658)
- 75 cm2 flasks (Techno Plastic Products, cat no. 90025)

PROCEDURE

1. Weight the rat
2. Anesthetize the rat with 5% Isoflurane till it has achieved desired level of sedation (decreased breathing rate of ~60 bpm),
3. Open the mouth of the rat and gently pull the tongue out to one side with tweezers.
4. Gently insert the glass instillation glass tube trought the trachea

Confirm it is well intubated by watching air condensation inside the glass instillation tube

5. Raise the rat to a 45° incline and secure the intubation tube while inserting the precision syringe containing the HCl 0,01M at a concentration of 1.2 µL/ g body wt. of the rat.

Figure A2. Instillation process. (Left) *Open the mouth and pull the tongue to introduce the instillation tube.* ***(Right)*** *Rise the rat and instill the solutions*

6. Dispense the solution directly into the lung in a single fluid motion and immediately remove the syringe and instillation tube.
7. Return the mouse to a cage and allow recovery from anesthesia.
8. After 2h anesthetize again with isoflurane 5% and intratracheally instill LPS from *E. Coli* at a concentration of 30 µg/g body w of the rat.
9. Return the rat to a cage and allow recovery from anesthesia.

○ Intratracheal instillation of L-HG

10. 16h after LPS hit instill the rat again with 200 µl L-HG at 3 mg/ml (diluted from 20mg/ml), MSCs or saline.
11. Trypsin the rBM-MSCs cells previously stained for the liophilic fluorophore PKH26 according to the manufacturer's instructions.
    a. Remove the medium with a sterile glass Pasteur pipette.
    b. Add 5 mL of PBS 1X to completely remove the medium
    c. Add 2mL of Tryple Trypsin and leave it for 5 minutes in the cell incubator at 37ºC.
    d. Add 5mL of TNS to stop the solution (check first that the cells are completely detached from the glass)
    e. Transfer the content to a falcon and centrifuge during 5 minutes at 250G.
    f. Aspirate the TNS and resuspend in 1mL of complete medium.
12. Count the cells:
    a. Take a small aliquot of the cell suspension and dilute it in 1:10 v/v with trypan blue. Mix it well with micropipette. ´
    b. Place 10 µL of the solution and place it carefully in the hemocytometer chamber.
    c. Count the cells and calculate the cell concentration.
13. Take the needed volume of cell suspension to have a final concentration 2×10^6 cells suspended in 200 µl of sterile saline.
14. Centrifuge 5 minutes at 250G and resuspend in 200 µl of sterile saline.

Keep the cells on ice until usage.

15. Weight the rat every day

o Sample collection

16. After 72h of the induction of therapy the rat is anesthetized with an intraperitoneal injection of 7.5 mL/kg of animal weight of urethane at 20%.
17. Check the animal reflexes and administrate half of the previous dose if needed. Check again the reflexes after some minutes.
18. The rat is placed in supine position and ethanol soaked.
19. The abdominal cavity is opened, and the vena cava is cut off to release the blood.
20. The diaphragm is cut off and the chest cavity is opened to show the lungs and the heart.
21. The lung and the heart are excised *en bloc* keeping the trachea. Then the heart and the trachea are removed.

APPENDIX D. CELL CULTURE ON TISSUE SLICES PROTOCOL

The decellalurazitaion process offers the possibility to study the tissue mechanics and the composition of determined region. In this case, lung slices are decellularized to test their biomechanical characteristics and composition, further culture with MSCs is conducted to test their viability and proliferation capacity. Here I explain the whole process to obtain the decellularized lung scaffold and culture the MSCs in every replicate.

MATERIALS:

- 6 month and 24-month C57BL/6J mice
- hBMMSCs (ATCC, catalog number: PCS-500–012)
- Coverslips (Labbox, catalog number: COVN-050-100)
- Vacuum filters (Nalgene, cat no Z358207-1CS)
- Blades (Ted Pella, Inc. St/Steel, Single Edge, 38 mm, catalog number: 121.4)
- Slide tray (Histoline, Tray Slide Staining System, catalog number: M920-1)
- 250 mL glass beaker (VWR, catalog number: 213-1124)

- Pasteur pipettes 3 mL (Deltalab, catalog number: 200006.C.)
- SuperFrost Plus glass slides (ThermoFisher, Epredia TM SuperFrost Plus TM Adhesion slides, catalog number: 10149870)
- Optimum cutting temperature (OCT) compound (Sakura, Tissue-Tek ®, catalog number: 4583)
- Cryomolds (Sakura, Tissue-Tek ® Cryomold ® Standard 25 × 20 × 5 mm, catalog number: 4557)
- Corning ® 50 mL centrifuge tubes (Sigma-Aldrich, catalog number: CLS430290-500EA)
- Tweezers (rubisTech, catalog number: 1-SA)

REAGENTS:

- Deoxyribonuclease I from bovine pancreas (Sigma-Aldrich, catalog number: DN25-1G)
- MgCl2 (Sigma-Aldrich, catalog number: M8266-1KG)
- CaCl2 (Sigma-Aldrich, catalog number: C1016-500G)
- 1 M Tris-HCl, pH 7.5 (ThermoFisher, Invitrogen, catalog number: 15567027)
- Sodium deoxycholate (Sigma-Aldrich, catalog number: D6750-500G)
- Milli-Q water
- MSCs Basal Medium (ATCC, catalog number: PCS-500–030, ATCC)
- Amphotericin B solution (Sigma, cat. no. A2942)
- Fetal Bovine Serum (Gibco, cat. no. 10270106)
- Penicillin/streptomycinin solution (Sigma, cat. no P4333)
- PBS 1X (Gibco, Massachusetts, cat. no. 10010-015)
- Ethanol 70% (Sigma Aldrich, Misuri)
- TrypLE Express Enzyme (1X) (Gibco, 11558856)
- Trypan Blue (Sigma, cat. no. T8154)
- DNase solution: 0.3mg/mL of DNase, 10% Tris-HCl, 10mM $MgCl_2$, 10 mM $CaCl_2$ in MiliQ
- SDC solution: 2% of SDC in MiliQ

EQUIPMENT:

- Cryostat (Leica, model: CM3050S)
- Milli-Q Gradient (Millipore, catalog number: ZMQ55V001)
- Centrifuge (Heraeus Instruments, Labofuge 400R model)
- Scale (Sartorius Lab Instruments, ENTRIS124l-1S, catalog number: 31603742)
- Cell culture incubator (Thermo Scientific Heracell 150i CO2 incubator)
- Laminar flow cabinet for cell culture (Scanlaf Mars Safety Class 2)
- Optical microscope (Olympus Life Science, CKX31 model)

PROCEDURE:

Lung harvesting and sample preparation

1. Euthanize the mice by dislocation and harvest the lungs *en bloc* with the heart.
2. Inflate the lungs immediately with with 1:3 dilution of OCT with 0.3 mL to reach FV. Keep another group without inflation, at RV. Put both samples ina cryomold OCT embedded.
3. Perform 100 µm cryosections using a cryostat with a −24°C temperature setting in a positively charged glass slide and allowed to air-dry 15 min before being stored at −80°C until needed.

Slide preparation and decellularization

4. Withdraw samples from the freezer and allow them to thaw inside a Laminar flow cabinet for cell culture at room temperature for 40 min.

From now on the whole procedure will be at sterile conditions, therefore all the reagents must be made with sterile PBS or MiliQ and filtered through 0.20µm filters.

5. Cover the whole slide in PBS 1× 1% AA for 30 min to remove the OCT compound.
6. Remove the PBS 1X 1% AA by inverting the glass slide over a glass beaker.

Be quick in between washes to never let the sample completely dry.

7. Cover the whole sample in Milli-Q water for 10 min to provoke cell lysis.
8. Remove the Milli-Q water by inversion and repeat step 6.
9. Remove the Milli-Q water by inversion.
10. Cover the sample in SDC 2% solution for 15 min.
11. Remove the SD 2% solution by inversion.
12. Cover the sample again in SD 2% solution for 15 min.
13. Remove the SD 2% solution by inversion.
14. Incubate with PBS 1× 1% AA for 5 min and remove it by inverting the sample.
15. Repeat step 11 three times.
16. Cover the sample in DNase solution and incubate at 37ºC for 40 min.
17. Remove the DNase by inversion and repeat step 14 three times.
18. Leave the sample in PBS 1X 1% AA until further testing. Do not allow to dry.

o MSCs culturing on slices

19. Trypsin the cells:
    a. Remove the medium with a sterile glass Pasteur pipette.
    b. Add 5 mL of PBS1X to completely remove the medium
    c. Add 2mL of Tryple Trypsin and leave it for 5 minutes in the cell incubator at 37ºC.
    d. Add 5mL of TNS to stop the solution (check first that the cells are completely detached from the glass)
    e. Transfer the content to a falcon and centrifuge during 5 minutes at 250G.
    f. Aspirate the TNS and resuspend in 1mL of complete medium.
20. Count the cells:
    a. Take a small aliquot of the cell suspension and dilute it in 1:10 v/v with trypan blue. Mix it well with micropipette. ´
    b. Place 10 µL of the solution and place it carefully in the hemocytometer chamber.
    c. Count the cells and calculate the cell concentration.

21. Add the desired number of cells according to the experimental design on top of the lung scaffold and complete with the MSCs medium to reach the medium well volume.